博士論文

論文題目

Neuromuscular control during split-belt locomotor adaptation in humans

（スプリットベルト歩行適応における神経筋制御）

2020 年度入学

氏名　大島 惇史（1415200002）

指導教員　中村 康雄 教授

Acknowledgments

First, I would like to express my gratitude to my supervisor, Dr. Kiyotaka Kamibayashi, for his continuous support. I could not have accomplished my work without your support. Your technical assistance in experiments and our discussions in preparation for papers and conferences as well as your informal comments in the lab have greatly advanced my work. I would also like to express my thanks to you for teaching me the pleasure of research.

In addition, I would like to thank my co-supervisor, Dr. Yasuo Nakamura, for his technical assistance in experiments and meaningful comments in the preparation of the papers for publication. My thanks also go to Dr. Yoshiyuki Fukuoka and Dr. Masaki Takeda for valuable comments in the review of this thesis.

Furthermore, I received support from Dr. Hikaru Yokoyama at The University of Tokyo and Dr. Benio Kibushi at Kobe University on how to analyze and interpret the results of my work. I appreciate their kind support.

I would also like to thank all members of Dr. Kamibayashi's laboratory for their useful comments on my work, those who participated in my experiments for their kindness, and my colleagues who worked hard at BANJYOKAN at Doshisha University for their support.

Finally, I wish to express my greatest appreciation to my father, mother, and older brother for their endless support in my professional and private life.

博士論文に関わったすべての方々に感謝申し上げます

Atsushi Oshima

November 2022

TABLE OF CONTENTS

List of abbreviations **1**

Chapter 1: General Introduction **3**

1-1. Preface 3

1-2. Literature review 4

1-2.1. Biomechanics of steady-state walking 4

1-2.2. Neural control of steady-state walking 10

1-2.3. Outline of split-belt locomotor adaptation 22

1-2.4. Biomechanics of split-belt locomotor adaptation 25

1-2.5. Neural control of split-belt locomotor adaptation 29

1-3. Purpose and outline of thesis 33

Chapter 2: Study 1 ..... **35**

Time-series changes in intramuscular coherence associated with split-belt treadmill adaptation in humans

2-1. Introduction and purpose 35

2-2. Methods 39

2-3. Results 45

2-4. Discussion 50

2-5. Conclusion 56

Chapter 3: Study 2 ..... **57**

Modulation of muscle synergies in lower-limb muscles associated with split-belt locomotor adaptation

3-1. Introduction and purpose 57

3-2. Methods 61

3-3. Results 69

3-4. Discussion 78

3-5. Conclusion 83

Chapter 4: General Discussion **84**

4-1. Summary of the results 84

4-2. Neuromuscular control of individual muscle through the corticospinal tract in the course of split-belt locomotor adaptation 85

4-3. Neuromuscular control of multiple muscles through muscle synergies in the course of split-belt locomotor adaptation 87

4-4. Comprehensive understanding of neuromuscular control in the course of split-belt locomotor adaptation 89

4-5. Limitations 91

4-6. The future direction of split-belt locomotor adaptation study 92

4-7. Implications for clinical rehabilitation and sports science 94

Chapter 5: Conclusion **97**

References **98**

List of abbreviations

Abbreviation	Term
AL	adductor longus
ANOVA	analysis of variance
BF	biceps femoris
CBI	cerebellar brain inhibition
CNS	central nervous system
CPG	central pattern generator
EEG	electroencephalography
EMG	electromyography
fMRI	functional magnetic resonance imaging
Gmax	gluteus maximus
Gmed	gluteus medius
GRF	ground reaction force
LG	lateral gastrocnemius
MEPs	motor evoked potentials
MG	medial gastrocnemius
MLR	mesencephalic locomotor region
NNMF	non-negative matrix factorization
PCA	principal component analysis
PPC	posterior parietal cortex
RF	rectus femoris
RMS	root mean square
SCI	spinal cord injury
SLR	subthalamic locomotor region
SOL	soleus
SPECT	single photon emission computed tomography
ST	semitendinosus
TA	tibialis anterior
tDCS	transcranial direct current stimulation

List of abbreviations

TFL	tensor fasciae latae
TMS	transcranial magnetic stimulation
VAF	variability accounted for
VL	vastus lateralis
VM	vastus medialis

Chapter 1: General Introduction

1-1. Preface

Bipedal walking is a fundamental locomotion style in humans. The major characteristics of bipedal walking are upright posture and foot strike to the ground from the heel in front of the body (Nielsen, 2003; Grillner, 2011). This locomotion style began approximately 6 million years ago in central Africa, and the reason why human ancestors started bipedal walking seems to be to carry limited resources such as food (Carvalho et al., 2012). Bipedal walking is thought to be fully developed approximately 3.6 million years ago (Simonsen, 2014). Freeing the forelimbs (i.e., upper limbs) by walking only with the hindlimbs (i.e., lower limbs) enabled our ancestors to use tools, which might have contributed to the development of human culture (Nielsen, 2003). The study of human bipedal walking is considered to have originated with Aristotle in Ancient Greece (Baker, 2007). Although this study was qualitative and observational, it would have a significant effect on subsequent human walking studies. With the development of measurement technology, studies on human bipedal walking have been rapidly progressing. At present, we can obtain data on physiological phenomena, such as muscle and brain activities, as well as biomechanics such as joint angle and ground reaction force during walking.

Human bipedal walking is undoubtedly flexible and adaptable in response to changes in walking environments (Nielsen, 2003). For example, when we face an unfamiliar walking surface, our walking pattern is temporarily disrupted; however, a few seconds or minutes later, we adjust our walking patterns and can adapt to the environment. In the field of motor control research, adjustment of walking patterns in response to changes in environments is called locomotor adaptation (Torres-Oviedo et al., 2011). Although many researchers have studied the neural mechanism underlying

locomotor adaptation, its detailed neural mechanism is not yet fully understood. Therefore, this thesis focuses on the adaptability of human bipedal walking and aims to investigate the underlying neural control thereof.

Chapter 1 reviews previous studies on biomechanics and neural control of steady-state walking and locomotor adaptation. The purpose and outline of this thesis are then presented.

1-2. Literature review

1-2.1. Biomechanics of steady-state walking

Basic terms in walking studies

The basic terms used in walking analysis, based on the right leg for convenience, are outlined below. Generally, the gait cycle is determined by the time between heel strikes of the same foot (Neumann, 2002). In other words, one gait cycle is from the heel strike of the right foot to the subsequent that of the right foot. The one cycle length is conventionally normalized to 100% to describe events within one gait cycle and to compare data on different cycles. This cycle comprises the stance and swing phases (Fig. 1-1). The stance phase is when the foot is on the ground (i.e., from heel strike of the right foot to toe-off of the right foot). This phase composes approximately 60% of one gait cycle at a normal walking speed of approximately 5 km/h in healthy young adults (Bohannon and Williams Andrews, 2011). The stance phase is further subdivided into four periods. The first is a loading response period from the right heel strike to the left toe-off (0–10% of one gait cycle). This period corresponds to an initial double support phase in which both feet are on the ground. The second period is a mid-stance period from the left toe-off to the right heel-off (10–30%). The third period is the terminal stance period from the right heel-off to the left heel strike (30–50%). The fourth period is the pre-swing period

from the left heel strike to the right toe-off (50–60%). This period corresponds to a second double support phase. Unlike the stance phase, the swing phase is when the foot is not on the ground (i.e., from the right toe-off to the right heel strike). This phase makes up approximately 40% of one gait cycle at normal walking speed, which is subdivided into three periods. The first of these is an initial swing period from the right toe-off to the intersection of both feet in the sagittal plane (60–73%). The second is the mid-swing period, which is from the intersection of both feet to the point at which the right tibia is vertical (73–87%). The third period is the terminal swing period, which is from the point at which the right tibia is vertical to the right heel strike (87–100%). On the other hand, in spatial terms, stride length of the right leg is defined as the anterior-posterior distance between the right heel strike and the subsequent right heel strike (Fig. 1-2). Furthermore, step length of the right leg is the anterior-posterior distance between the left heel strike and subsequent right heel strike.

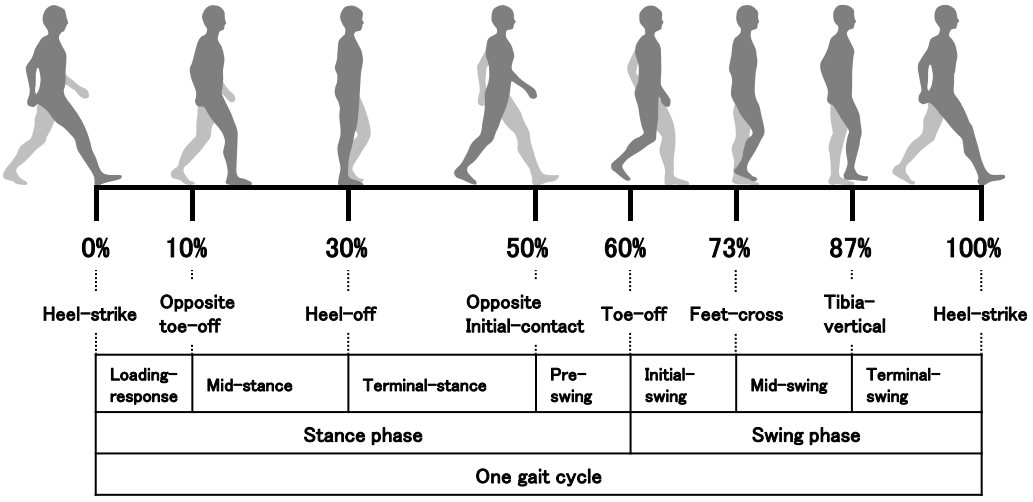

Figure 1-1 Events and each period within one gait cycle
Each event in this figure is described based on movement of the right leg (dark gray side) (modified from Neumann, 2002).

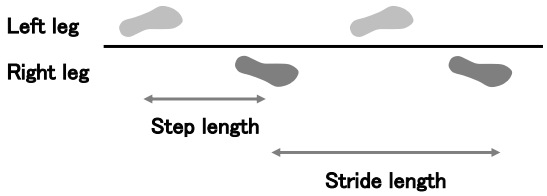

Figure 1-2 Spatial parameters for walking analysis (modified from Neumann, 2002)

Kinematics

Kinematic parameters of steady-state walking, the angles of three lower limb joints in the sagittal plane during the gait cycle, are described below (Fig. 1-3). Firstly, the hip joint is in a position of approximately 30° flexion at heel strike (Neumann, 2002). Subsequently, the joint extends throughout the stance phase and reaches a maximum of approximately 10° extension just before toe-off. Following this, the hip joint flexes throughout the swing phase and reaches its original heel strike position. Thus, the range of motion of the hip joint within one gait cycle is approximately 40°. Concurrently, the knee joint flexes approximately 20° after heel strike. Although this joint becomes a neutral position near midpoint of the stance phase, it flexes again from before toe-off to midpoint of the swing phase. The knee joint then returns to a neutral position just before heel strike. Thus, the angular change of this joint within one gait cycle is approximately 60° and is bimodal. Finally, a slight plantarflexion of the ankle joint occurs just after the heel strike (< 5°), followed by the dorsiflexion of approximately 10° in the midpoint of the stance phase. Subsequently, the plantarflexion of approximately 30° occurs from the pre-swing period to the toe-off. Lastly, the ankle joint dorsiflexes in the early phase of the swing phase and is in a neutral position since the middle of the swing phase. Thus, the range of motion of the ankle joint within one gait cycle is approximately 30°.

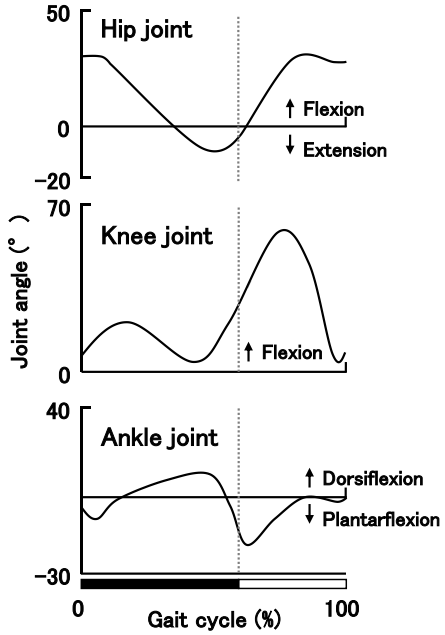

Figure 1-3 Angular changes in three lower limb joints within one gait cycle
Vertical axis is angle (°), and horizontal axis is normalized gait cycle (%). Solid black and white bars indicate stance and swing phases, respectively. Vertical dashed lines indicate borders between stance and swing phases (modified from Neumann, 2002).

Kinetics

Ground reaction force (GRF) is a kinetic parameter in walking analysis (Fig. 1-4). The GRF is the reaction force generated by the contact area between the sole of the foot and the floor and comprises three directions components, medial-lateral, anterior-posterior, and vertical components. For the medial-lateral component, an inward reaction force continues to occur throughout one gait cycle (Neumann, 2002). The peak size of this component is approximately 5% body weight. Secondly, a backward reaction (braking) force of the anterior-posterior component occurs after heel strike, followed by the forward reaction (propulsive) force in the last half of the gait cycle. The maximum magnitudes of backward and forward reaction forces are approximately 20% body weight. Finally, the upward reaction force of the vertical component rapidly increases just after heel strike. Although this force decreases marginally at the midpoint of one gait cycle, it then increases again. In other words, changes in the vertical component within one gait cycle are bimodal. The peak magnitude of the vertical component is slightly greater than body weight (> 100%).

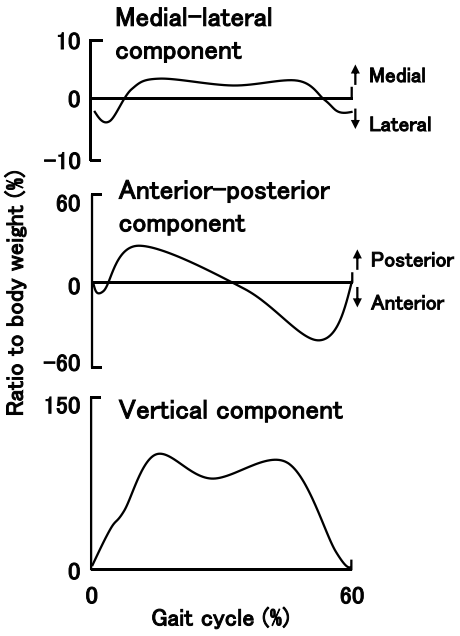

Figure 1-4 Changes in three components of ground reaction force within one gait cycle
Vertical axis is ratio to body weight and horizontal axis is normalized gait cycle (%) (modified from Neumann, 2002).

Muscle activities of lower limb

Figure 1-5 shows electromyography (EMG) waveforms of the lower limb muscles within one gait cycle during steady-state walking at various walking speeds (Cappellini et al., 2006). This section details the activities of the major muscles of the lower limb (Neumann, 2002). The activation of the gluteus maximus (Gmax) muscle, a hip extensor, begins just before the heel strike and persists during the loading response and mid-stance periods. This activation contributes to leg deceleration in the terminal swing period and hip extension in the stance phase. A similar activation pattern is observed in the gluteus medius (Gmed) muscle, a hip abductor. This activation contributes to preventing tilt to the contralateral side of the pelvis in the mid-stance and terminal stance periods. The tensor fasciae latae (TFL) muscle, a hip flexor, invertor, and abductor, is active throughout the stance phase. This activation assists the swing of the contralateral leg by advancing the opposite pelvis. The adductor longus (AL) muscle, a hip adductor, is mostly activated in the initial swing period. This activation assists the hip flexion and contributes to swing initiation. The biceps femoris (BF) and semitendinosus

(ST) muscles, hip extensors and knee flexors, are mainly activated from the terminal swing to the mid-stance periods. These activations contribute to leg deceleration in the late swing phase and hip extension in the early stance phase. The rectus femoris (RF), vastus medialis (VM), and vastus lateralis (VL) muscles, quadriceps muscle, are activated from the late swing phase to the early stance phase. The activations aid in the absorption of impact and stabilization of the knee joint at the heel strike. The RF is also active in the early swing phase, which contributes to hip flexion. The medial (MG) and lateral gastrocnemius (LG), and soleus (SOL) muscles, planter flexors, are mostly activated in the late stance phase. These activations contribute to generating propulsive force. Finally, the tibialis anterior (TA) muscle, an ankle dorsiflexor, is activated in the swing and early stance phases. This activation contributes to securing foot clearance and preventing striking of the sole at the heel strike.

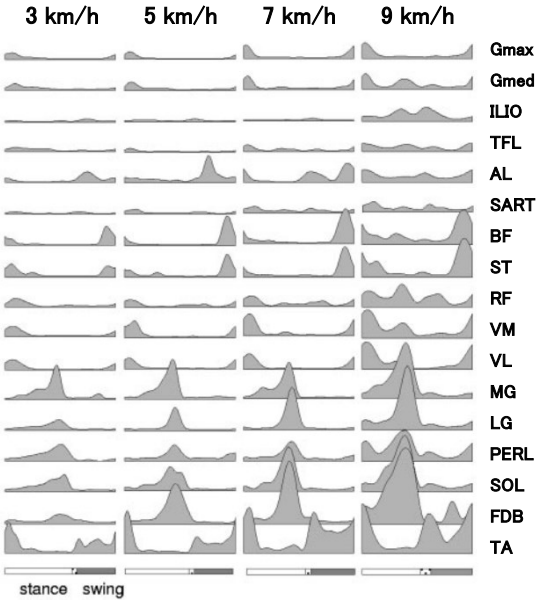

Figure 1-5 Muscle activities of the lower limb muscles within one gait cycle at different speeds
Gluteus maximus (Gmax), Gluteus medius (Gmed), Iliopsoas (ILIO), Tensor fasciae latae (TFL), Adductor longus (AL), Sartorius (SART), Biceps femoris (BF), Semitendinosus (ST), Rectus femoris (RF), Vastus medialis (VM), Vastus lateralis (VL), Medial gastrocnemius (MG), Lateral gastrocnemius (LG), Peroneus longus (PERL), Soleus (SOL), Flexor digitorum brevis (FDB), Tibialis anterior (TA) (modified from Cappellini et al., 2006)

1-2.2. Neural control of steady-state walking

Central pattern generators

Central pattern generators (CPGs) are thought to play an important role in the locomotion of vertebrates (Rossignol et al., 2006; Grillner and El Manira, 2020). CPGs are neural networks consisting of spinal interneurons and generate rhythmic muscle activities for locomotion (Latash, 2007). The basic concept of CPGs is the half-center model proposed by Graham Brown over a century ago (Brown, 1914). In this model, reciprocal inhibition mechanisms in spinal interneurons connecting to flexor- and extensor-innervating motoneurons are hypothesized to result in alternate flexor-extensor activities. Although many studies have investigated the presence of human CPGs, there is still no direct evidence. The major reason for this is that methods measuring neural activity in the spinal cord directly are invasive and are not applicable to humans. However, several studies have reported the presence of the CPG-like neural network in humans. For example, when a patient with an incomplete spinal cord injury (SCI) was in a supine posture with an extended hip joint, involuntary stepping-like movements appeared spontaneously (Calancie et al., 1994). This phenomenon suggests that CPG-like neural networks generating rhythmic stepping are present in the human spinal cord. Following this, Dimitrijevic et al. (1998) more directly assessed these neural networks using epidural spinal cord stimulation. According to the authors, when the non-patterned stimulation was applied to the posterior structures of the lumbosacral spinal cord in a patient with a complete SCI, patterned locomotion-like stepping movements and muscle activities were induced. The induction of such involuntary locomotion-like movements has also been reported in healthy participants (Gerasimenko et al., 2010). These findings provide the possibility that the human spinal cord possesses CPGs capable of generating rhythmic movements. Recently, a new model has also been proposed, in which a CPG has

two distinct layers, the rhythm generator and pattern formation circuits (McCrea and Rybak, 2008).

Reflex mechanisms

The Hoffmann reflex (H-reflex) is widely used to investigate the spinal reflex circuit, specifically motoneurons excitability and synaptic transmission in the Ia afferent nerve terminal. The H-reflex is a muscular response that occurs when ascending impulses elicited by electrical stimulation to the Ia afferent nerve excite motoneurons (Latash, 2007). In many previous studies on humans, H-reflex has been induced in the SOL muscle. The H-reflex is the same reflex circuit as the monosynaptic stretch reflex; however, the monosynaptic stretch reflex is evoked by mechanical stretching of the muscle spindle. The H-reflex has been shown to be modulated in a task-dependent manner. For example, Capaday and Stein (1986) reported that the H-reflex amplitude in the SOL was reduced in walking compared with standing with similar EMG levels. The H-reflex has also been shown to be modulated depending on the phase of walking. For example, it has been shown that although the amplitude of the H-reflex increased progressively through the stance phase, it was absent in the swing phase (Capaday and Stein, 1987). Moreover, the sensory input related to walking may affect the H-reflex excitability. A previous study investigated the effect of sensory input on H-reflex amplitude of the SOL using an exoskeleton robot on healthy participants. The results showed that the H-reflex during passive walking was modulated in a phase-dependent manner (Kamibayashi et al., 2010). The phase-dependent modulation pattern of the H-reflex during passive walking was similar to that during normal walking. Interestingly, this study also found that the extent of loading due to foot contact during walking did not affect the H-reflex. Hence, the H-reflex during walking is likely modulated by sensory information associated with lower limb movement rather than load-related information.

On the other hand, the stretch reflex in lower leg muscles during walking is also modulated in a phase-dependent manner. Sinkjaer et al. (1996) used a breakthrough system that was able to force the ankle joint to dorsiflex during walking and found that the stretch reflex in the SOL was phase-dependently modulated. Specifically, the reflex amplitude was maximal in the mid-stance phase, and the reflex amplitude in the swing phase was approximately 45% of the maximum value. Such modulation pattern within one gait cycle was almost similar to that of H-reflex (Capaday and Stein, 1987). Interestingly, the stretch reflex in the TA muscle is facilitated in the early stance phase in which the muscle activity is usually absent (Christensen et al., 2000). Because the latency of the reflex response was long, the reflex has been thought to be a long-latency reflex via the cerebrum. Such facilitation of the stretch reflex in the muscles around the ankle joint may function to stabilize the ankle joint in response to unexpected perturbations during walking (Nakazawa et al., 2004).

Brain stem and diencephalon

Over 50 years ago, Shik et al. (1966) discovered that electric stimulation of the midbrain could induce locomotion-like movements in decerebrated cats. The region is called the mesencephalic locomotor region (MLR) and includes part of the pedunculopontine tegmental nucleus (Takakusaki, 2013). Another region capable of evoking locomotor-like movements by electrical stimulation is also in the subthalamus, which is called the subthalamic locomotor region (SLR) (Takakusaki, 2013). Both MLR and SLR project to the reticular formation; this structure is the origin of the reticulospinal tract that influences CPG activation. Although it is not fully understood whether regions corresponding to the MLR and SLR are present in humans, it has been reported that the abilities to stand and step were impaired in patients with a lesion in the region corresponding to the MLR (Masdeu et al., 1994;

Hathout and Bhidayasiri, 2005). The literature supports the possibility that these regions are involved in human bipedal walking, especially in the initiation of walking.

Cerebellum

The cerebellum plays an important role in the generation of smooth and coordinated movements. The cerebellum forms the spinocerebellar loop with the spinal cord, which comprises the ventral and dorsal spinocerebellar tracts (Latash, 2007). The information regarding the activities of the CPGs and the somatosensory information during walking may be transmitted to the cerebellum via the ventral and dorsal spinocerebellar tracts, respectively. The region that can evoke locomotor-like movements by electric stimulation is also thought to be present in the cerebellum, which is called the cerebellar locomotor region (Takakusaki, 2013). Previous lesion studies have reported significant different walking patterns and locomotor muscle activity patterns between patients with cerebellar damage and healthy participants (Ebersbach et al., 1999; Martino et al., 2014, 2015). Moreover, the activity of the cerebellum has been estimated to increase after compared with before walking in previous studies using single photon emission computed tomography (SPECT) (Fukuyama et al., 1997; Hanakawa et al., 1999), a brain imaging technique that can estimate the neuronal activities in the deep brain regions based on the blood flow. These findings imply that the cerebellum plays an important role in walking.

Cerebrum

As mentioned above, the spinal cord plays an important role in generation of basic locomotive movements. Indeed, cats whose spinal cords were disconnected from their brains have been reported to be still able to walk (Armstrong, 1988). However, it has been indicated that the amplitude of

discharge in the motor cortex and posterior parietal cortex (PPC) of the cerebrum increased when cats faced complicated walking environments (Drew and Marigold, 2015). This suggests that the involvement of the cerebral cortex increases depending on walking environments, especially in a visually guided condition, in animals such as cats. In humans, although the involvement of the cerebral cortex in steady-state walking remains controversial, evidence indicating the importance of the cerebral cortex in walking has been accumulated with the development of brain imaging techniques. For example, previous studies using SPECT showed that the blood flow in the sensorimotor area increased with walking (Fukuyama et al., 1997; Hanakawa et al., 1999). Additionally, Dalla Volta et al. (2015) showed the changes in activations in the premotor and supplemental areas with locomotor-like movements using functional magnetic resonance imaging (fMRI). This technique measures the changes in blood oxygen levels due to brain neural activity. Moreover, recent studies using electroencephalography (EEG), which has a high temporal resolution compared with SPECT and fMRI, have identified detailed electrical activity in the cerebral cortex during walking. Gwin et al. (2011) showed that anterior cingulate, posterior parietal, and sensorimotor cortex activities were modulated during one gait cycle. Since then, many researchers have used the EEG to investigate brain activity during walking (Bulea et al., 2015; Bradford et al., 2016; Yokoyama et al., 2020a). The high temporal resolution and portability of EEG enable to non-invasive examination of the coupling between brain and muscle activities during walking. This synchronization is called corticomuscular (EEG-EMG) coherence (Liu et al., 2019). Many studies on corticomuscular coherence during walking have been published in last decade (Petersen et al., 2012; Jensen et al., 2019; Liu et al., 2019; Yokoyama et al., 2019, 2020b), and these studies have reported that the activities of the motor cortex and lower limb muscles during walking synchronize in the beta and low-gamma bands (approximately

10–45 Hz). These findings support the importance of the cerebral cortex in the generation of walking.

On the other hand, the deeply placed structures in the cerebrum is the basal ganglia, which comprises the striatum, globus pallidus, subthalamic nucleus, and substantial nigra. A dysfunction of the basal ganglia (Parkinson's disease) seriously impaired normal walking movements (Morris et al., 1994). Additionally, previous studies using SPECT reported that the blood flow in the basal ganglia increased with walking (Fukuyama et al., 1997; Hanakawa et al., 1999). These findings suggest the importance of the basal ganglia in walking. Further, the basal ganglia form a loop with the cerebral cortex and thalamus and the loop may play a role in voluntary control of walking movements according to the demand of environments. Meanwhile, the pathway between the basal ganglia and brain stem may contribute to the control of rhythmical walking movements and muscle tone (Takakusaki, 2013).

From the above, the cerebrum contribution to walking may be great (Nielsen, 2003). This may be evident when considering that gait function is impaired in patients with cerebrum damage such as stroke (Li et al., 2018).

Corticospinal tract

Primates, including humans, possess monosynaptic descending pathway named the corticospinal tract that runs from the primary motor cortex (layer V) to the spinal motoneurons (Nielsen, 2003). The excitability of the corticospinal tract has been examined based on amplitudes of motor evoked potentials (MEPs), which are muscular responses elicited by transcranial magnetic stimulation (TMS) to the primary motor cortex (Petersen et al., 2003). An early study applying TMS to the leg area in the primary motor cortex during walking reported that MEPs in the ankle plantar flexor and dorsiflexor were modulated in phase-dependent manners within one gait cycle (Schubert et al., 1997). Two years

later, Capaday et al. (1999) found that MEPs in the ankle dorsiflexor during walking were the same level as those during a voluntary ankle dorsiflexion task; conversely, MEPs in the ankle plantar flexor were reduced during walking compared with those during voluntary ankle plantar flexion task. Additionally, the corticospinal excitability of the ankle dorsiflexor was enhanced in the stance phase, in which the muscle is normally inactive. These results suggest that the corticospinal contribution to the ankle dorsiflexor is greater than that to the ankle plantar flexor during walking. On the other hand, Petersen et al. (2001) investigated the involvement of the primary motor cortex in activities in the ankle dorsiflexor during walking using a low-intensity (below motor threshold) TMS that is thought to activate inhibitory intracortical interneurons. The results showed that the muscle activities during walking were suppressed by applying such stimulation. Further, recovery of locomotor function with a rehabilitation training in patients with incomplete SCI has been indicated to be associated with increase in corticospinal excitability in the ankle dorsiflexor (Thomas and Gorassini, 2005; Yang and Gorassini, 2006). These results support that the importance of the corticospinal tract in walking. On the other hand, Kamibayashi et al. (2009) used a robot that can impose passive walking on participants to investigate how sensory input affects corticospinal tract excitability. In this study, excitability of corticospinal tract in the ankle dorsiflexor was phase-dependently modulated during passive walking with 40% body weight unloading but not with 100% body weight unloading. This implies that load-related afferent information facilitates corticospinal excitability in this muscle during walking.

In the last two decades, coherence analysis has been used to infer information about neural drive to spinal motoneurons during walking (Nielsen, 2002; Halliday et al., 2003; Charalambous and Hadjipapas, 2022). Coherence analysis is a mathematical method that calculates correlation between pairs of signals recorded simultaneously (e.g., paired surface EMG signals) in the time and frequency

domain (Halliday et al., 1995). In the frequency domain, EMG-EMG coherence between approximately 10 and 60 Hz (beta and gamma bands) has been thought to reflect the descending drive to the spinal motoneurons via corticospinal tract (Charalambous and Hadjipapas, 2022). EMG-EMG coherence in the ankle dorsiflexor has been reported to be observed in the beta band (8–20 Hz) during walking of healthy participants and be greater in the early and late swing phases than mid-swing phase (Halliday et al., 2003). Further, EMG-EMG coherence in the ankle plantar flexor during walking in healthy participants has also been indicated to be observed at approximately 10–45 Hz (Jensen et al., 2019). Such findings suggest involvement of descending corticospinal drive in the activities of the ankle dorsiflexor and plantar flexor during walking. On the other hand, EMG-EMG coherence in the beta and gamma bands during walking has been reported to be significantly reduced in patients with the central nervous system (CNS) disorders such as incomplete SCI (Hansen et al., 2005; Norton and Gorassini, 2006; Barthélemy et al., 2010; Zipser-Mohammadzada et al., 2022) and stroke (Nielsen et al., 2008; Kitatani et al., 2016) compared with healthy participants. Moreover, EMG-EMG coherence in the lower limb has been shown to increase with the improvement of locomotor function with rehabilitation training for several weeks (Norton and Gorassini, 2006; Willerslev-Olsen et al., 2015). These findings strongly support the hypothesis that the EMG-EMG coherence in the beta and gamma bands originates from descending neural drive through the corticospinal tract. Therefore, EMG-EMG coherence is thought to be a useful indicator for estimating the strength of corticospinal drive during walking.

Neural modules for control of multiple muscles

The role of individual CNS components in walking has reviewed until here. On the other hand, there

are numerous muscles in the body. This subsection describe how the CNS controls the multiple muscles to achieve walking.

Firstly, the numerous muscles in our body (i.e., many degrees of freedom) are essential to produce various physical movements in daily life. For example, when we walk, the many muscles in the trunk and lower limbs are activated. If the CNS controlled the activity of each of these multiple muscles separately, the amount of computation in the brain would be huge. This problem has been known as the problem of degrees of freedom, proposed by Nikolai Bernstein (Bernstein, 1966). Thus, the CNS is considered to implement motor control strategies to solve this problem. The muscle synergy concept has been proposed as a promising motor control strategy. The concept is that the CNS activates a few neural modules which are organized by some functionally related muscles to control activities of multiple muscles (Fig. 1-6). In other words, the brain may simplify muscular control by sending commands to a few neural modules rather than to each muscle individually (Dominici et al., 2011; Bizzi and Cheung, 2013). Then, where are the neural modules encoded in the CNS? Although the answer to this question is still under debate, previous studies on vertebrates have suggested that neural modules are encoded in the spinal cord (Bizzi and Cheung, 2013; Cheung and Seki, 2021). Therefore, neural modules may reflect the spinal neural network, including CPGs. Considering the commonality of the spinal neural network between vertebrates (Dominici et al., 2011; Yokoyama et al., 2016), neural modules may also be present in the human spinal cord. Such neural modules have been thought to be represented as muscle synergies that are inherent in the activities of multiple muscles (i.e., low-dimensional structures in EMG signals recorded from multiple muscles during physical movements).

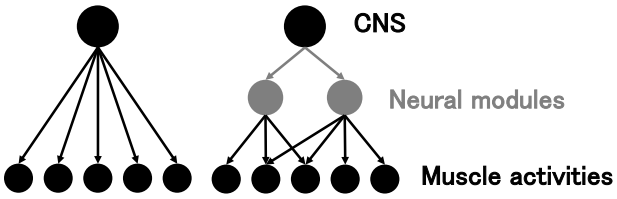

Figure 1-6 Conceptual scheme of neural modules for control of multiple muscles
Left and right panels show neuromuscular control when the central nervous system (CNS) controls multiple muscles individually and via a few neural modules, respectively.

Computational methods are employed to extract muscle synergies from multiple muscles activities. Although there are various computational methods [e.g., principal component analysis (PCA) (Ivanenko et al., 2004)], non-negative matrix factorization (NNMF) has been used in many previous studies (Dominici et al., 2011; Chvatal and Ting, 2013). NNMF is a dimension reduction technique, which approximately decomposes a given non-negative matrix into two non-negative matrices by minimizing error (Lee and Seung, 1999). Specifically, the EMG signals of multiple muscles recorded while performing a task are decomposed as follows:

$$E = WC + e$$

In this equation, E is an $m \times t$ matrix (m is the number of muscles and t is the number of recorded time points), W is an $m \times n$ matrix (n is the number of extracted synergies), C is a $n \times t$ matrix, and e is a residual. In other words, E comprises original EMG data, W indicates the weightings of muscle synergies and C indicates temporal activation patterns of the muscle synergies (Fig. 1-7 and 1-8).

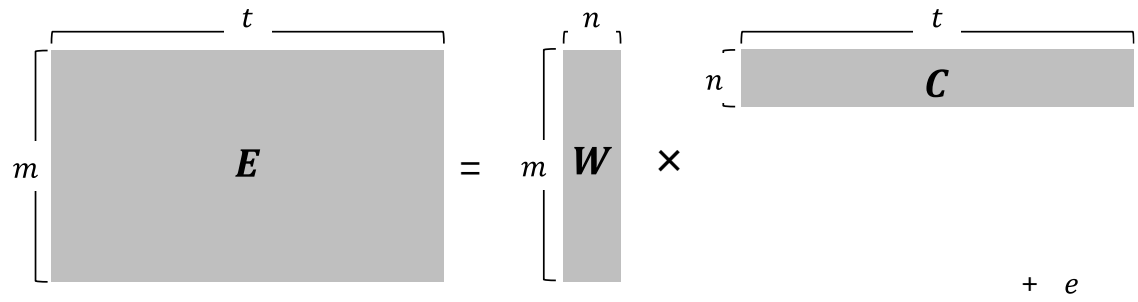

Figure 1-7 Scheme of muscle synergy analysis using non-negative matrix factorization
E is original EMG data consisted of an $m \times t$ matrix (m is the number of muscles and t is the number of recorded time points), W is the weightings of muscle synergies consisting of an $m \times n$ matrix (n is the number of extracted synergies), C is the temporal activation patterns consisting of a $n \times t$ matrix, and e is a residual.

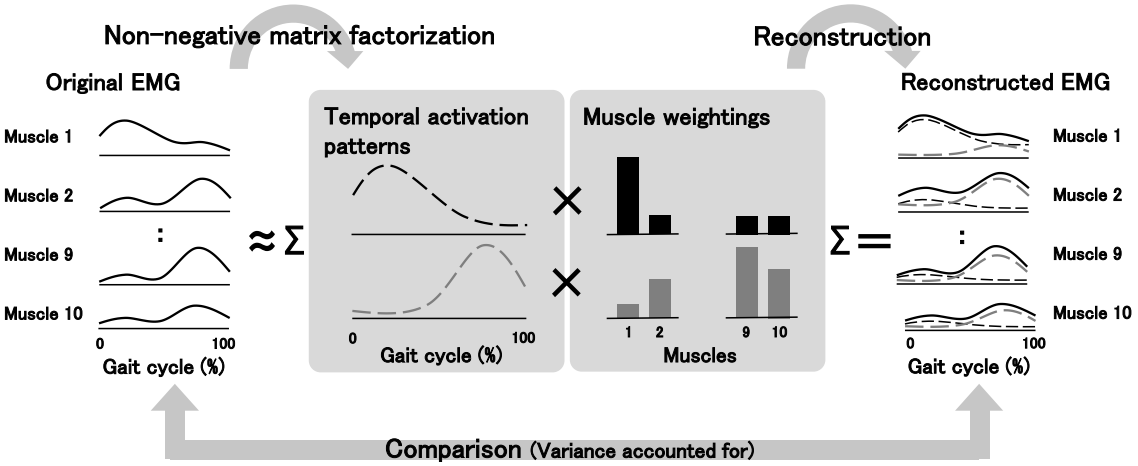

Figure 1-8 Scheme of temporal activation patterns and muscle weightings of muscle synergies
In this figure, the original EMG data consisting of 10 muscles (left panel) are decomposed by two muscle synergies (black and dark gray in middle panel). EMG data reconstructed by the extracted muscle synergies is shown in right panel.

Previous studies on muscle synergies during walking are reviewed below. Ivanenko et al. (2004) applied the PCA method to EMG data recorded from 25 muscles during normal walking and found that the EMG data were reconstructed by five basic activation patterns sufficiently. Similarly,

previous studies using NNMF have also indicated that activities of multiple muscles in the lower limb during normal walking are expressed by four or five muscle synergies (Oliveira et al., 2016; Yokoyama et al., 2016; Kibushi et al., 2018). Regarding the number of muscle synergies, Yokoyama et al. (2016) reported that the number of muscle synergies changed with walking speed. Furthermore, it has been indicated that the number of muscle synergies decreased in stroke patients (Clark et al., 2010) and Parkinson's disease patients (Mileti et al., 2020) compared with healthy participants. Moreover, Clark et al. (2010) showed that the few muscle synergies correlated with slow walking speed in post-stroke patients. Conversely, the number of muscle synergies has been indicated to increase with development from neonates to adults (Dominici et al., 2011). From the above, it is considered that the number of muscle synergies may change depending on walking speed, neurological disorders, and development. On the other hand, activation patterns in muscle synergies, which reflect neural commands sent to each muscle synergy, have been indicated to change in association with walking speed (Hagio et al., 2015; Kibushi et al., 2018) and surfaces (Martino et al., 2015; Santuz et al., 2018, 2020). Kibushi et al. (2018) extracted muscle synergies from activities of multiple trunk and lower limb muscles and found that the activation timings in several of the extracted muscle synergies shifted to an earlier or later phase in one gait cycle with an increase in walking speed. Martino et al. (2015) investigated the durations of the activation patterns in muscle synergies extracted from multiple lower limb muscles while walking in unfamiliar environments. The authors found that the duration of the activation patterns in most muscle synergies extracted during walking in unfamiliar environments was significantly longer than those extracted during walking on an even floor. The extended duration of the activation patterns may reflect a strategy to cope with the unstable walking environments. Such prolonged duration of activation patterns was also observed while walking in other unstable environments set up by a special

treadmill (Santuz et al., 2018). Therefore, the CNS may flexibly control the timing and duration of activation patterns of muscle synergies to adapt to various walking environments. Regarding the muscle weighting in the muscle synergies, a previous study reported that imposed walking environments did not significantly affect weightings of muscle synergies (Yokoyama et al., 2021); however, muscle weightings are likely to change with long-term training (Sawers et al., 2015).

In summary, the CNS may control multiple muscles during walking through a few neural modules. These neural modules may be represented as the muscle synergies. The muscle synergies are partially modulated according to external (i.e., imposed perturbation) and internal environments (i.e., disease and aging).

Summary of neural control of steady-state walking

Knowledge about neural control in walking has been accumulated with the development of various neuroimaging, electrophysiological, and computational methods. The knowledge tells us that human bipedal walking is produced by the interaction of various regions in the CNS.

1-2.3. Outline of split-belt locomotor adaptation

Locomotor adaptation has been broadly defined as an error-driven motor learning process to adjust spatio-temporal elements of walking in response to changes in walking environments (Reisman et al., 2010; Torres-Oviedo et al., 2011; Helm and Reisman, 2015; Vasudevan et al., 2017). Thus far, several methods have been proposed to investigate human locomotor adaptation; these include a robot-driven gait orthosis that controls lower limb joints in the swing phase during walking (Severini et al., 2020) and an application of weight in the swing phase during walking (Savin et al., 2010). In addition to

these methods, a special treadmill with two belts, each driven by an independent motor, has been widely used (Reisman et al., 2005; Choi and Bastian, 2007). This type of treadmill, called a split-belt treadmill (Fig. 1-9), allows walking not only in a normal walking environment (tied-belt condition) but also in a novel walking environment with different walking speeds on the left and right sides (split-belt condition). The first study in humans using the split-belt treadmill was performed on infants 35 years ago (Thelen et al., 1987). A few years later, a study on healthy adults was conducted (Dietz et al., 1994). However, these early studies only investigated immediate adjustments of lower limb coordination for a few seconds. Then, Bastian and her colleagues imposed walking in the split-belt condition for several minutes on healthy adults and reported that several kinematics parameters changed gradually (Reisman et al., 2005). With this as a trigger, many locomotor adaptation studies using the split-belt treadmill have been conducted in various research groups. In September 2022, PubMed returned 278 results when queried using search terms “split-belt treadmill” and “humans.”

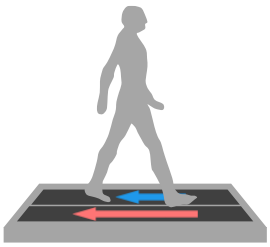

Figure 1-9 Split-belt treadmill
This treadmill has two belts that are separately controlled, providing participants with a novel walking environment in which the two belts move at different speeds (split-belt condition). Short bule and long red arrows indicate belts moving at a slow and fast speeds, respectively.

A typical split-belt treadmill paradigm that has been used in previous studies (Fig. 1-10) and general features observed under the paradigm in healthy adults are introduced below. The detailed methodology for the split-belt study has been described in a recent comprehensive review (Vasudevan

et al., 2017). First, participants are positioned with one leg on each belt. They walk in the tied-belt condition at a fast speed and then at a slow speed for approximately 2 min (baseline period). Following this, participants are exposed to the split-belt condition for approximately 10 min (adaptation period), in which one belt is set at the faster speed and one at the slower speed. A belt speeds ratio of 1:2 has been typically used in previous studies (e.g., a slow speed is 0.7 m/s and a fast speed is 1.4 m/s) (Reisman et al., 2005; Hamzey et al., 2016). Other ratios (e.g., 1:1.2 and 1:4) have also been occasionally used in several previous studies (Reisman et al., 2005; Yokoyama et al., 2018). Immediately after exposure to the split-belt condition, their walking patterns are temporarily disrupted. Specifically, the step length of each leg becomes asymmetric, resembling a limp. In other words, the split-belt condition is an obvious perturbation to bipedal walking. However, several minutes later, the walking patterns approach symmetry despite the split-belt condition. Thus, participants adapted their walking patterns to the novel walking condition based on trial-and-error practice (Reisman et al., 2010; Helm and Reisman, 2015); this implies that an internal model was updated. Finally, participants are again exposed to the tied-belt condition at the slower belt speed (post-adaptation period). They demonstrate asymmetric walking patterns again just after the exposure, a phenomenon called an aftereffect. This aftereffect reflects that the CNS learned and stored new walking patterns appropriate for the split-belt condition (Reisman et al., 2010; Torres-Oviedo et al., 2011). Subsequently, the aftereffects are washed out and walking patterns return to normal, suggesting that a recalibration of an internal model occurs again (i.e., de-adaptation to the tied-belt condition).

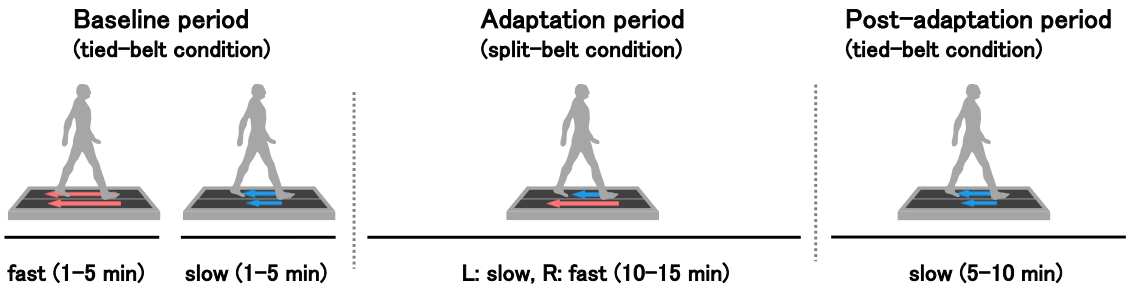

Figure 1-10 Typical split-belt treadmill paradigm
Tied-belt condition is one in which the belts move at the same speed and split-belt condition is one in which the belts move at different speeds. In the split-belt condition, a belt speeds ratio of 1:2 has been usually used in previous studies. Short blue and long red arrows indicate belts moving at slow and fast speeds, respectively.

1-2.4. Biomechanics of split-belt locomotor adaptation

Locomotor adaptation on a split-belt treadmill is characterized by two adaptive processes; the first is a predictive feedforward adaptation and the second is a reactive feedback adjustment (Reisman et al., 2005; Morton and Bastian, 2006; Sato and Choi, 2021; Severini and Zych, 2022). The following subsections provide an overview of the two distinct processes.

Predictive feedforward adaptation

Predictive feedforward adaptation is defined as an anticipatory adjustment of motor command to reduce the mismatch between the expected information and actual sensory input (i.e., error) generated in the prior movement in the subsequent movement (Ogawa et al., 2015; Sato and Choi, 2021). In other words, this adaptation is an update of an internal model in the brain based on trial-and-error practice. This adaptation is characterized by the occurrence of an aftereffect when an imposed perturbation (split-belt condition) is removed (Reisman et al., 2010; Severini and Zych, 2022) and has

been shown in walking parameters reflecting interlimb coordination. The representative indicators are step length symmetry and double support time symmetry (Reisman et al., 2005; Morton and Bastian, 2006). When calculating the step length symmetry, the following equation has been frequently used (Malone and Bastian, 2010).

$$Step\ length\ symmetry = \frac{Step\ length\ in\ limb\ on\ fast\ belt - step\ length\ in\ limb\ on\ slow\ belt}{Step\ length\ in\ limb\ on\ fast\ belt + step\ length\ in\ limb\ on\ slow\ belt}$$

A positive or negative step length symmetry value indicates that the step length in the left and right limbs is different (asymmetry), whereas a value of 0 indicates that the step length in both limbs is equal (symmetry). The symmetry of the other walking parameters is also calculated in the same way.

The step length symmetry changes throughout the split-belt paradigm in healthy participants as follows (Fig. 1-11) (Malone and Bastian, 2010). Initially, since the step length of the left and right limbs in the tied-belt condition (baseline-period) is almost equal, the step length symmetry becomes almost 0. Following this, because the step length of the left and right limbs becomes asymmetric when exposed to the split-belt condition (adaptation period), the step length symmetry becomes negative values, which reflects that the step length in the limb on the slower belt is longer than that on the faster belt. However, the step length asymmetry is gradually corrected, and a few minutes later the step length symmetry approaches 0 again. In the case of the belt speed ratio of 1:3, the stride number required to approach a plateau level is approximately 200 (Malone and Bastian, 2010; Finley et al., 2014). Subsequently, when the tied-belt condition is reintroduced (post-adaptation period), step length asymmetry is observed again, indicating the presence of an aftereffect. The size of the aftereffect has

been shown to be greater when the speed of both belts was set at the slower speed than the faster speed in the split-belt condition (Vasudevan and Bastian, 2010). Because the aftereffect is then washed out within a few minutes and symmetrical walking patterns are retrieved, the step length symmetry returns almost 0.

Although it has also been reported that the double support time symmetry slowly changes throughout the split-belt treadmill paradigm, as does the step length symmetry (Morton and Bastian, 2006; Musselman et al., 2011; Sato and Choi, 2022), the rate of adaptation is faster in double support time symmetry than in step length symmetry (Malone and Bastian, 2010; Malone et al., 2012). From the above, step length symmetry and double support time symmetry are thought to act as error signals in the predictive feedforward adaptation of split-belt locomotor adaptation (Malone et al., 2012).

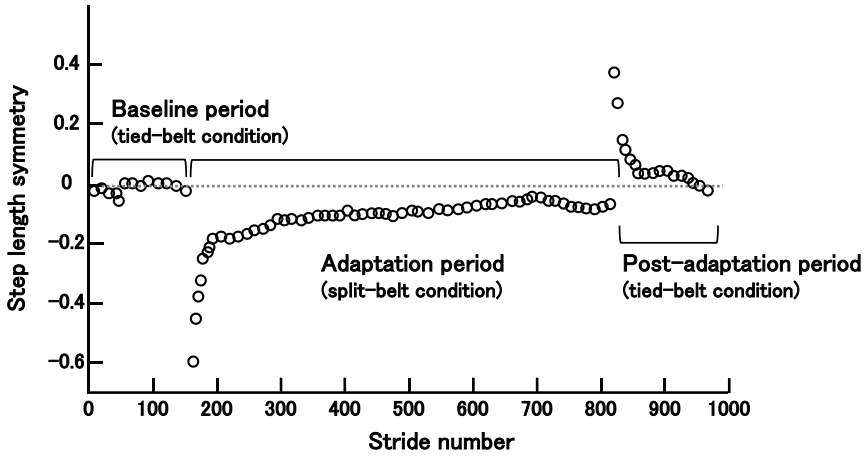

Figure 1-11 Typical example of time-series changes in step length symmetry throughout the split-belt treadmill paradigm

A belt speed ratio of 1:3 was used in this paradigm. Vertical axis is step length symmetry and horizontal axis is stride number. Horizontal dashed line indicates that step length in left and right limbs is equal (modified from Malone and Bastian, 2010).

Reactive feedback adjustment

Reactive feedback adjustment is a rapid adjustment of movements based on afferent feedback

information from the periphery (Sato and Choi, 2021; Severini and Zych, 2022). These adjustments are observed in the walking parameters indicating intralimb coordination such as the stance time and stride length (Reisman et al., 2005; Morton and Bastian, 2006). For example, stance time symmetry exhibits rapid changes when walking conditions are altered and remains almost constant throughout each condition (Fig. 1-12). Unlike predictive feedforward adaptation, slow changes during the split-belt condition and the aftereffect after the split-belt condition are not observed (Fig. 1-11 and 1-12).

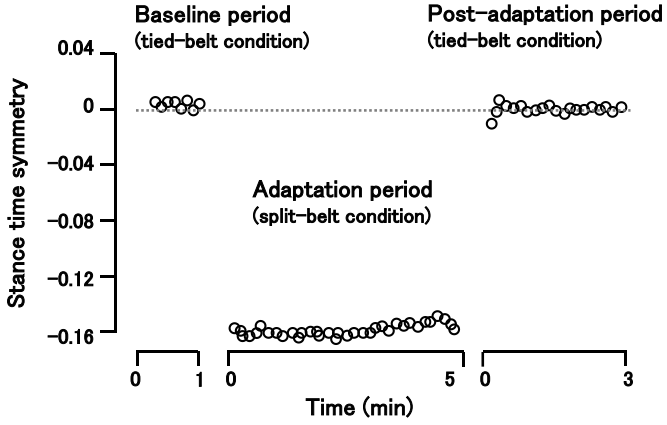

Figure 1-12 Typical example of time-series changes in averaged stance time symmetry among participants throughout the split-belt treadmill paradigm
A belt speed ratio of 1:2 was used in this paradigm. Horizontal dashed line indicates that stance time in left and right limbs is equal (modified from Yokoyama et al., 2018).

Summary of biomechanics in split-belt locomotor adaptation

Predictive feedforward adaptation and reactive feedback adjustment in split-belt locomotor adaptation are reflected by different walking parameters (i.e., interlimb parameters and intralimb parameters). These distinct adaptation processes are hypothesized to be controlled by different neural structures. The following section provides an overview of neural control of split-belt locomotor adaptation.

1-2.5. Neural control of split-belt locomotor adaptation

This section reviews the neural structures that may be involved in a split-belt locomotor adaptation based on lesions, electrophysiological, neuromodulation, and brain imaging studies.

Spinal cord

To date, many studies have reported that neurological impairment at the supraspinal level such as the cerebellum and cerebrum does not disrupt reactive feedback adjustment in stride length and stance time (see following subsections) (Morton and Bastian, 2006; Choi and Bastian, 2007; Reisman et al., 2007; Vasudevan et al., 2014). For example, it has been reported that the patients with cerebral or cerebellar damage show a quick decrease and increase in stance time in the limbs on the faster and slower belts, respectively, immediately after exposure to the split-belt condition, as do healthy participants (Morton and Bastian, 2006; Reisman et al., 2007). The adjusted stance time persisted throughout the split-belt condition. When returning to the tied-belt condition, the stance time was quickly adjusted again and then returned to the baseline levels. Therefore, the spinal circuit, rather than the supraspinal structures, may possess sufficient ability to make reactive feedback adjustments.

Cerebellum

The cerebellum plays a critical role when modifying movements based on error information (Bastian, 2006). Previous lesion studies have reported that split-belt locomotor adaptation is impaired in individuals with cerebellar damage (Morton and Bastian, 2006). Specifically, healthy participants were able to correct step length asymmetry over the course of the split-belt condition and then showed an aftereffect, whereas patients with cerebellar damage showed minimal improvement of step length

asymmetry and only a small aftereffect. Furthermore, double support time asymmetry was also not fully corrected in the patients. It has also been reported that the extent of impairment of split-belt locomotor adaptation is associated with the degree of cerebellar damage (Morton and Bastian, 2006; Statton et al., 2018).

A previous study investigating the role of the cerebellum on the split-belt locomotor adaption using TMS reported that adaptation to split-belt condition was associated with depressed cerebellar excitability [i.e., reduction in cerebellar brain inhibition (CBI)] (Jayaram et al., 2011). This study also showed that the degree of reduction in the CBI correlated with the extent of adaptation to the split-belt condition. These findings strongly suggest an involvement of the cerebellum in split-belt locomotor adaptation. On the other hand, using transcranial direct current stimulation (tDCS), some studies have investigated the effect of neuromodulation of the cerebellum on split-belt locomotor adaptation. tDCS is a non-invasive brain stimulation method capable of modulating the excitability of underlying cortical tissue in polarity specific manner (Nitsche and Paulus, 2000). In general, cathodal stimulation and anodal stimulation have been considered to induce a decrease and increase in cortical excitability, respectively. Jayaram et al. (2012) reported that anodal tDCS over the cerebellum accelerated the predictive feedforward adaptation in the split-belt condition compared with sham stimulation and cathodal tDCS. Conversely, Kumari et al. (2020) recently reported that the anodal tDCS over the cerebellum did not affect the predictive feedforward adaptation in the split-belt condition. Hence, because there are no consistent results, further studies would be needed to show the importance of the cerebellum for split-belt locomotor adaptation in terms of neuromodulation.

Based on these findings from clinical and electrophysiological studies, the cerebellum contribution is thought to be great in the predictive feedforward adaptation in split-belt locomotor

adaptation. In addition, a recent neuroimaging study indicated the importance of the inferior cerebellar peduncle, which connects the cerebellum and olivary nucleus, in split-belt locomotor adaptation (Jossinger et al., 2020).

Cerebrum

There is mixed evidence about the role of the cerebrum in split-belt locomotor adaptation. Bastian and colleagues observed that patients with focal cerebrum damage due to stroke showed predictive feedforward adaptation and aftereffects similar to that of healthy participants (Reisman et al., 2007, 2009). Given their results, cerebral contribution to the split-belt locomotor adaptation seems to be minor. Conversely, Tyrell et al. (2014) reported that the rate of predictive feedforward adaptation to the split-belt condition was slowed in patients with stroke compared with healthy participants. Additionally, another study by Choi et al. (2009) on patients whose cerebral hemisphere was completely removed in surgery showed that predictive feedforward adaptation in the split-belt condition and aftereffects were partially impaired. Therefore, cerebral contribution to split-belt locomotor adaptation cannot be ruled out.

On the other hand, some researchers investigated the effect of dual tasks requiring cognitive processing on split-belt locomotor adaptation. The results showed that the imposition of dual tasks slowed predictive feedforward adaptation to the split-belt condition (Malone and Bastian, 2010; Conradsson et al., 2019). This implies that split-belt locomotor adaptation was inhibited by the devotion of cerebral cognitive resources to the dual task, supporting the idea that the cerebrum is involved in split-belt locomotor adaptation.

Then, is the excitability of the cerebrum, especially the motor cortex, modulated in

association with the split-belt locomotor adaptation? To my knowledge, one study only addressed this question using TMS and showed that the excitability of the motor cortex was enhanced with the adaptation to the split-belt condition (Jayaram et al., 2011). However, this modulation of the excitability was also observed with a complex walking task in which the walking speeds change every few seconds in tied-belt condition, not an adaptation task. Hence, the modulation of excitability in the motor cortex might not be adaptation-specific and be due to the complexity of walking tasks. It should be noted that although the previous study used the MEPs to evaluate the excitability of the motor cortex, the amplitudes of MEPs also include the modulation of excitability in spinal motoneurons.

Recently, Young et al. (2020) used tDCS to investigate whether the neuromodulation to the PPC in the cerebrum affects the split-belt locomotor adaptation. They found that the predictive feedforward adaptation was impaired when cathodal and anodal tDCS were applied over the left and right PPC, respectively, compared with the sham condition. From the findings, they have remarked that the left PPC, which has been implicated in the creation of internal representation and integration of various sensory information, may play an important role in split-belt locomotor adaptation.

Taken together, although there is still conflicting evidence, the cerebrum is thought to be involved in the predictive feedforward adaptation in the split-belt locomotor adaptation.

Summary of neural control in split-belt locomotor adaptation

As reviewed, multiple neural structures contribute to split-belt locomotor adaptation. Specifically, the supraspinal center and the spinal cord have been suggested to be involved in the predictive feedforward adaptation and reactive feedback adjustment in the split-belt locomotor adaptation, respectively. Recently, not only the specific brain regions involved in the split-belt locomotor adaptation but also

the role of the neural network between the brain regions (e.g., the cerebellum-thalamus-motor cortex) in the split-belt locomotor adaptation has been uncovered with the development of the neuroimaging technique (Mawase et al., 2017). Hence, although there are still questions that need to be clarified, our knowledge of neural control in split-belt locomotor adaption is being accumulated (Hinton et al., 2020; Sato and Choi, 2021; Severini and Zych, 2022).

1-3. Purpose and outline of thesis

The role of each neural structure in the two distinct adaptation processes in the split-belt locomotor adaptation (i.e., predictive feedforward adaptation and reactive feedback adjustment) seems to be gradually being understood. However, previous lesion, electrophysiological, and neuroimaging studies have not provided findings regarding neural control in the course of split-belt locomotor adaptation. Therefore, neural control during split-belt locomotor adaptation is still not fully understood. In particular, our comprehension of how the CNS controls muscle activities during split-belt locomotor adaptation is limited. Therefore, the present thesis aimed to clarify neuromuscular control during split-belt locomotor adaptation by resolving the following research questions.

- Does the descending drive through the corticospinal tract change in the course of split-belt locomotor adaptation?
- How does the CNS control activities of multiple muscles in the course of split-belt locomotor adaptation?

To answer each research question, two separate studies, Study 1 and 2, were undertaken. The computational methods that have been used to noninvasively investigate neuromuscular control during walking (i.e., EMG-EMG coherence and muscle synergy analyses) were adopted in each study.

Therefore, the specific research contents are as follows.

- Study 1 (Chapter 2): Investigation of time-series changes in EMG-EMG coherence in a lower-limb muscle during split-belt locomotor adaptation
- Study 2 (Chapter 3): Investigation of time-series changes in muscle synergies in lower-limb muscles during split-belt locomotor adaptation

The completion of these two studies is academically significant as it expands our understanding of neuromuscular control during split-belt locomotor adaptation. Furthermore, these findings are clinically and socially significant as they may be fundamental knowledge to interpret and discuss locomotor adaptability of individuals poststroke and older people.

Chapter 4 will discuss neural control of split-belt locomotor adaptation, combining previous research and findings obtained from Study 1 and 2. In addition, this chapter will describe limitation of this thesis, future direction of split-belt locomotor adaptation study, and implications to walking rehabilitation and sports science. Finally, Chapter 5 will remark conclusion of this thesis.

Chapter 2: Study 1
Time-series changes in intramuscular coherence associated with split-belt treadmill adaptation in humans

This study has been published as: Oshima, A., Wakahara, T., Nakamura, Y., Tsujiuchi, N., and Kamibayashi, K. Time-series changes in intramuscular coherence associated with split-belt treadmill adaptation in humans. Experimental Brain Research, 239, pp. 2127-2139, 2021

2-1. Introduction and purpose

Walking is a fundamental movement in humans and is a highly automated behavior involving many muscle activities (Dietz, 2002; Nielsen, 2003). The basic neural control for walking is concerned with descending commands from the brain and the CPGs in the spinal cord (Yang and Gorassini, 2006). In addition, reactive (feedback) and predictive (feedforward) controls in the CNS are important in flexibly modifying walking patterns to meet the demands of various environments (Sinkjaer et al., 1996; Bastian, 2006). Regarding the reactive control, the facilitated stretch reflex pathway in the spinal cord during walking may function to stabilize the ankle joint at the heel strike (Nakazawa et al., 2004) and may contribute to stable locomotion. In contrast, the cerebellum may play a role in predictive control (Bastian, 2006). In patients with damage to the cerebellum, the parameters of walking, such as step length, were not adjusted under a novel walking condition (Morton and Bastian, 2006).

A split-belt treadmill is a useful experimental apparatus for studying locomotor adaptation (Reisman et al., 2005; Malone and Bastian, 2010; Vasudevan and Bastian, 2010; Bruijn et al., 2012; Jayaram et al., 2012; Ogawa et al., 2014; Yokoyama et al., 2018). This apparatus has two belts controlled separately and can generate a novel walking environment in which the belt speeds in the

right and left legs are different (i.e., split-belt condition). Previous studies have shown that step length symmetry became asymmetric during the initial phase of split-belt walking compared to normal walking (Reisman et al., 2005; Jayaram et al., 2012). However, the step length symmetry gradually approached symmetry during split-belt walking for several minutes. Similarly, the anterior component of the GRF (braking force) also changed slowly during split-belt walking (Ogawa et al., 2014; Yokoyama et al., 2018). These adjustments of walking motion are called locomotor adaptation, which is considered to be an error-driven motor learning process (Torres-Oviedo et al., 2011). This adaptation may occur by reducing the error signal that may be caused by asymmetric movement between the legs in split-belt walking. The cerebellum, which calibrates an internal model, may play a critical role in locomotor adaptation (Morton and Bastian, 2006). In addition, it has been reported that the cerebrum might also contribute to modifying the walking pattern (Choi et al., 2009). Subsequently, when returning to the belt condition in which two belts move at the same speed (i.e., tied-belt condition), the step length symmetry and the anterior component of the GRF showed a robust aftereffect (Reisman et al., 2005; Ogawa et al., 2014). This phenomenon indicates that the CNS learned a new walking pattern suitable for the novel walking environment (Helm and Reisman, 2015).

However, the knowledge based on walking parameters, as described above, is not sufficient to discuss the neural control underlying split-belt locomotor adaptation. Therefore, it would be more important to focus on EMG signals that reflect neural control commands. Although some previous studies using EMG signals have investigated changes in timing, patterns, and levels of individual muscle activities in the lower limb during and after split-belt walking (Dietz et al., 1994; Maclellan et al., 2014; Ogawa et al., 2014), detailed neural control for adaptation to split-belt walking and de-adaptation after split-belt walking is still unclear. Investigating coherence between paired EMG signals

recorded from the lower limb muscles would contribute to further understanding the neural control of locomotor adaptation. Coherence analysis is a mathematical analysis method that estimates the strength of correlation at a specific frequency component between two signals recorded simultaneously (Farmer et al., 1993; Halliday et al., 1995). A coherence (EMG-EMG coherence) analysis using paired EMG signals recorded from two parts over one muscle (e.g., proximal and distal parts of the TA muscle) or two different muscles (e.g., synergistic muscles) has been defined as an intramuscular or intermuscular coherence analysis, respectively. A previous study proposed that EMG-EMG coherence analysis can explore the frequency component and strength of the common synaptic drives to different motoneuron pools during walking (Halliday et al., 2003).

For the frequency domain, the intramuscular coherence between paired EMG signals recorded from two parts over the TA muscle during walking in healthy participants has been observed in beta (15–35 Hz) and gamma (35–60 Hz) bands (Halliday et al., 2003; Jensen et al., 2018; Spedden et al., 2019). On the other hand, it has been reported that intramuscular coherence in these frequency bands during walking in neurological patients with incomplete SCI (Hansen et al., 2005; Barthélemy et al., 2010) and stroke (Nielsen et al., 2008; Kitatani et al., 2016) was obviously lower than that in healthy participants. Moreover, intermuscular coherence in the beta band during isometric contraction increased following the facilitation of cortical excitability by anodal tDCS over the primary motor cortex (Power et al., 2006). Hence, these results indicate that EMG-EMG coherence in the beta and gamma bands reflects cortical involvement, such as descending drive from the primary motor cortex to the motoneurons during motor tasks. It has also been reported that intramuscular coherence is modulated depending on the difficulty of motor tasks in healthy participants. For instance, intramuscular coherence in the beta and gamma bands during visually guided treadmill walking

(precision stepping task) was significantly higher than that during normal treadmill walking (Jensen et al., 2018). Thus, it is likely that an increase in intramuscular coherence in the beta and gamma bands is related to an increased cortical contribution.

Based on the results of these previous studies, intramuscular coherence is expected to change during and after split-belt walking. Sato and Choi (2019) have already investigated the changes in intramuscular coherence during and after split-belt walking and showed interesting results that intramuscular coherence in the TA muscle was significantly higher at the beginning of split-belt walking than during normal treadmill walking before split-belt walking. Subsequently, intramuscular coherence was significantly lower in the late phase than at the beginning of split-belt walking. However, they only showed the results at the initial and late phases of split-belt walking and normal treadmill walking after split-belt walking. Hence, although many previous studies on locomotor adaptation have shown the time-series changes in the walking parameters, such as step length symmetry and double support time (Reisman et al., 2005; Bruijn et al., 2012), it has not yet been clarified how intramuscular coherence changes during split-belt walking and during tied-belt walking following split-belt walking.

Therefore, this study aimed to investigate the time-series changes in intramuscular coherence in the TA muscle associated with split-belt locomotor adaptation. In particular, we focused on the manner of changes in intramuscular coherence during and after split-belt walking. Choi et al. (2009) reported that the cerebrum might be involved in adjustment of walking parameter, such as a double support time, which became symmetric gradually throughout the split-belt walking. Therefore, we hypothesized that involvement of the cerebral cortex would gradually weaken during split-belt walking; that is, intramuscular coherence in the beta and gamma bands would gradually decrease

during split-belt walking. In addition, when returning to the tied-belt condition after split-belt walking, it has been reported that the walking pattern became asymmetric again (Reisman et al., 2005). Therefore, it is assumed that cortical control is needed again to revert the walking pattern from asymmetric to normal. Thus, intramuscular coherence would increase at the beginning of normal walking following split-belt walking. The present results would provide new insights into the cortical control in locomotor adaptation.

2-2. Methods

Participants

Twelve healthy young men (age 21.1 ± 1.0 years) participated in this study. We excluded participants with any neurological or orthopedic impairments. All participants provided written informed consent prior to the start of the study. All procedures were approved by the Doshisha University Research Ethics Review Committee regarding Human Subject Research (Approval No. 18045), and this study was performed in accordance with the Declaration of Helsinki. None of the participants had prior walking experience on a split-belt treadmill.

Experimental protocol

Participants were asked to walk on a split-belt treadmill (Tec Gihan Co., Ltd.) with two belts controlled separately by an independent motor. During the experiment, the treadmill was operated in either a tied-belt condition (i.e., two belts moving at the same speed) or split-belt condition (i.e., two belts moving at different speeds). In both belt conditions, the belts moved from front to back. The belt speed was set at 0.5 m/s (slow) or 1.25 m/s (fast). Figure 2-1A shows the experimental paradigm, which is a

typical paradigm used in split-belt treadmill research (Reisman et al., 2005). The experiment started with a familiarization period which was the tied-belt condition at 0.5 and 1.25 m/s for 2 min each. Subsequently, the baseline period was the tied-belt condition at 0.5 m/s for 2 min. The adaptation period was the split-belt condition with the left belt at 0.5 m/s and the right belt at 1.25 m/s for 10 min (belt speed ratio of 1:2.5). Thus, the leg moving faster during the adaptation period was assigned to the right leg in all participants. In this assignment, the dominant leg of each participant was not considered. We defined the leg on the slow or fast belt during the adaptation period as the "slow leg" or "fast leg," respectively. In the post-adaptation period, the belt condition was again the tied-belt at 0.5 m/s for 6 min to assess the aftereffect following the split-belt walking and its washout. Throughout the experiment, the belts were not stopped, and changes in the belt speed between periods were performed with acceleration or deceleration of 0.15 m/s^2. Participants were informed verbally about the next belt speed approximately 10 s before the actual belt speed change by an experimenter during walking. They were also instructed to look at an X mark on a wall approximately 2.4 m ahead from the treadmill and to refrain from looking down as much as possible while walking. For safety, one experimenter stood by the treadmill during the experiment and an emergency button was installed within the reach of the participant and experimenter.

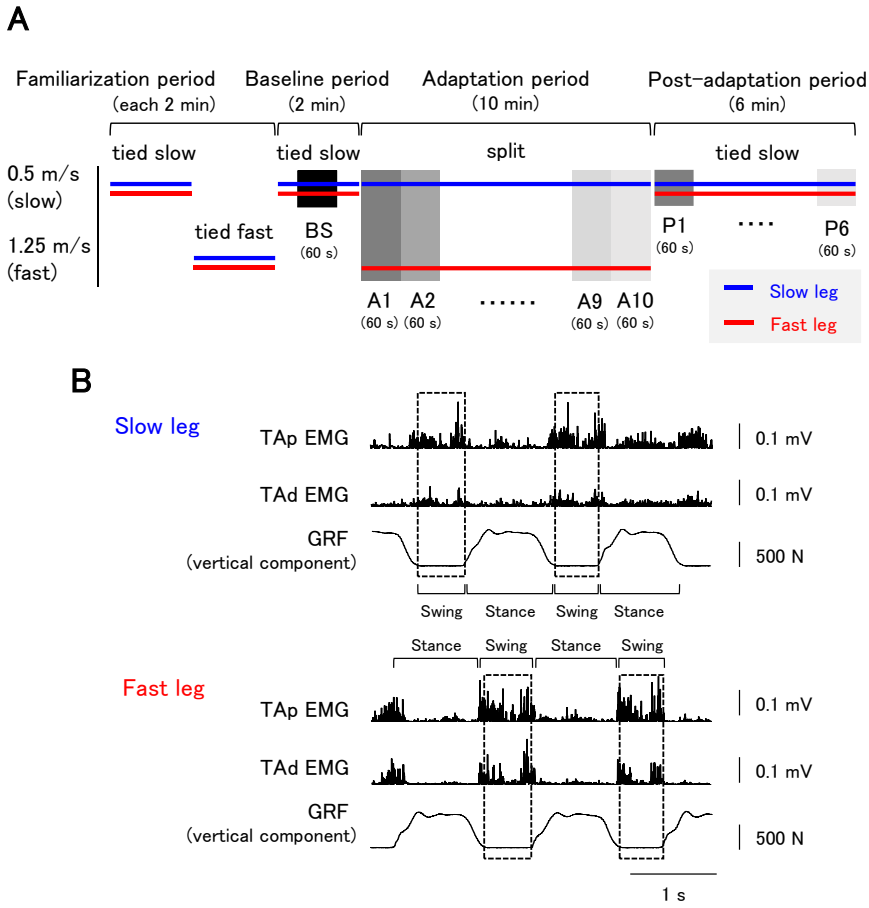

Figure 2-1 (A) Experimental paradigm and statistical analysis sections (tied: two belts moving at the same speed, split: two belts moving at different speeds)
The blue and red horizontal lines depict the slow and fast legs, respectively. Each rectangle in the baseline, adaptation, and post-adaptation periods represents the statistical analysis section for 60 s (BS, A1–10, and P1–6). (B) Typical waveforms of the rectified electromyography (EMG) in the proximal and distal parts of the tibialis anterior (TAp and TAd, respectively) muscle and the vertical component of the ground reaction force (GRF) in each leg at BS from one participant
The areas surrounded by dashed lines are the epochs used to calculate the EMG activity level and intramuscular coherence (TAp–TAd)

Data collection

Surface EMG electrodes (Trigno Wireless System, Delsys Inc.) were placed over the proximal and distal parts of the TA muscle (TAp and TAd) in each leg. The bandwidth of the EMG electrodes was

10–850 Hz. The locations of the electrodes for the TAp and TAd were 20% and 55% of the lower leg length between the lateral knee joint space (0%) and the lateral malleolus (100%), respectively. Before placement of the electrodes, the skin was lightly rubbed with fine sandpaper and cleaned with alcohol swabs to reduce impedance. The recorded EMG signals were amplified (with a 300-gain preamplifier) before further amplification (total effective gain of 909) and stored on a computer for later analyses after A/D conversion at 2000 Hz of a sampling frequency (PowerLab 16/35, AD Instruments Inc.). The vertical component of the GRF data measured from the force plate mounted underneath each belt was recorded and sampled at 2000 Hz with the EMG signals simultaneously.

Data analyses

From the vertical component of the GRF, the instants of the heel strike and toe-off during walking were detected (threshold: 10 N), and the averages of the stance (from the heel strike of one leg to the subsequent toe-off of the same leg) and swing (from the toe-off of the one leg to the subsequent heel strike of the same leg) durations at each analysis section (see “Statistical analyses”) were calculated (Fig. 2-1A).

Muscle activity levels in the TAp and TAd during the swing phase at each analysis section were quantified by calculating the root mean square (RMS) value. Data processing and analyses were performed using custom programs written in MATLAB (MathWorks Inc.).

Coherence analysis was performed to describe the frequency domain coupling between TAp and TAd EMG signals using MATLAB functions from NeuroSpec software (http://www.neurospec.org) (Halliday et al., 1995). An epoch used for coherence analysis was the entire swing phase (Fig. 2-1B). All epochs included in each analysis section (60 s each) were used for

the analysis. The EMG signals in each epoch were passed through a Tukey window to reduce the waveform discontinuity at the joins between epochs and concatenated without overlapping (Norton and Gorassini, 2006). For coherence analysis, the EMG data were full-wave rectified.

The intramuscular coherence between paired rectified EMG signals recorded from the TAp and TAd (x and y) was defined at frequency i according to the following equation:

$$\left|R_{xy}(i)\right|^2 = \frac{\left|f_{xy}(i)\right|^2}{f_{xx}(i)f_{yy}(i)}$$

In this equation, $f_{xx}(i)$ and $f_{yy}(i)$ are the values of the power spectra of x and y at frequency i. $f_{xy}(i)$ is the value of the cross spectrum between x and y at frequency i and is estimated in a similar manner to the auto-spectrum. The values were estimated by a periodogram approach using a fast Fourier transform algorithm with a non-overlapping Hanning window in each segment of 1024 points. A frequency resolution was approximately 1.95 Hz (2000 sampling rate/1024 points). These periodograms were then averaged across all segments. The coherence between x and y was calculated as the ratio of the squared magnitude of the cross spectrum to the product of the power spectra. The coherence functions provided normative measures of linear association on a scale from 0 to 1. Zero signifies that the two signals are completely independent at that frequency, and 1 signifies that the two signals have a perfect linear relationship at that frequency (Halliday et al., 1995). The upper 95% confidence limit for individual coherence was given by the following equation:

$$1 - (\alpha)^{\frac{1}{L-1}}$$

where α is the significance level (0.05) and L is the number of segments used for the coherence analysis (Halliday et al., 1995) (see horizontal dashed lines in Fig. 2-4). In the present study, to quantitatively evaluate changes in intramuscular coherence during walking, the values of the cumulative sum (i.e., area) under the coherence curve in the beta (15–35 Hz) and gamma (35–60 Hz) bands at each analysis section were calculated (Kitatani et al., 2016; Jensen et al., 2018; Sato and Choi, 2019). The values were defined as the amount of intramuscular coherence in the present study.

Statistical analyses

Statistical analyses were performed for each variable (stance and swing durations, EMG RMS value, and amount of intramuscular coherence). The analysis sections for the statistics were one section for 60 s from 30 s after the baseline period start (BS), 10 sections divided into every 60 s in the adaptation period (A1–10), and six sections divided into every 60 s in the post-adaptation period (P1–6) (Fig. 2-1A). In the present study, since we focused on how the intramuscular coherence changes during split-belt walking, the values in each variable during the adaptation period were compared with those in the first analysis section in the adaptation period (A1). On the other hand, the values of each variable in the post-adaptation period were compared with those in the baseline period (BS) to investigate the aftereffect following split-belt walking and washout. The collected data were checked using the Shapiro-Wilk test to assess the normality of distribution. If the data in each section for each statistical analysis (i.e., A1–10 for the adaptation period or BS and P1–6 for the post-adaptation period) were normally distributed, a one-way analysis of variance (ANOVA) test was conducted. When statistical significance was found using ANOVA, Dunnett's multiple comparison tests were used to test for

differences between the A1 and the other adaptation sections (A2–10) as well as between the BS and the post-adaptation sections (P1–6). If the data were not normally distributed, a non-parametric Friedman test was conducted. When statistical significance was found using the Friedman test, the Wilcoxon signed-rank sum test with *P* values adjusted by Holm's method was used to test for differences between sections. All statistical analyses were performed using SPSS 26.0 (IBM). Statistical significance was set at $P < 0.05$. Data are presented as mean ± standard deviation (SD).

2-3. Results

Stance and swing durations

Figure 2-2 shows the time-series changes in stance and swing durations in the slow and fast legs. Regarding the adaptation period, the one-way ANOVA test indicated that the section difference was significant in the stance duration of the slow leg ($F_{2.69, 29.68} = 3.81$, $P < 0.05$) (Fig. 2-2A), and Dunnett's multiple comparison tests revealed that the stance duration from A5 to A10 was significantly longer than that at A1 (all $P < 0.05$). The Friedman test indicated that the section difference was significant in the swing duration of the slow leg [Chi^2 (df = 9) = 77.67, $P < 0.01$]. The Wilcoxon signed-rank sum test revealed that the swing duration at the adaptation sections from A2 was significantly longer than that at A1 (all $P < 0.05$). As for the fast leg in the adaptation period, the section difference was significant in both stance and swing durations [Chi^2 (df = 9) = 81.43, 22.38, both $P < 0.01$] (Fig. 2-2B). The stance duration at the adaptation sections from A2 was significantly longer than that at A1 (all $P < 0.05$), while the swing duration at A10 was significantly longer than that at A1 ($P < 0.05$).

On the other hand, for the baseline and post-adaptation periods, the ANOVA test indicated that the section difference was significant in the swing duration of the fast leg ($F_{4.56, 50.17} = 2.65$, $P <$

0.05) (Fig. 2-2D). The swing duration in the fast leg at P1 was significantly shorter than that at BS (P < 0.05). A significant main effect was found in the stance duration in the slow leg ($F_{2.88, 31.73}$ = 3.05, P < 0.05) (Fig. 2-2C), but Dunnett's multiple comparison tests did not reveal a significant difference (all P > 0.05). In the swing duration in the slow leg and stance duration in the fast leg, no significant main effects were found [swing (slow leg): $F_{3.01, 33.20}$ = 2.24, P > 0.05; stance (fast leg): $F_{2.95, 32.50}$ = 1.63, P > 0.05] (Fig. 2-2C and D).

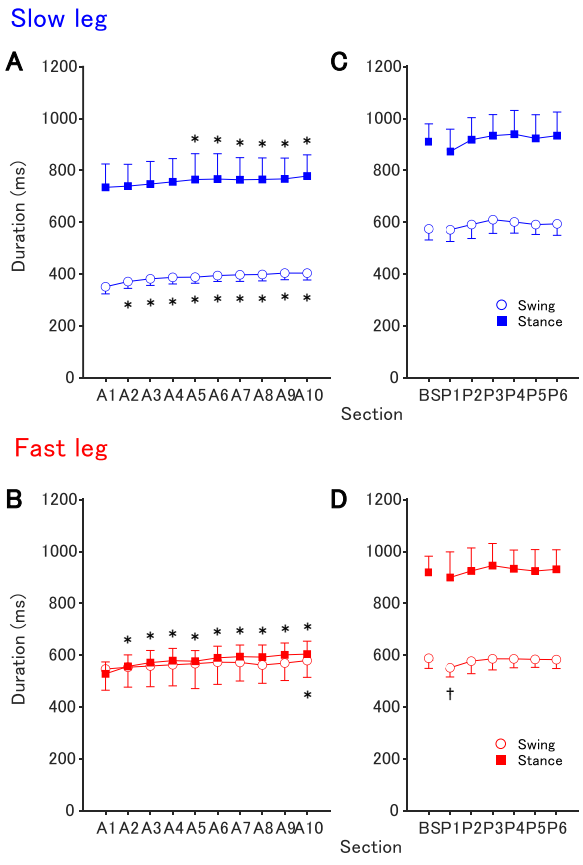

Figure 2-2 Time-series changes in the stance and swing durations in the slow leg (A and C) and fast leg (B and D)
The circle and square depict the swing and stance durations, respectively. The left (A and B) and right (C and D) sides denote the swing and stance durations in the split-belt [adaptation period (A1–10)] and tied-belt [baseline (BS) and post-adaptation periods (P1–6)] conditions, respectively. Each plot represents the mean from all participants and the error bar indicates the standard deviation (SD). *P < 0.05 versus A1. †P < 0.05 versus BS

Muscle activity levels

Figure 2-3 shows the time-series changes in the muscle activity levels of TAp and TAd in the slow and fast legs. For the adaptation period, section differences were significant in the TAp and TAd muscle activity levels in the slow leg [TAp: $F_{2.36, 26.04}$ = 20.46, P < 0.01; TAd: Chi^2 (df = 9) = 55.14, P < 0.01]

(Fig. 2-3A). Subsequent multiple comparison tests revealed that the activity levels in the TAp and TAd in the slow leg at all adaptation sections from A2 were significantly lower than those at A1 (all $P < 0.05$). In contrast, the muscle activity levels in the TAp and TAd of the fast leg did not show significant main effect differences [TAp: Chi^2 (df = 9) = 6.72, $P > 0.05$; TAd: $F_{3.00, 33.01} = 0.78$, $P > 0.05$] (Fig. 2-3B).

Regarding the baseline and post-adaptation periods, the respective muscle activity levels in the TAp and TAd were not significantly different among sections in both legs [TAp (slow leg): $F_{1.98, 21.77} = 0.28$, $P > 0.05$; TAd (slow leg): Chi^2 (df = 6) = 7.71, $P > 0.05$; TAp (fast leg): Chi^2 (df = 6) = 11.85, $P > 0.05$; TAd (fast leg): Chi^2 (df = 6) = 11.96, $P > 0.05$] (Fig. 2-3C and D).

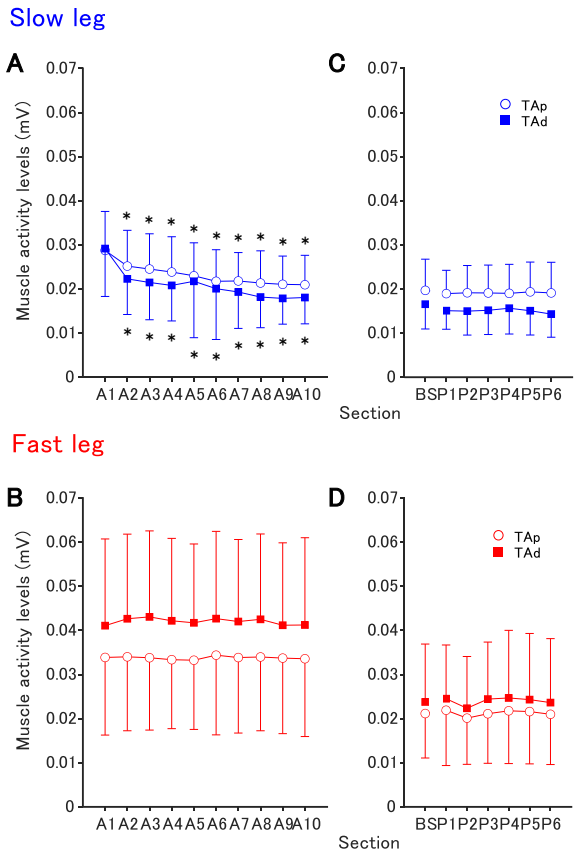

Figure 2-3 Time-series changes in the muscle activity level during the swing phase in the proximal and distal parts of the tibialis anterior (TAp and TAd) muscles in the slow leg (A and C) and fast leg (B and D)
The circle and square depict the TAp and TAd muscle activity levels, respectively. The left (A and B) and right (C and D) sides denote the muscle activity levels in the split-belt [adaptation period (A1–10)] and tied-belt [baseline (BS) and post-adaptation periods (P1–6)] conditions, respectively. Each plot represents the mean from all participants and the error bar indicates the standard deviation (SD). *$P < 0.05$ versus A1

Intramuscular coherence

Figure 2-4 depicts typical patterns of intramuscular coherence (TAp-TAd) at A1, A4, A7, A10, BS, P1, P3, and P6 from one participant. In these sections, significant coherence in the beta and/or gamma bands was observed. Some significant peaks of the intramuscular coherence in the beta and gamma bands in the slow leg during the adaptation period were higher at A1, particularly at approximately 16, 30, and 37 Hz (Fig. 2-4A). In addition, significant peaks of intramuscular coherence in the beta and gamma bands in the fast leg at P1 were higher than those at BS (Fig. 2-4D). In particular, peaks were observed at approximately 18, 47, and 55 Hz. On the other hand, the intramuscular coherence was similar among sections in the fast leg during the split-belt condition (Fig. 2-4B) and among sections in the slow leg during the tied-belt condition (Fig. 2-4C).

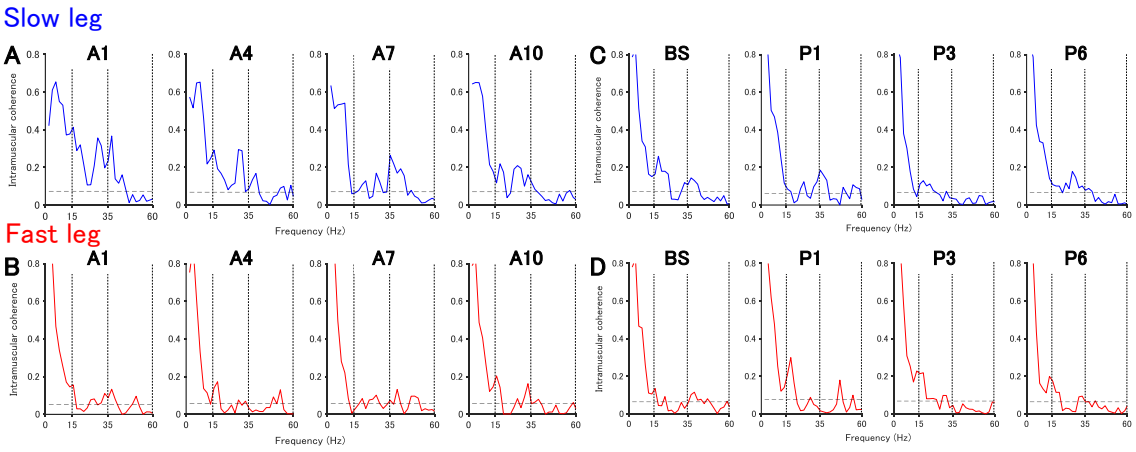

Figure 2-4 Typical intramuscular coherence (TAp-TAd) in the slow leg (A and C) and fast leg (B and D) from one participant

The left (A and B) and right (C and D) figures depict typical examples of intramuscular coherence in the split-belt [adaptation period (A1, A4, A7, and A10)] and tied-belt [baseline (BS) and post-adaptation periods (P1, P3, and P6)] conditions, respectively. The horizontal dashed lines indicate the upper 95% confidence limit and the vertical dotted lines indicate the frequency range of the beta (15–35 Hz) and gamma (35–60 Hz) bands

Amount of intramuscular coherence

The time-series changes in the amount of intramuscular coherence (TAp-TAd) in the beta and gamma bands in the slow and fast legs are shown in Figure 2-5. With regard to the slow leg during the adaptation period, the ANOVA test indicated that the section difference was significant in the amount of intramuscular coherence in the beta band ($F_{5.61, 61.76} = 2.58$, $P < 0.05$) (Fig. 2-5A). The amount of intramuscular coherence in the beta band at A7, A8, A9, and A10 was significantly smaller than that at A1 (all $P < 0.05$). In addition, the Friedman test showed a significant main effect on the amount of intramuscular coherence in the gamma band in the slow leg [Chi^2 (df = 9) = 18.14, $P < 0.05$] (Fig. 2-5A). The amount of intramuscular coherence in the gamma band at A10 was also significantly smaller than that at A1 ($P < 0.05$). In contrast, the Friedman test revealed no significant main effect for the beta band in the fast leg [Chi^2 (df = 9) = 9.10, $P > 0.05$] (Fig. 2-5B). For the gamma band in the fast leg, although the Friedman test showed a significant main effect [Chi^2 (df = 9) = 22.58, $P < 0.05$] (Fig. 2-5B), subsequent multiple comparison tests did not reveal a significant difference between A1 and the other adaptation sections.

Regarding the slow leg in the baseline and post-adaptation periods, there were no significant main effects on the amount of intramuscular coherence in both beta and gamma bands [beta: $F_{3.34, 36.82} = 1.35$, $P > 0.05$; gamma: Chi^2 (df = 6) = 11.64, $P > 0.05$] (Fig. 2-5C). In contrast, for the fast leg, the ANOVA test for the beta band and the Friedman test for the gamma band revealed significant main effects [beta: $F_{6, 66} = 4.89$, $P < 0.01$; gamma: Chi^2 (df = 6) = 24.28, $P < 0.01$] (Fig. 2-5D). Subsequent multiple comparison tests indicated that the amount of intramuscular coherence in both beta and gamma bands in the fast leg at P1 was significantly larger than that at BS (all $P < 0.05$).

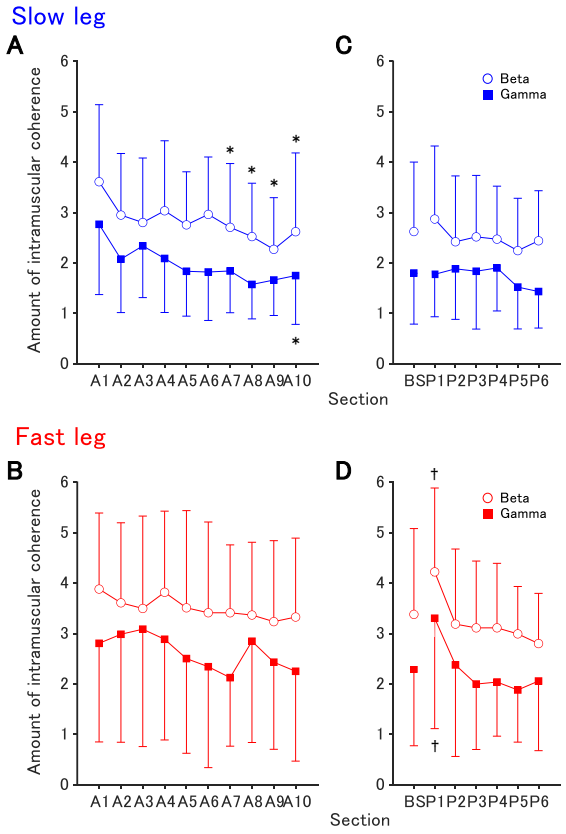

Figure 2-5 Time-series changes in the amount of intramuscular coherence (TAp–TAd) in the slow leg (A and C) and fast leg (B and D)
The circle and square depict the amount of intramuscular coherence in the beta (15–35 Hz) and gamma (35–60 Hz) bands, respectively. The left (A and B) and right (C and D) sides denote the amount of intramuscular coherence in the split-belt [adaptation period (A1–10)] and tied-belt [baseline (BS) and post-adaptation periods (P1–6)] conditions, respectively. Each plot represents the mean from all participants and the error bar indicates the standard deviation (SD). *$P < 0.05$ versus A1. †$P < 0.05$ versus BS

2-4. Discussion

This study aimed to investigate the time-series changes in intramuscular coherence in the ankle dorsiflexor muscle associated with split-belt locomotor adaptation. In particular, we focused on the manner of changes in intramuscular coherence during and after split-belt walking. The main results of this study are as follows. The amount of intramuscular coherence in the slow leg at the adaptation sections from A7 (beta band) was significantly smaller than that at A1 (Fig. 2-5A). In addition, the amount of intramuscular coherence in both beta and gamma bands in the fast leg at P1 of the post-adaptation period was significantly larger than that at BS, and there were no differences between the BS and each post-adaptation section from P2 (Fig. 2-5D). Below, we discuss the time-series changes in the stance and swing durations, TA muscle activity levels, and amount of intramuscular coherence

during and after split-belt walking.

Time-series changes in stance and swing durations and TA muscle activity levels during and after split-belt walking

In the present study, we used the typical split-belt treadmill paradigm, which has been widely used in previous studies that investigated locomotor adaptation (Reisman et al., 2005; Malone and Bastian, 2010; Vasudevan and Bastian, 2010; Bruijn et al., 2012; Jayaram et al., 2012; Ogawa et al., 2014; Yokoyama et al., 2018). Therefore, it is thought that the gait behavior observed in the present study was comparable to that observed in previous studies.

Previous studies have reported that the step length symmetry and anterior component of the GRF changed slowly during split-belt walking (Reisman et al., 2005; Jayaram et al., 2012; Ogawa et al., 2014; Yokoyama et al., 2018). In contrast, it has been reported that some temporal walking parameters (e.g., stance duration) changed quickly at the beginning of split-belt walking and the changed values of the walking parameter remained constant during split-belt walking (Ogawa et al., 2014; Yokoyama et al., 2018). Similarly, in the present study, there were significant differences in swing duration in the slow leg and stance duration in the fast leg between A1 and A2 (Fig. 2-2A and B). Hence, these results suggest that the swing duration in the slow leg and stance duration in the fast leg were adjusted quickly in the initial phase of the split-belt condition.

Regarding the EMG activity levels in the slow leg during the adaptation period, activity levels in TAp and TAd at A1 were significantly higher than those in the other adaptation sections (A2–10) (Fig. 2-3A). This excessive TA muscle activity might have occurred in response to the sudden reduction of the swing duration in the slow leg due to the increased contralateral belt speed [from the

tied-belt condition (BS) to the split-belt condition] (Fig. 2-2A and C). In the shorter swing duration in the slow leg, quick dorsiflexion to avoid stumbling might be associated with increased muscle activity in the TA. On the other hand, TA muscle activity during the late swing is related to the adjustment of ankle stiffness toward the heel strike during walking (Capaday, 2002). Ogawa et al. (2014) indicated that the anterior component of the GRF (braking force) in the slow leg at the early adaptation period was larger than that at the late adaptation period. Thus, the impact of the heel strike in the slow leg might be larger in the early adaptation period. Therefore, since it might be necessary for the ankle joint to be stiffened to prepare for the large heel impact, the EMG activity level may have increased at A1. Subsequently, muscle activity levels gradually decreased (Fig. 2-3A), which was likely related to the adjustment of the ankle stiffness by adaptation (Ogawa et al., 2014). Regarding the EMG activity levels in the post-adaptation period, a robust aftereffect following split-belt walking was not observed in either leg (Fig. 2-3C and D). Participants may be able to adjust the ankle stiffness rapidly after a change in the belt condition, because the belt condition of the post-adaptation period was a tied-belt condition similar to normal walking. However, the activity levels of the antagonist muscles (i.e., ankle plantar flexor muscles) need to be considered to discuss the details of the adjustment of ankle stiffness during and after split-belt walking (De Luca and Mambrito, 1987).

Time-series changes in intramuscular coherence during and after split-belt walking

In the present study, there were significant coherence peaks in the beta and/or gamma bands during and after split-belt walking (Fig. 2-4) as observed in previous studies (Halliday et al., 2003; Barthélemy et al., 2010; Jensen et al., 2018). When focusing on the slow leg during the adaptation period, the amount of intramuscular coherence in the beta and gamma bands appears to gradually

decrease throughout the entire adaptation period (Fig. 2-5A), which is consistent with our hypothesis. From the results of statistical analyses, the amount of intramuscular coherence in the beta band from 6 min after exposure to the split-belt condition were significantly smaller than that at A1 (Fig. 2-5A). It has been found that patients with cerebellar damage could not adapt walking patterns during split-belt walking and showed little or no aftereffect in tied-belt walking just after split-belt walking (Morton and Bastian, 2006). Thus, adjustments of walking patterns may depend on an update of an internal model by the cerebellum (Morton and Bastian, 2006). In addition, a previous study by Choi et al. (2009) indicated that cerebral hemisphere damage disrupted adaptation in double support time during split-belt walking. Thus, it is thought that the cerebral cortex also functions to modify walking patterns. In healthy participants, the double support time rapidly became asymmetric just after exposure to the split-belt condition, and then gradually changed back toward the baseline values (i.e., symmetry) (Reisman et al., 2005). Hence, it is thought that the participants learned a new walking pattern, taking several minutes after exposure to the split-belt condition. For each participant, the new walking pattern may become a “new normal walking pattern” (Iturralde and Torres-Oviedo, 2019). Therefore, after the middle of the adaptation period in the present study, cortical involvement in the activity of the TA muscle in the slow leg might weaken notably compared with that at the beginning of the adaptation period.

On the other hand, when focusing on the post-adaptation period, the amount of intramuscular coherence in both beta and gamma bands in the fast leg at P1 was significantly larger than that at BS despite the same belt condition (Fig. 2-5D). This result supports our hypothesis. The increase in the amount of intramuscular coherence implies that cortical involvement increased at P1 compared to BS. In the initial phase of tied-belt walking just after split-belt walking, it has been reported that the double

support time became asymmetric (Reisman et al., 2005), indicating that the CNS learned a new walking pattern by split-belt walking (Helm and Reisman, 2015). Thus, it is considered that the increase in cortical involvement at P1 is associated with the correction of the asymmetric walking pattern to de-adapt to the normal walking pattern in daily life. However, there were no significant differences between the BS and each post-adaptation section from P2 (Fig. 2-5D). Hence, the extent of cortical involvement might return to the baseline level approximately 1 min after returning to the tied-belt condition. Since the left and right belt speeds in the condition in which participants walked after split-belt walking were the same (i.e., normal walking environment), it is thought that the intramuscular coherence quickly decreased at the initial phase of the post-adaptation period.

Taken together, these results provide the following novel findings. When adapting to the split-belt condition, the involvement of the cerebral cortex might decrease gradually for several minutes (Figs. 2-4A and 2-5A). On the other hand, when de-adapting from the “new normal walking pattern” (i.e., adapted walking pattern) to the normal walking pattern, the involvement of the cerebral cortex might increase temporarily and then decrease quickly (Figs. 2-4D and 2-5D). Although it has been suggested that cats with spinal cord transections could adapt to split-belt walking based on sensory inputs from peripheral mechanoreceptors located in the left and right hindlimbs that sense loading, pressure, and muscle length (Frigon et al., 2013), the cortical involvement for locomotion is assumed to be greater in humans than in cats and lower vertebrates (Nielsen, 2003). Thus, changes in cortical involvement may occur during and after split-belt walking in humans. On the other hand, although it has been proposed that the intramuscular coherence in the beta and gamma bands could reflect the neural drive from the cerebral cortex (Hansen et al., 2005; Nielsen et al., 2008), we could not exclude the possibility that the sensory input from the periphery and neural drive via descending

pathways other than the corticospinal pathway were reflected in the intramuscular coherence (Fisher et al., 2002; Kilner et al., 2004). Thus, there may be diversity in the origin of the signal included in the intramuscular coherence, which is important in interpreting our results. However, considering several previous studies using EMG-EMG coherence analysis (Hansen et al., 2005; Power et al., 2006; Nielsen et al., 2008; Barthélemy et al., 2010; Kitatani et al., 2016; Jensen et al., 2018; Sato and Choi, 2019), the time-series changes in the intramuscular coherence observed in the present study suggest that the cortical contribution to TA muscle changed in association with split-belt locomotor adaptation.

It is important to note that these phenomena of intramuscular coherence were specific to the leg assigned in the split-belt paradigm (i.e., in the slow leg during the adaptation period and in the fast leg during the post-adaptation period). The sequence of changes in the intramuscular coherence observed in the slow leg during the adaptation period was not observed in the fast leg (Fig. 2-5A and B). One possible explanation for this is that the contralateral belt speed in the slow leg was fast. In the adaptation period, the swing duration in the slow leg was shorter (approximately 390 ms) than that in the fast leg (approximately 570 ms) (Fig. 2-2A and B). Hence, a stronger contribution of the cerebral cortex to control the swing movement of the slow leg might be needed during the first several minutes of split-belt walking. Then, as the participants learned the swing movement appropriate to the split-belt condition and neural adaptation occurred, the amount of intramuscular coherence in the slow leg might decrease gradually. In contrast, throughout the post-adaptation period, the changes in the intramuscular coherence observed in the fast leg were not found in the slow leg (Fig. 2-5C and D). Therefore, when de-adapting to the normal walking pattern after split-belt walking, the increase in cortical involvement in the swing movement of the fast leg might be important. Although the swing duration in the fast leg was similar to that in the slow leg (approximately 560 ms in both legs) at the

beginning of the post-adaptation period (Fig. 2-2C and D), the participants may have felt that the contralateral belt (slow leg side) moved faster than the ipsilateral belt (fast leg side) immediately after the adaptation period because of the sensory recalibration induced by split-belt walking (Statton et al., 2018). Thus, cortical contribution to the TA muscle during the swing phase of the fast leg might increase at the initial post-adaptation period, which might result in a change in intramuscular coherence in the fast leg.

2-5. Conclusion

Our results suggest that cortical contribution to the ankle dorsiflexor muscle gradually decreases during split-belt walking. On the other hand, in tied-belt walking following split-belt walking, cortical contribution might increase temporarily and then decrease quickly. These phenomena of intramuscular coherence were specific to the leg assigned in the split-belt paradigm. The findings of the present study would contribute to the understanding of neural control underlying adaptation to various walking environments and the construction of a rational program for walking rehabilitation.

Chapter 3: Study 2
Modulation of muscle synergies in lower-limb muscles associated with split-belt locomotor adaptation

This study has been published as: Oshima, A., Nakamura, Y., and Kamibayashi, K. Modulation of Muscle Synergies in Lower-Limb Muscles Associated With Split-Belt Locomotor Adaptation. Frontiers in Human Neuroscience, 16, 852530, 2022

3-1. Introduction and purpose

Humans change their walking patterns flexibly and adapt to novel and challenging walking environments. The use of a split-belt treadmill provides one way to assess adaptability (Reisman et al., 2005; Choi and Bastian, 2007). This type of treadmill can impose a novel walking condition on participants in which the speed of the belts is different on the left and right sides (i.e., split-belt condition). As an indicator that reflects an adaptation during split-belt walking, step length symmetry, calculated as the difference between the step length of each leg, has been widely used in previous studies (Malone and Bastian, 2010; Bruijn et al., 2012; Yokoyama et al., 2018). In the case of healthy participants, step length symmetry becomes asymmetrical in the initial phase of the split-belt condition (Bruijn et al., 2012). Interestingly, after approximately 10 min of exposure to the split-belt condition, steps become symmetrical. When the belts return to the same speed (i.e., tied-belt condition), step asymmetry appears, before becoming symmetrical again. This series of adjustments in walking patterns has been called locomotor adaptation (Reisman et al., 2010). Thus, the split-belt treadmill is useful to understand the processes of adaptation and de-adaptation simultaneously in human locomotion, and to highlight the adaptability of the CNS to changes in the environment (Torres-Oviedo

et al., 2011; Helm and Reisman, 2015). Impaired split-belt locomotor adaptation has been observed in patients with neurological disorders, such as cerebellar damage (Morton and Bastian, 2006) and hemispherectomy (Choi et al., 2009), indicating that the supraspinal structures play a role in the split-belt locomotor adaptation (Hinton et al., 2020). However, how the CNS achieves split-belt locomotor adaptation remains an open question.

EMG-EMG coherence analysis has been used as one of the methods for non-invasive investigation of neural control in physical movements (Halliday et al., 2003; Danna-Dos-Santos et al., 2014; Kenville et al., 2020). This analysis is a mathematical method that measures similarity in the frequency domain between a pair of EMG signals, which provides information concerning a neural drive to the motoneuron pools during physical movement (Nielsen, 2002). In particular, it has been suggested that EMG-EMG coherence in the beta band (approximately 15–35 Hz) is related to the corticospinal drive (Norton and Gorassini, 2006; Barthélemy et al., 2010). In recent years, a few studies have indicated that the EMG-EMG coherence in the beta band in an ankle dorsiflexor muscle changed when adapting walking patterns to the split-belt condition and de-adapting walking patterns to the tied-belt condition after the split-belt condition (Sato and Choi, 2019; Oshima et al., 2021).

However, previous studies using EMG-EMG coherence analysis focused on only one specific muscle. Considering that multiple muscles in the body are related to walking, knowledge obtained by focusing on one specific muscle would be insufficient to understand a neural control strategy underlying the split-belt locomotor adaptation. The muscle synergy concept has been proposed as a neural strategy to control multiple muscles relating to the generation of physical movements. This concept implies that the CNS controls a small number of modules (referred to as muscle synergies) consisting of some functionally related muscles instead of controlling muscles

individually (Ivanenko et al., 2004; Dominici et al., 2011; Bizzi and Cheung, 2013). The muscle synergies are supposed to contribute to solving the degree of freedom or redundancy problem in the musculoskeletal system (Bernstein, 1966; Tresch et al., 1999). Although the origin of muscle synergies has been debated (Bizzi and Cheung, 2013; Abd et al., 2021), evidence accumulated from previous animal studies has suggested that muscle synergies are neurophysiological entities to facilitate motor control and are encoded in the spinal cord (Ting et al., 2015; Cheung and Seki, 2021). The muscle synergies in human locomotion are extracted by applying decomposition techniques, such as PCA and NNMF to EMG data recorded from a large number of muscles during walking (Ivanenko et al., 2004; Yokoyama et al., 2021). A muscle synergy is represented by temporal activation pattern and muscle weighting. The temporal activation pattern is the timing of muscle activity during a gait cycle and muscle weighting is the extent of contribution to the activation pattern per individual muscle (Safavynia et al., 2011; Lacquaniti et al., 2012). Previous studies have shown that in healthy adults four or five muscle synergies can explain the variability in muscle activity patterns during normal walking (Cappellini et al., 2006; Ivanenko et al., 2006). It has also been indicated that each extracted muscle synergy has a particular function in a gait cycle (e.g., weight acceptance or propulsion during the stance phase) (Neptune et al., 2009; Lacquaniti et al., 2012). Thus far, presence of neurological disorders (Clark et al., 2010), development from neonatal to toddler stages (Dominici et al., 2011), and walking speeds (Yokoyama et al., 2016) have been reported to alter the number of muscle synergies. Further, the temporal activation patterns have been shown to be modified according to the walking speed (Hagio et al., 2015; Kibushi et al., 2018) and walking surfaces (Martino et al., 2015; Santuz et al., 2018). The muscle weightings recruited during an imposed walking task have been shown to be dependent on the training history (Sawers et al., 2015). Thus, the number, temporal

activation patterns, and muscle weightings of muscle synergies may change depending on the situation during walking. Hence, studies focusing on such muscle synergies can deepen the understanding of neuromuscular control underlying the split-belt locomotor adaptation. A recent study using cats focused on muscle synergies during walking on a split-belt treadmill; however changes in muscle synergies associated with adaptation and de-adaptation were not investigated (Desrochers et al., 2019). Maclellan et al. (2014) have extracted muscle synergies in the initial and late phases of split-belt walking and tied-belt walking following split-belt walking in humans but did not examine changes in muscle synergies over time. Therefore, it remains unclear whether muscle synergies change gradually or quickly in the adaptation and de-adaptation processes on the split-belt treadmill.

When examining changes in muscle synergies over time on the split-belt treadmill, one of the following patterns is expected to occur, given the hypotheses proposed in previous studies (Severini et al., 2020; Abd et al., 2021):

1) changes in the number of muscle weightings and temporal activation patterns

2) no changes in the muscle weightings but changes in the temporal activation patterns

3) changes in the muscle weightings and temporal activation patterns

4) both 1 and 3

Thus, in this study, we aim to investigate changes in muscle synergies over time and test which one of the four abovementioned hypotheses is valid in the adaptation and de-adaptation processes on the split-belt treadmill. To accomplish this, we extracted muscle synergies from the lower-limb muscles chronologically during split-belt walking and tied-belt walking after split-belt walking. The present study may provide new knowledge about the neuromuscular control in the split-belt locomotor adaptation.

3-2. Methods

Participants

Twelve healthy young men (22.1 ± 2.9 years, 170.3 ± 5.5 cm, and 62.9 ± 4.5 kg) participated in this study. The dominant leg was the right leg in all participants. We excluded participants with neurological impairments. All participants provided written informed consent prior to participating in the experiment. The procedures in this study were approved by the Doshisha University Research Ethics Review Committee regarding Human Subject Research, and this study was performed in accordance with the Declaration of Helsinki. Participants who had experience walking on a split-belt treadmill before were not included in the present study.

Experimental design

We applied an experimental design established by Bastian and colleagues (Reisman et al., 2005). The participants walked on a split-belt treadmill (HPT-1980D-DU, Tec Gihan Co., Ltd.) with two belts controlled separately by independent motors. The treadmill was operated in either a tied-belt condition (i.e., the two belts move at the same speed) or a split-belt condition (i.e., the two belts move at different speeds). The belts moved from the front to the back throughout the experiment. The belt speed was set at 3.0 km/h (slow) or 5.4 km/h (fast). Figure 3-1 illustrates the experimental paradigm. The baseline condition was the tied-belt condition at 3.0 km/h for 2 min. The adaptation condition was the split-belt condition with the left belt at 3.0 km/h and the right belt at 5.4 km/h for 9 min (belt speed ratio of 1:1.8). The leg moving faster during the adaptation condition was assigned to the dominant leg in all participants. We defined the leg on the slow and fast belts during the adaptation condition as the “slow

leg" and the "fast leg," respectively. In the post-adaptation condition, the belt condition was again the tied-belt condition at 3.0 km/h for 5 min. The belts were stopped between the baseline and adaptation conditions, but not between the adaptation and post-adaptation conditions. All changes in belt speeds (e.g., from 5.4 to 3.0 km/h between the adaptation and post-adaptation conditions) took 5 s. Participants were verbally informed of the next belt speed by an experimenter about 10 s before the actual changes in the belt speed. They were instructed to look at the centerline on a screen about 2 m ahead without looking down as much as possible while walking. All participants wore a safety harness around the upper chest to prevent falls during walking. The harness was mounted on the suspension device, but it did not support their body weight. Additionally, emergency buttons were placed within the reach of the participant and experimenter.

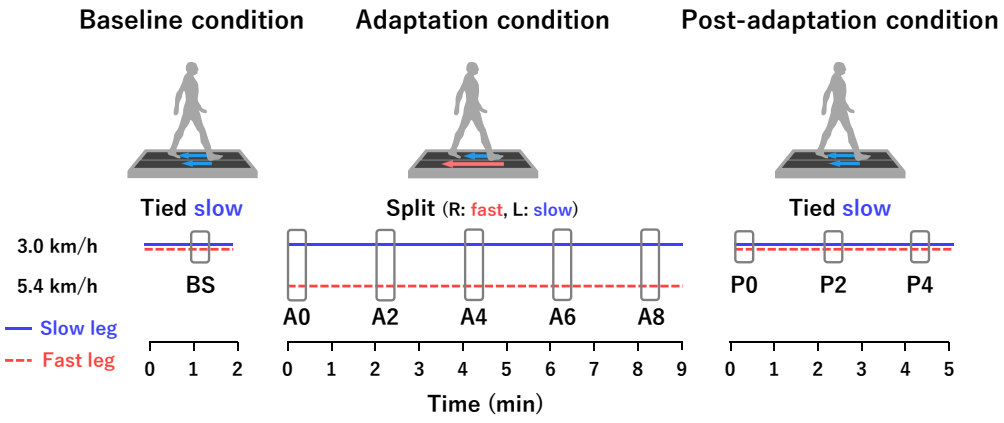

Figure 3-1 Experimental paradigm and analysis sections

Tied is a belt condition in which both belts move at the same speed. Split is a belt condition in which each belt moves at a different speed. In the adaptation condition, the right belt was fast (5.4 km/h), and the left belt was slow (3.0 km/h) for all participants. The horizontal blue solid and red dotted lines represent the slow leg and fast leg, respectively. The horizontal axis indicates time. Each rectangle in the baseline, adaptation, and post-adaptation conditions represents the analysis sections consisting of 20 gait cycles.

Data collection

Kinematic data were collected at 100 Hz using a motion capture system with eight cameras (OptiTrack motion capture system, NaturalPoint Inc.). Infrared reflective markers were attached bilaterally on the ankles (lateral malleolus). Three-dimensional GRF data [mediolateral (Fx), anterior-posterior (Fy), and vertical (Fz) components] were recorded at 1,000 Hz from a force plate mounted underneath each belt of the treadmill (TFH-40120-EL and TFH-40120-ER, Tec Gihan Co., Ltd.). Surface EMG electrodes (Trigno Wireless System, Delsys Inc.) were used to record EMG bilaterally from the following 13 muscles: Gmax, Gmed, AL, TFL, BF, ST, RF, VL, VM, MG, LG, SOL, and TA muscles. The electrode locations were determined by referring to the Surface Electromyography for the Non-Invasive Assessment of Muscles (SENIAM) guidelines (http://www.seniam.org) and confirmed using an ultrasonic device (Prosound α7, Hitachi-Aloka Medical, Ltd.). Before placing the electrodes, the skin was lightly rubbed with fine sandpaper and cleaned with alcohol swabs. The recorded EMG signals were amplified (with a 300-gain preamplifier) before further amplification (total effective gain of 909), band-pass filtered (20–450 Hz), and stored on a computer for later analyses after A/D conversion at 1,000 Hz (PowerLab 16/35, AD Instruments Inc.). The timing for recording the kinematic, GRF, and EMG data was synchronized.

Data analysis section

Multiple analysis sections were set for the analyses of the spatio-temporal parameters and the muscle synergy (Figure 3-1). Each section consisted of 20 consecutive gait cycles. One section was set from 1 min after the start of the baseline condition (BS). In the adaptation condition, five sections were set as follows: immediately after the start of the adaptation condition (A0), 2 min after the start (A2), 4

min after the start (A4), 6 min after the start (A6), and 8 min after the start (A8). In the post-adaptation condition, three sections were set as follows: immediately after the start of the post-adaptation condition (P0), 2 min after the start (P2), and 4 min after the start (P4).

Analysis of spatio-temporal parameters

The kinematic and GRF data were low-pass filtered at 6 and 15 Hz, respectively (Reisman et al., 2005; Sato and Choi, 2019). From the Fz component of the GRF, the timings of the heel strike and toe-off of each leg were determined (threshold: 5% of the bodyweight). Based on the timings of the heel strike and toe-off, stance time, swing time, and double support time were calculated. These temporal parameters were normalized to the duration of one gait cycle.

From the kinematic data, step length symmetry was calculated. Step length symmetry was defined as the normalized difference between the step length of each leg following the equation:

$$Step\ length\ symmetry = \frac{Step\ length\ of\ fast\ leg - Step\ length\ of\ slow\ leg}{Step\ length\ of\ fast\ leg + Step\ length\ of\ slow\ leg}$$

In this equation, the step length was the anterior-posterior distance between the ankle markers of each leg at the heel strike of the leading leg (Reisman et al., 2005). The step length for the slow leg was measured at the heel strike of the slow leg. A positive value of the step length symmetry indicates that the step length of the fast leg was longer than that of the slow leg (i.e., asymmetry) (Figure 3-2). A value of 0 indicates that the step lengths of the fast leg and slow leg are equal (i.e., symmetry).

Muscle synergy analysis

Muscle synergy analysis was performed in the slow leg and fast leg, respectively. Twenty consecutive gait cycles at each section were used to extract muscle synergies (Oliveira et al., 2016). The recorded EMG signals were high-pass filtered (40 Hz) with a zero-lag fourth-order Butterworth filter, demeaned, full-wave rectified, and low-pass filtered (10 Hz) with a zero-lag fourth-order Butterworth filter (Clark et al., 2010; Kibushi et al., 2018). We confirmed visually that there were no obvious artifacts in the smoothed EMG signals. The smoothed EMG data were time-interpolated to 200-time points per one gait cycle (Cappellini et al., 2016). The EMG envelopes were then ensemble-averaged (Nazifi et al., 2017; Saito et al., 2018). Thus, the EMG matrix, which consisted of 13 rows and 200 columns was generated in each leg at each section. The EMG amplitude of each muscle in each matrix was normalized to the maximum amplitude across the sections used in the statistics (see "Statistics" section: A0–A8 for the adaptation analysis, and BS and P0-P4 for the de-adaptation analysis) per participant (Yokoyama et al., 2019), indicating that the amplitude of each muscle was scaled from 0 to 1. Then, the data of each muscle in each matrix was normalized to the standard deviation of that muscle to have unit variance (Chvatal and Ting, 2012; Hagio and Kouzaki, 2014). This normalization was removed after extracting muscle synergies to rescale the data to the original scaling.

The NNMF was used to extract muscle synergies from each EMG matrix (Lee and Seung, 1999; Yokoyama et al., 2016; Boccia et al., 2018), which has previously been described as a linear decomposition technique according to the following equation:

$$E = W \cdot C + e = Er + e$$

In this equation, E is an $m \times t$ matrix [where m is the number of muscles (13) and t is the time point (200)] that is an original EMG matrix, W is an $m \times n$ matrix (where n is the number of muscle synergies) that indicates muscle weightings, C is an $n \times t$ matrix that indicates temporal activation patterns, e is the residual error matrix, and Er is a reconstructed EMG matrix from the multiplication of W and C. Each vector in the extracted muscle weightings (each column of W) was normalized to its maximum and each vector in the extracted temporal activation patterns (each row of C) was scaled by the value used in the normalization of muscle weighting corresponding to the temporal activation pattern. Thus, each vector in muscle weightings was a unit vector.

The extraction was performed using a possible n between 1 and 13 and in each n the extraction was iterated 100 times. To select the optimal number of muscle synergies, in each n, a goodness of fit between the original EMG matrix (E) and reconstructed EMG matrix (Er) was calculated using the variability accounted for (VAF). The VAF describes the extent to which the variability of the original EMG data was accounted for by the reconstructed EMG data. The value of VAF was calculated as 100 $\times$ the coefficient of determination from the uncentered Pearson correlation coefficient in the entire EMG data (global VAF) and each muscle EMG data (muscle VAF) (Hagio et al., 2015) (Figure 3-3). The optimal number of muscle synergies was defined as the minimum number of muscle synergies required to achieve a global VAF > 90% and a muscle VAF > 75% (Barroso et al., 2014; Boccia et al., 2018; Kibushi et al., 2018). After determining the optimal number of muscle synergies in each participant, we determined the number of muscle synergies at each section as a rounded mean number of muscle synergies across participants for further analysis.

To sort the muscle synergies extracted by the rounded mean number of muscle synergies in all participants at each section, the cosine similarity value that was calculated as a scalar product

between a pair of vectors normalized by the product of the norm of each vector was used (Oliveira et al., 2014; Singh et al., 2020). The cosine similarity values close to 0 and 1 were considered dissimilar and highly similar, respectively. In this study, when the cosine similarity value was over 0.684 ($P < 0.01$), the pair of vectors were determined to be similar. First, the cosine similarity values between each vector in the muscle weightings of an arbitrary reference participant and that of the remaining participants were calculated (Hagio et al., 2015; Kibushi et al., 2018), and an average muscle weighting set was made using similar vectors. Subsequently, the cosine similarity values were again calculated between each vector in the average muscle weighting set and that in the muscle weightings of each participant. If two vectors in one participant were categorized into one vector in the average muscle weighting set, a vector with the highest correlation was selected. The average muscle synergies, consisting of the muscle synergies finally categorized as similar muscle synergies across participants by sorting vectors of muscle weightings, were then made. Through these steps, several muscle synergies in some participants were not included in any of the average muscle synergies. We also calculated the cosine similarity value of each vector in the muscle weightings of the average muscle synergies between A0 and the remaining sections in the adaptation condition, as well as between the BS and all sections in the post-adaptation condition. The average muscle synergies that were similar across sections are shown in Figures 3-4 and 3-5. The principal muscles within similar muscle synergies across sections were defined as muscles that showed weighting values ≥ 0.5 in more than half of the number of sections for statistics (see “Statistics” section: A0–A8 for the adaptation analysis and BS and P0–P4 for the de-adaptation analysis) (Tables 3-1 and 3-2). We calculated the areas under the curves of the temporal activation patterns in participants included in the average muscle synergies at each section to investigate changes in the temporal activation patterns (Hayes et al., 2014; Sawers

et al., 2015). All data processing and analysis were performed using custom software written in MATLAB R2020b (MathWorks Inc.).

Statistics

We focused on the respective changes in the muscle synergies of each leg when adapting walking patterns to the split-belt condition and de-adapting walking patterns to the tied-belt condition after the split-belt condition. Thus, statistical analysis was performed using the following combination of sections: A0–A8 for the adaptation analysis, and BS and P0–P4 for the de-adaptation analysis. Regarding the statistical analysis of the areas of the temporal activation patterns, when the number of participants who recruited a certain muscle synergy throughout all sections selected for each statistical analysis of adaptation and de-adaptation was more than six (see filled markers and dotted lines in Figures 3-4C, F and 3-5C, F), we performed the statistical analysis on those participants. The statistical analysis for step length symmetry was conducted on all participants in the same combination of sections. The normal distribution of data was evaluated using the Shapiro-Wilk test. If the data at each section used in each statistical analysis were normally distributed, we performed a one-way repeated-measures ANOVA. When the assumption of sphericity (Mauchly's test) was violated, Greenhouse-Geisser adjustments were applied to adjust the degrees of freedom. When statistical significance was found using the repeated-measures ANOVA (Significance level alpha = 0.05), Sidak-correction post hoc comparisons [1−(1−significance level alpha of 0.05) ^ (1/number of compared pairs)] were performed to examine the differences among sections [Sidak-adjusted alpha level for the adaptation analysis = 0.0051 (10 pairs), and sidak-adjusted alpha level for the de-adaptation analysis = 0.0085 (six pairs)]. If the data were not normally distributed, a non-parametric Friedman test was conducted.

When statistical significance was found using the Friedman test (Significance level alpha = 0.05), the Wilcoxon signed-rank sum test (Sidak-correction) was used to examine the differences among sections. Data are presented as mean ± standard error (SE). All statistical analyses were performed using SPSS (IBM SPSS Statistics for Windows, Version 27.0, IBM Corp.).

3-3. Results

Step length symmetry

Figure 3-2 shows the time-series changes in the step length symmetry. Although the step length symmetry exhibited a negative value in the initial phase of the adaptation condition, it gradually approached 0 by the late phase of the adaptation condition. In the initial phase of the post-adaptation condition, the step length symmetry became a positive value despite the tied-belt condition being identical to the baseline condition. This value of step asymmetry reduced gradually toward the baseline value. In the adaptation condition, there was a significant main effect of section [Chi^2 (df = 4) = 40.00, $P < 0.05$]. The post-hoc tests showed significant differences in the following pairs of sections: A0–A4, A0–A6, A0–A8, and A2–A8 (all $P < 0.0051$). In the baseline and post-adaptation conditions, there was a significant main effect of section [$F_{(1.30, 14.36)} = 36.72$, $P < 0.05$]. The step length symmetry at P0 was significantly different compared with that at BS, P2, and P4 (all $P < 0.0085$), and there was also a significant difference between BS and P2 ($P < 0.0085$).

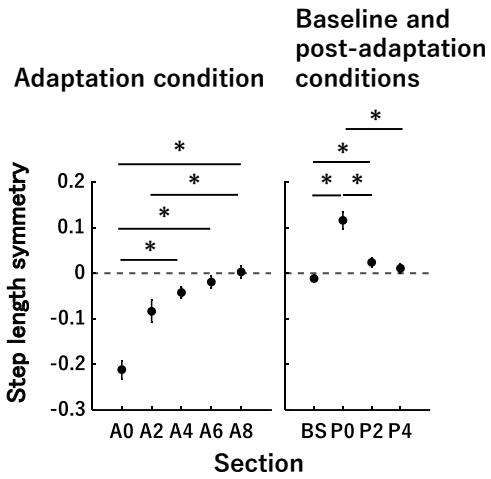

Figure 3-2 Time-series changes in the step length symmetry

The vertical axis indicates the step length symmetry, and the horizontal axis indicates the sections in each panel. A value of 0 in the vertical axis (dotted lines) indicates that the step lengths of the slow leg and fast leg are equal (i.e., symmetry). The panels represent time-series changes in the step length symmetry in the adaptation condition (left panel) as well as the baseline and post-adaptation conditions (right panel). Error bars indicate mean ± SE. *P < 0.0051 (adaptation condition) and 0.0085 (baseline and post-adaptation conditions).

Number of extracted muscle synergies

Figure 3-3 shows the global VAF curves in each leg at each section in the adaptation condition (Figures 3-3A and B) and the baseline and post-adaptation conditions (Figures 3-3C and D). The mean number of muscle synergies in the slow leg at each section was as follows: 4.17 ± 0.21 (A0), 4.42 ± 0.15 (A2), 4.50 ± 0.15 (A4), 4.58 ± 0.15 (A6), 4.75 ± 0.18 (A8), 4.75 ± 0.13 (BS), 4.17 ± 0.17 (P0), 4.92 ± 0.19 (P2), and 4.92 ± 0.23 (P4). Thus, we determined the number of muscle synergies at A0, A2, and P0 to be four and the other sections to be five. The mean number of muscle synergies in the fast leg at each section was as follows: 4.75 ± 0.13 (A0), 4.75 ± 0.18 (A2), 4.67 ± 0.22 (A4), 4.83 ± 0.27 (A6), 4.92 ± 0.23 (A8), 4.75 ± 0.18 (BS), 4.42 ± 0.19 (P0), 4.92 ± 0.23 (P2), and 5.17 ± 0.17 (P4). Therefore, the number of muscle synergies was five in all sections, except for four muscle synergies at P0.

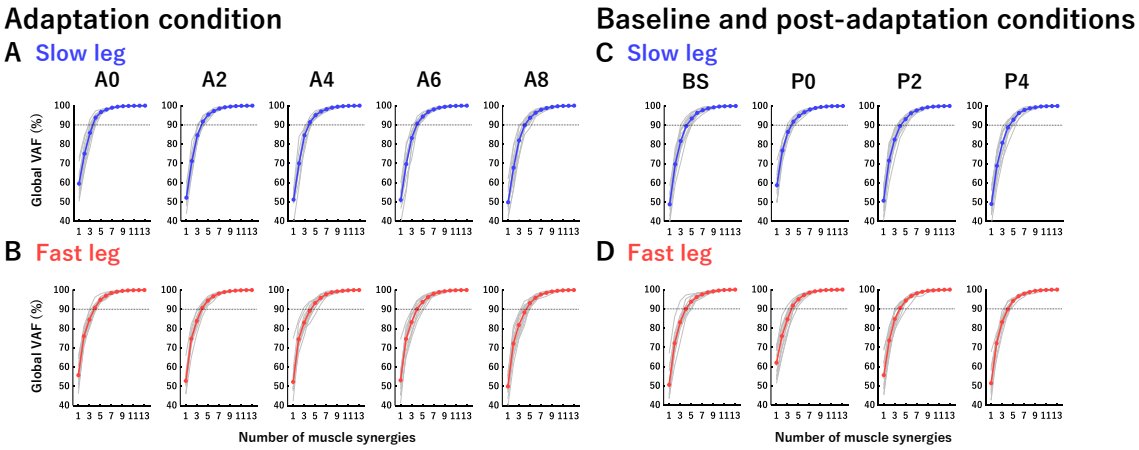

Figure 3-3 Global variability accounted for (VAF) curves in each leg at each section

The vertical axis indicates global VAF (%) and the horizontal axis indicates the number of muscle synergies. Horizontal dotted lines at 90% VAF indicate the threshold of global VAF. (A, B) Global VAF curves of the slow leg and fast leg at each section in the adaptation condition. (C, D) Global VAF curves of the slow leg and fast leg at each section in the baseline and post-adaptation conditions. Thin gray curves indicate the global VAF curve of each participant and colored curves (blue and red) indicate the averaged global VAF curves from all participants.

Extracted muscle synergies in adaptation condition

Figure 3-4 shows the average muscle weightings (heatmaps, Figures 3-4A and D), average temporal activation patterns (waveforms, Figures 3-4B and E), and areas under the curves of temporal activation patterns (scatter plots, Figures 3-4C and F) in each leg at each section in the adaptation condition. In Figures 3-4B and E, the average stance time at each section is indicated with the gray area at the bottom surface of the figure. In addition, the average time of double stance and single limb support in each section is identified by the timing of the heel strike or toe-off in the contralateral leg, indicated by the vertical dotted lines in the temporal activation patterns. The muscle synergies were aligned based on the timing of the activation during a gait cycle from stance to swing. The principal muscles and main activation timings in each muscle synergy are summarized in Table 3-1. Synergy #1 mainly

represented the activation of the Gmax, Gmed, VL, and VM. These muscles were mainly active during the initial double stance phase. They were also active during single limb support phase in the slow leg at A0 and A2. Synergy #2 mainly represented the activation of the TFL, which was active during the stance phase and early swing phase. This synergy was not recruited in either leg at A0 and in the slow leg at A2. Synergy #3 represented the activation of the MG, LG, and SOL, which were mainly observed during the late stance phase. Synergy #4 mainly represented the activation of the AL in both legs and the RF in the slow leg. The muscles in this synergy were active during the terminal double stance phase. Further, in the slow leg at A0 and A2, this synergy represented activation of the TFL that was also active during the single limb support phase. Synergy #5 represented the activation of the BF and ST that occurred in the late swing phase. In the fast leg at A0, the BF and ST muscles were also active throughout the swing phase. Furthermore, in the fast leg at A0, a section-specific muscle synergy that was not sorted from Synergy #1 to #5 was extracted. This synergy represented the activation of the Gmed, BF, ST, MG, LG, and SOL during the initial double stance phase and the single limb support phase.

Regarding areas of the temporal activation patterns in the slow leg (Figure 3-4C), there was a significant main effect of section in Synergy #1 [Chi^2 (df = 4) = 30.55, $P < 0.05$]. The area at A0 was significantly greater than that at A4, A6, and A8 (all $P < 0.0051$). The area at A2 was also significantly greater than that at A6 ($P < 0.0051$). In Synergy #2, a significant main effect of section was not observed [$F_{(2, 14)} = 0.29$, $P > 0.05$]. In Synergy #3, there was a significant main effect of section [$F_{(4, 44)} = 3.02$, $P < 0.05$], but the post-hoc tests did not show significant differences among sections. In Synergy #4, a significant main effect of section was shown [$F_{(1.83, 10.96)} = 26.05$, $P < 0.05$], and the area at A0 was significantly greater than that at the other sections (all $P < 0.0051$). In Synergy #5, there

was also a significant main effect of section [Chi^2 (df = 4) = 25.53, $P < 0.05$] and the area at A0 was significantly greater than that at A4, A6, and A8 (all $P < 0.0051$). For the fast leg (Figure 3-4F), there was no significant main effect of section in Synergy #1, #2, and #3 [Synergy #1: $F_{(4, 40)} = 1.63$; Synergy #2: $F_{(3,15)} = 0.89$; Synergy #3: $F_{(4, 44)} = 1.10$, all $P > 0.05$]. In Synergy #4, since only one participant recruited this muscle synergy at all sections, we did not perform a statistical analysis. In Synergy #5, a significant main effect of section was shown [Chi^2 (df = 4) = 17.90, $P < 0.05$] and the area at A0 was significantly greater than that at A6 and A8 (both $P < 0.0051$).

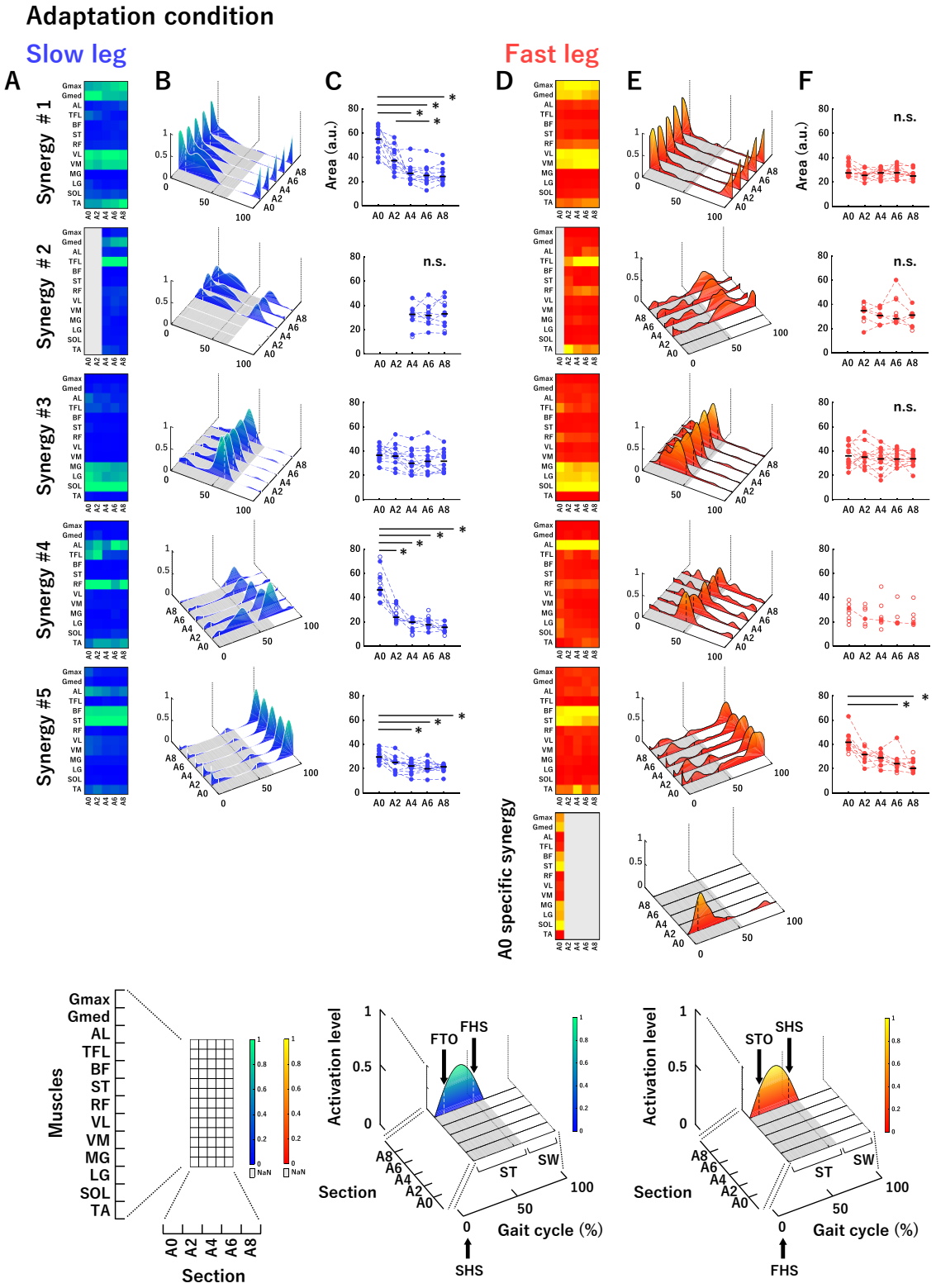
Adaptation condition
Slow leg
Fast leg
A
B
C
D
E
F
Synergy # 1
Synergy # 2
Synergy #3
Synergy #4
Synergy #5
A0 specific synergy
Area (a.u.)
n.s.
Muscles
Section
Activation level
FTO
FHS
STO
SHS
ST
SW
Gait cycle (%)

Figure 3-4 Average muscle synergies across participants in the slow leg (A–C) and the fast leg (D–F) at each section in the adaptation condition

(A, D) Each heatmap represents the muscle weightings of muscle synergies. The vertical axis indicates muscle names, and the horizontal axis indicates sections. Bright color (green or yellow) indicates high weighting. The parts filled with gray in the heatmap mean that a corresponding muscle synergy was not extracted. (B, E) Each waveform represents the temporal activation patterns of muscle synergies. The vertical axis indicates activation level and the two axes in the bottom plane indicate sections and gait cycle (%). Bright color (green or yellow) indicates high activation. The bottom part of the figure, shown with gray, represents stance phase and the vertical white or black dotted lines depicted within the temporal activation patterns represent boundaries of the double support phase. An enlarged view of each axis of each heatmap and waveform is shown in the lowest row. (C, F) The areas under the curves of the temporal activation patterns of muscle synergies. The vertical axis indicates the area (a.u.) and the horizontal axis indicates the sections. The area of each participant is denoted by circles. The filled circles connected by dotted lines were used in the statistical analysis. Horizontal black bars indicate the median value across participants. n.s. indicates no significant difference in the one-way repeated measures ANOVA or Friedman test. ST, stance phase; SW, swing phase; FTO, fast leg toe-off; FHS, fast leg heel strike; STO, slow leg toe-off; SHS, slow leg heel strike. *$P < 0.0051$.

Extracted muscle synergies in baseline and post-adaptation conditions

Figure 3-5 shows the average muscle weightings, average temporal activation patterns, and the areas under the curves of temporal activation patterns in each leg at each section in the baseline and post-adaptation conditions with the same convention as that of Figure 3-4. The principal muscles and main activation timings in each muscle synergy in baseline and post-adaptation conditions were almost the same as those in the adaptation condition (Tables 3-1 and 3-2). However, some characteristic changes in the muscle synergies were observed among sections in the baseline and post-adaptation conditions. Synergy #2 was not extracted in both legs at P0. For Synergy #3 of the slow leg at P0, the activation level of the temporal activation patterns was high even in the early stance phase. In Synergy #4 of both

legs, although the activation of the AL was mainly represented at all sections, the activation of the TFL and RF was also represented at P0. The muscles involved in this synergy were also active during the single limb support phase in the fast leg at P0. Further, in Synergy #5 at P0, additional activation was observed during the stance phase in the slow leg, and during the swing phase in the fast leg.

Regarding the areas of the temporal activation patterns in the slow leg (Figure 3-5C), there was a significant main effect of section in Synergy #1 and #5 [Synergy #1: $F_{(3, 21)} = 11.22$; Synergy #5: $F_{(3, 21)} = 25.40$, both $P < 0.05$]. The post-hoc tests showed that the area at P0 was significantly greater than that at the other sections (all $P < 0.0085$). In Synergy #2, there was no significant main effect of section [$F_{(2, 16)} = 0.05$, $P > 0.05$]. In Synergy #3, a main effect of section was significant [Synergy #3: Chi^2 (df = 3) = 16.20, $P < 0.05$] and the area at P0 was significantly greater than that at BS and P4 (both $P < 0.0085$). In Synergy #4, a significant main effect of the section was observed [$F_{(3, 15)} = 8.50$, $P < 0.05$], and the area at P0 was significantly greater than that at P2 and P4 (both $P < 0.0085$). For the fast leg (Figure 3-5F), although a significant main effect of the section was shown in Synergy #1 [$F_{(3, 24)} = 5.93$, $P < 0.05$], significant differences among sections were not observed. In Synergy #2, since only three participants recruited this muscle synergy throughout all sections, statistical analyses were not conducted. In Synergy #3, there was a significant main effect of section [Chi^2 (df = 3) = 8.70, $P < 0.05$], and the area at BS was significantly greater than that at P4 ($P < 0.0085$). In Synergy #4, a significant main effect was not observed [Chi^2 (df = 3) = 7.00, $P > 0.05$]. In Synergy #5, there was a significant main effect of section [$F_{(3, 30)} = 8.80$, $P < 0.05$], and the area at P0 was significantly greater than that at the other sections (all $P < 0.0085$).

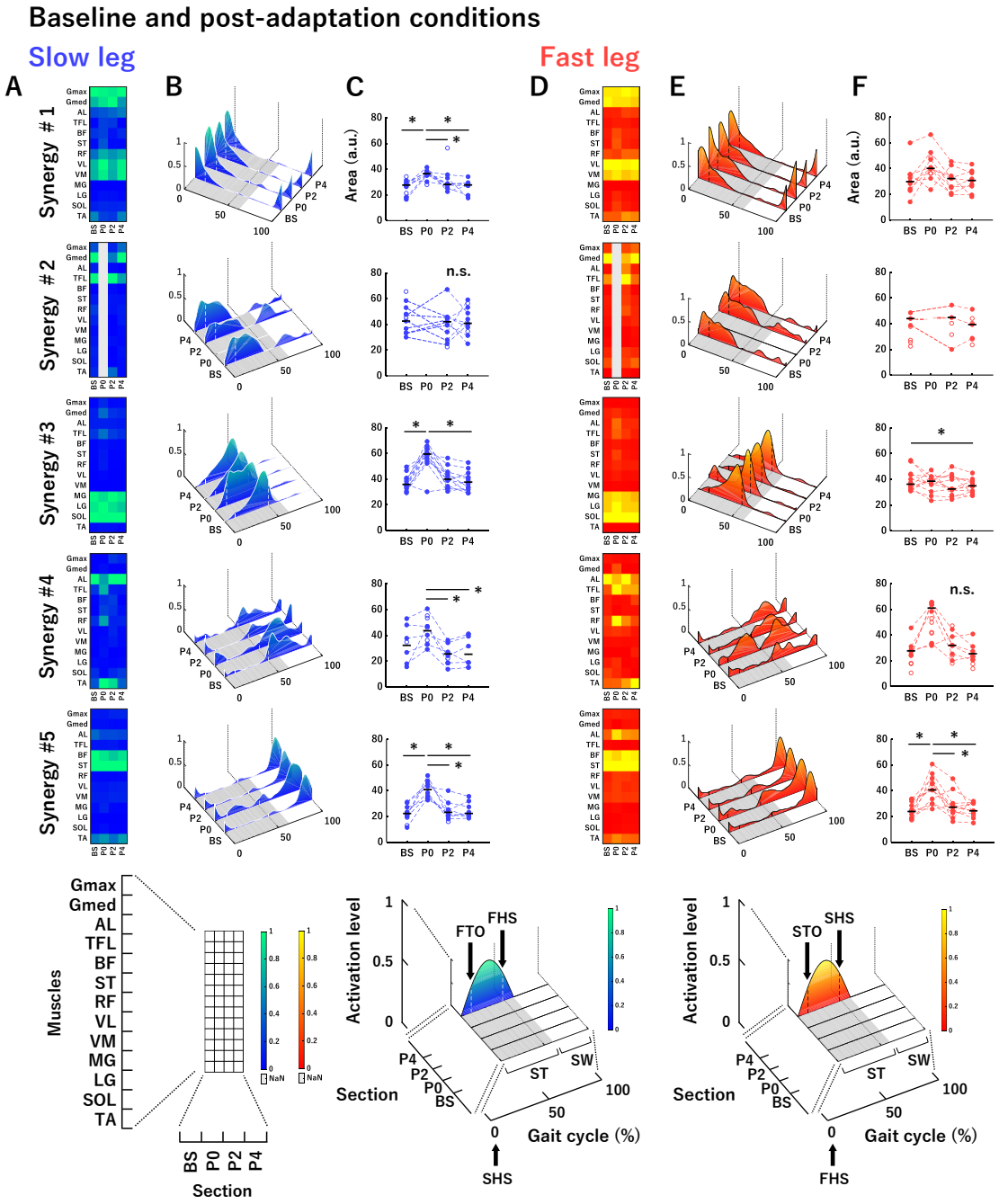

Figure 3-5 Average muscle synergies across participants in the slow leg (A–C) and the fast leg (D–F) at each section in the baseline and post-adaptation conditions

(A, D) Each heatmap represents the muscle weighting of muscle synergies. (B, E) Each waveform represents the temporal activation patterns of muscle synergies. (C, F) The areas under the curves of temporal activation patterns of muscle synergies. The conventions of each panel are the same as those in Figure 3-4. *$P < 0.0085$.

Table 3-1 Principal muscles and main activation timing of each muscle synergy in the adaptation condition

Adaptation condition		
	Principal muscles	Timing
Synergy #1	Gmax, Gmed, VL, VM	Initial double stance
Synergy #2	TFL	Stance · Early swing
Synergy #3	MG, LG, SOL	Late stance
Synergy #4	AL	Terminal double stance
Synergy #5	BF, ST	Late swing
Specific synergy (F)	Gmed, BF, ST, MG, LG, SOL	Initial double stance · Single limb support

F, Fast leg

Table 3-2 Principal muscles and main activation timing of each muscle synergy in the baseline and post-adaptation conditions

Baseline and post-adaptation conditions		
	Principal muscles	Timing
Synergy #1	Gmax, Gmed, VL, VM	Initial double stance · Mid stance
Synergy #2	Gmed, TFL	Initial double stance · Single limb support
Synergy #3	MG, LG, SOL	Late stance
Synergy #4	AL	Early swing
Synergy #5	BF, ST	Late swing

3-4. Discussion

We studied changes in muscle synergies over time and tested which one of the four sub-hypotheses were valid in the adaptation and de-adaptation processes on the split-belt treadmill. The main findings were that the number of muscle synergies changed in the slow leg during split-belt walking and in both legs during tied-belt walking after split-belt walking. Moreover, one section-specific muscle synergy was extracted in the fast leg in the initial phase of split-belt walking. The areas of the temporal activation patterns in a few specific muscle synergies decreased during split-belt walking (Figures 3-

4C and F). Meanwhile, the areas of the temporal activation patterns in a few specific muscle synergies increased temporarily in the initial phase of tied-belt walking following split-belt walking and then decreased (Figures 3-5C and F). We discuss these changes in muscle synergies below.

Changes in the number of extracted muscle synergies

The series of changes in the step length symmetry identified in the present study (Figure 3-2) was almost consistent with those in previous studies that investigated the split-belt locomotor adaptation (Malone and Bastian, 2010; Bruijn et al., 2012; Yokoyama et al., 2018). We performed a muscle synergy analysis under the premise that split-belt locomotor adaptation had occurred. Overall, the number of muscle synergies extracted during split-belt and tied-belt walking (i.e., four or five muscle synergies) was similar to that identified in previous studies that had examined muscle synergies during walking (Clark et al., 2010; Dominici et al., 2011; Janshen et al., 2017). Thus far, some researchers have indicated the possibility that the number of muscle synergies does change depending on walking speeds (Yokoyama et al., 2016; Kibushi et al., 2018). Interestingly, in the present study, the number of muscle synergies changed at the constant walking speed (i.e., at 3.0 km/h in the slow leg in the adaptation condition or 3.0 km/h in both legs in the baseline and post-adaptation conditions). Specifically, the EMG data in the slow leg at A0 and A2, and in both legs at P0 were well accounted for by four muscle synergies temporarily, not five. This result likely reflects that the independence of muscular control reduced immediately after exposure to the split-belt condition and tied-belt condition following the split-belt condition (Clark et al., 2010; Ting et al., 2015). On the other hand, each muscle synergy extracted during normal walking has been assumed to have particular functions (Neptune et al., 2009; Lacquaniti et al., 2012). In the present study, the muscle synergy that was not extracted at

the section where the number of muscle synergies was four was Synergy #2. The muscle synergy mainly represented the activation of the TFL (Figures 3-4 and 3-5), whose function is considered to be body stabilization (Rimini et al., 2017). The body stabilization might be complemented partially by Synergy #4 because the activation of the TFL was included in Synergy #4 immediately after changing walking conditions. Subsequently, since Synergy #2 might have become controllable independently as adaptation and de-adaptation progressed, the number of muscle synergies would have increased from four to five. Thus, the number of muscle synergies was shown to change according to the split-belt locomotor adaptation.

Section-specific muscle synergy

Although the change in the number of muscle synergies was not observed in the fast leg in the adaptation condition, a section-specific muscle synergy was included within the five muscle synergies extracted at A0 (Figures 3-4D and E). The muscle weightings of this muscle synergy consisted of the extensor muscles in the lower limb, which might work to maintain balance immediately after being imposed to walk at different belt speeds on the left and right sides. Subsequently, the section-specific muscle synergy might not be extracted after A2 because the balance was restored with adaptation to the disturbance caused by the unfamiliar walking environment. Thus, the muscle weightings were shown to change in the fast leg during split-belt walking. The appearance and disappearance of the extra muscle synergy are considered to reflect how the CNS deals with a new walking condition.

Changes in the temporal activation patterns of extracted muscle synergies

In the adaptation condition, significant changes in the areas among sections were observed in three

muscle synergies of the slow leg and one muscle synergy of the fast leg (Figures 3-4C and F). In a previous study, it was reported that the temporal activation patterns changed abruptly without changes in muscle weightings in several muscle synergies just after a robot-driven perturbation was given to the lower limb during walking (Severini et al., 2020). The abrupt changes in the temporal activation patterns are considered to be a reactive response to the perturbation via the feedback mechanism. Thus, the great areas in the initial phase of the adaptation condition might also reflect a reactive response to novel constraints with a split-belt treadmill at the muscle synergy level (Hoogkamer, 2017; Severini et al., 2020). On the other hand, since we analyzed muscle synergies within the same belt condition (i.e., within the split-belt condition or tied-belt condition), biomechanical task constraints that would affect muscle synergies are believed to be constant. Nevertheless, the areas of a few specific muscle synergies decreased during split-belt walking (Figures 3-4C and F), which would result from mainly a decrease in activation levels in the temporal activation patterns. For Synergy #4 in the slow leg, a decrease in the area would result from the disappearance of an additional activation in the stance phase. The manners of these decreases in the areas, in a few specific muscle synergies, appear to be gradual. Thus, this result likely reflects that temporal activation patterns were adjusted via the feedforward mechanism (Severini et al., 2020). These adaptive changes in the temporal activation patterns have also been observed by repeating an imposed walking task in another previous study (Martino et al., 2015). The feedforward control is characterized by an aftereffect, occurring when a perturbation was removed (Torres-Oviedo et al., 2011). In the present study, the greater areas at P0 than at BS have been observed in several muscle synergies (Figures 3-5C and F), suggesting that aftereffect occurred at the muscle synergy level. The aftereffect was then washed out and the areas returned to the baseline level. The series of changes in the areas imply that adaptation and de-adaptation occurred in the temporal

activation patterns of a few specific muscle synergies in association with the split-belt locomotor adaptation.

Regarding the feedforward control, as mentioned in the previous paragraph, the supraspinal structures have been suggested to be involved (Choi et al., 2009). Therefore, the changes in the temporal activation patterns observed in the present study might reflect that the involvement of supraspinal structures changed in the split-belt locomotor adaptation. In particular, since cortical activation has been reported to be related to the activation of muscle synergies during walking (Yokoyama et al., 2019), it is considered that the involvement of the cortex changed. The changes in the cortical involvement associated with the split-belt locomotor adaptation have also been indicated in recent studies using the EMG-EMG coherence analysis, albeit at the individual muscle level (Sato and Choi, 2019; Oshima et al., 2021). Additionally, afferent signals from the lower limb have been considered to be one of the factors that influence the activation of muscle synergies in animal studies (Cheung et al., 2005; Bizzi and Cheung, 2013). The amount of various somatosensory information would change during split-belt walking (Hoogkamer, 2017). Ogawa et al. (2014) showed that the magnitude of the GRF associated with the load-related sensory information significantly changed during split-belt walking. Therefore, changes in both supraspinal origin and somatosensory information might be related to changes in the temporal activation patterns in a few specific muscle synergies.

It should be noted that the changes in the areas were more prominent in the slow leg than in the fast leg (Figure 3-4). The results would indicate that the CNS tried to adjust the slow leg rather than the fast leg. This idea appears to be consistent with the contention of a previous study that the CNS might give importance to a slow leg during split-belt walking (Vasudevan and Bastian, 2010).

Thus, the significant changes in the areas would be observed in more muscle synergies of the slow leg compared with the fast leg as an aftereffect when the belts returned to the same speed (Figure 3-5).

3-5. Conclusion

Our results showed changes in the number of muscle synergies, appearance and disappearance of extra muscle synergy, and modulation of the temporal activation patterns of a few specific muscle synergies in the adaptation and de-adaptation processes on the split-belt treadmill. These results support hypothesis 4 and suggest that adaptation and de-adaptation have occurred at the muscle synergy level. The understanding of neural control strategies underlying the split-belt locomotor adaptation is advanced by our findings, based on the muscle synergy concept.

Chapter 4: General Discussion

4-1. Summary of the results

This thesis aimed to investigate the neuromuscular control that underlies split-belt locomotor adaptation in humans. Specifically, solving the following two research questions may advance our understanding of neuromuscular control during split-belt locomotor adaptation.

- Does the descending drive through the corticospinal tract change in the course of split-belt locomotor adaptation?
- How does the CNS control the activities of multiple muscles in the course of split-belt locomotor adaptation?

I addressed two separate studies, Study 1 and 2, to answer these research questions. The findings and suggestions obtained from each study are summarized below.

In Study 1 (Chapter 2), time-series changes in intramuscular coherence in the ankle dorsiflexor (TA) muscle during split-belt locomotor adaptation were investigated to answer the first research question. The results showed that 1) the intramuscular coherence in the beta and gamma bands, the frequency bands of interest, in the slow leg gradually decreased in the split-belt condition, and 2) when returning to the tied-belt condition after the split-belt condition, the intramuscular coherence in both bands in the fast leg temporarily increased and then quickly returned to the baseline levels (Fig. 2-5). The results suggest that the corticospinal drive from the primary motor cortex to the motoneurons of the TA muscle in the slow leg was gradually reduced with adaptation to the split-belt condition. Furthermore, the corticospinal drive from the primary motor cortex to the motoneurons of the TA muscle in the fast leg temporarily increased and then quickly returned to baseline levels when

de-adapting to the normal walking condition after learning new walking patterns.

In study 2 (Chapter 3), changes in muscle synergy during split-belt locomotor adaptation were investigated to answer the second research question. The results showed that 1) the number of muscle synergies increased in the slow leg with adaptation to the split-belt condition and in both legs with de-adaptation to the tied-belt condition after the split-belt condition, 2) the extra muscle synergy temporarily appeared in the fast leg just after exposure to the split-belt condition, and 3) the temporal activation patterns of a few specific muscle synergies were modulated with adaptation and de-adaptation (Fig. 3-4 and 3-5). Overall, the results suggest that there is a neuromuscular adjustment at the muscle synergy level by the CNS behind the split-belt locomotor adaptation.

The neural control of split-belt locomotor adaptation in humans is discussed below, combining the findings of this thesis and the existing literature. Furthermore, the limitations of this thesis, future direction of the split-belt locomotor adaptation study, and implications for clinical rehabilitation and sports science are described.

4-2. Neuromuscular control of individual muscle through the corticospinal tract in the course of split-belt locomotor adaptation

To date, the cerebellum has been suggested to play a critical role in predictive feedforward adaptation in split-belt locomotor adaptation based on lesions (Morton and Bastian, 2006) and electrophysiological studies (Jayaram et al., 2011, 2012). Furthermore, it has also been implied that the cerebrum plays a role in predictive feedforward adaptation in split-belt locomotor adaptation. For example, Choi et al. (2009) have indicated that hemispherectomy disrupts predictive feedforward adaptation in the split-belt condition. Therefore, the involvement of the cerebrum in the split-belt

locomotor adaptation does not appear to be ruled out (Hinton et al., 2020). In particular, the primary motor cortex in the cerebrum is believed to be involved in error-driven locomotor adaptation (Choi et al., 2015). Thus, it is expected that corticospinal control of the primary motor cortex is also important in split-belt locomotor adaptation, but there is little understanding of corticospinal control during split-belt locomotor adaptation. One of the possible causes for this would be the methodological difficulty. Although TMS is a method to noninvasively investigate corticospinal control in humans walking, it is difficult to use it during walking due to problems such as fixing the TMS coil at a predetermined location on the scalp. Jayaram et al. (2011) investigated the corticospinal control associated with split-belt locomotor adaptation using TMS, but only showed changes in the excitability of the corticospinal tract before and after walking in the split-belt condition. In other words, they could not show corticospinal control during split-belt locomotor adaptation. Therefore, in Study 1 (Chapter 2), EMG-EMG coherence analysis was used to examine corticospinal control during split-belt locomotor adaptation. EMG-EMG coherence analysis has been used to examine corticospinal control during human walking noninvasively (Halliday et al., 2003; Barthélemy et al., 2010; Jensen et al., 2018; Charalambous and Hadjipapas, 2022). Recently, Sato and Choi (2019) used EMG-EMG coherence analysis to investigate corticospinal control in split-belt locomotor adaptation; however, they only showed differences in EMG-EMG coherence between initial and end of each walking condition (i.e., split-belt condition and tied-belt condition following split-belt condition). Therefore, it was unclear how corticospinal control changes during split-belt locomotor adaptation.

The present results imply that the strength of the descending drive from the primary motor cortex to the motoneurons of the TA muscle was modulated with adaptation to the split-belt condition and de-adaptation to the tied-belt condition after the split-belt condition, albeit leg specific.

Specifically, considering that intramuscular coherence increased in phases in which motor error became large (i.e., initial phases of both the split-belt condition and tied-belt condition after the split-belt condition), corticospinal control may contribute to the correction of motor error. This idea is supported by recent findings that the size of the motor error was correlated with the amount of intramuscular coherence in the TA muscle in the initial phase of the split-belt condition (Sato and Choi, 2019). Subsequently, the descending corticospinal drive may gradually decrease with adaptation and rapidly decrease with de-adaptation. In other words, flexible adjustment of the corticospinal drive may underlie the split-belt locomotor adaptation. From the above, the findings obtained from Study 1 would be novel and meaningful in that they showed changes in descending corticospinal drive during split-belt locomotor adaptation.

4-3. Neuromuscular control of multiple muscles through muscle synergies in the course of split-belt locomotor adaptation

In Study 2 (Chapter 3), changes in muscle synergies during split-belt locomotor adaptation were investigated. To date, some researchers have investigated activity levels and activation patterns in individual muscles to infer neuromuscular control during split-belt locomotor adaptation (Maclellan et al., 2014; Ogawa et al., 2014). Study 1 also investigated neuromuscular control during split-belt locomotor adaptation, focusing on the activity of one specific muscle (Oshima et al., 2021). There is no doubt that such studies at the individual muscle level are of considerable significance to clarify neural control during split-belt locomotor adaptation. Meanwhile, the question of how the CNS controls redundant degrees of freedom in the musculoskeletal system to produce physical movements has been a matter of interest for many years in the field of motor control research (Bernstein, 1966).

The concept of muscle synergy has been considered an answer to the question, and so far many studies have been performed based on the concept (Ivanenko et al., 2004; Dominici et al., 2011; Yokoyama et al., 2016). In the case of human steady-state walking, it has been suggested that the CNS controls the activities of multiple muscles by activating a small number of muscle synergies (e.g., the activities of 12 muscles during walking are controlled via four muscle synergies) (Ivanenko et al., 2004; Cappellini et al., 2006; Dominici et al., 2011). In other words, muscle synergy may be a fundamental system for the coordinated activity of multiple muscles during walking (Ting et al., 2015). Previous studies have reported that the number of muscle synergies could change in association with development (Dominici et al., 2011; Bach et al., 2021), changes in walking speed (Yokoyama et al., 2016; Kibushi et al., 2018), and CNS disorders such as stroke (Clark et al., 2010), cerebral palsy (Shuman et al., 2017), and SCI (Danner et al., 2015). Meanwhile, the present findings would be interesting in that they showed the possibility that the number of muscle synergies increases with adaptation to a novel walking environment (i.e., split-belt condition) and de-adaptation to an original walking environment (i.e., tied-belt condition), not the factors mentioned above. However, the mechanism behind the increase in muscle synergies might differ between adaptation and de-adaptation. Specifically, in the case of an adaptation, the increase in the number of muscle synergies might result from the recruitment of a newly formed muscle synergy by the CNS (synergy #2). Meanwhile, in the case of de-adaptation, the increase in the number of muscle synergies may be due to the re-recruitment of muscle synergies that were originally recruited in the baseline condition. Regarding the fast leg in the adaptation, although a new muscle synergy (synergy #2) was recruited 2 min after exposure to the split-belt condition similar to the slow leg, the number of muscle synergies was five throughout the split-belt condition due to the appearance of a characteristic muscle synergy immediately after exposure to the split-belt

condition. This characteristic muscle synergy consisting of extensor muscles in the thigh and lower leg has not been generally observed during normal walking (Yokoyama et al., 2016), even in unfamiliar environments such as uneven surfaces (Santuz et al., 2018), slippery surfaces, and narrow width beam (Martino et al., 2015). Therefore, the appearance of such characteristic muscle synergy might depend on whether an exposed walking environment is an unexperienced (i.e., split-belt condition) or an unfamiliar but experienced (e.g., uneven or slippery surface) walking environment. Furthermore, an interesting point revealed in Study 2 is that the activation patterns of a few specific muscle synergies were modulated by adaptation and de-adaptation in the split-belt locomotor adaptation. To date, activation patterns have been shown to be flexibly modulated when exposed to unfamiliar environments (Sawers et al., 2015; Santuz et al., 2018). However, they did not show whether the activation patterns change along with repeated exposure or exposure for several minutes (e.g., 10 min) to unfamiliar walking environments. Therefore, the present findings are novel in that the activation patterns of muscle synergies would be modulated by continuous walking in a novel walking environment. In addition, the findings that changes in activation patterns were observed in a few, but not all, muscle synergies suggest that the CNS selectively fine-tunes the timing and amount of recruitment of a few muscle synergies with adaptation and de-adaptation in the split-belt locomotor adaptation. From the above, the findings from Study 2 may be novel and meaningful in that they showed neuromuscular control of multiple muscles by the CNS during split-belt locomotor adaptation.

4-4. Comprehensive understanding of neuromuscular control in the course of split-belt locomotor adaptation

Previous studies suggest that human locomotor muscle activities are controlled through muscle

synergies (Ting et al., 2015). A recent previous study has also indicated that the cerebral cortex may control locomotor muscle activity through muscle synergies rather than individually, by an analysis method using EEG and EMG (Yokoyama et al., 2019). Meanwhile, it has also been shown that there is a significant correlation between the activities of the primary motor cortex and a lower limb muscle (e.g., TA muscle) during human walking (i.e., corticomuscular coherence) (Petersen et al., 2012; Yokoyama et al., 2020b). Therefore, both neuromuscular control at the individual muscle level and multiple muscle level plays a critical role in the production of human walking. This thesis investigated the neuromuscular controls during split-belt locomotor adaptation from the two perspectives. Although the detailed experimental procedures differed between Study 1 and 2 (e.g., belt speed ratio in the split-belt condition), the findings obtained from both studies suggest the following. In adaptation to the split-belt condition, significant modulation of activation patterns in most muscle synergies was observed approximately 4 min after exposure to the split-belt condition, while significant changes in intramuscular coherence were shown from 6 min after exposure to the split-belt condition. These findings suggest that neuromuscular adjustments occur relatively quickly at the multiple muscle level compared to the individual muscle level when adapting to the split-belt condition. Meanwhile, in the de-adaptation to the tied-belt condition after the split-belt condition, changes in intramuscular coherence and activation patterns in a few specific muscle synergies promptly occurred. This suggests that neuromuscular adjustments at both the individual muscle level and multiple muscle level may be performed rapidly when de-adapting to a well-experienced walking environment (i.e., tied-belt condition) after learning new walking patterns. From the above, the CNS is considered to perform neuromuscular adjustments at the two levels flexibly, resulting in split-belt locomotor adaptation.

4-5. Limitations

In the following, the methodological limitations of each analysis used in this thesis are described. Regarding the EMG-EMG coherence analysis used in Study 1, previous studies have shown that the beta and gamma bands of EMG-EMG coherence are useful as physiological markers that reflect a descending drive through the corticospinal tract (Hansen et al., 2005; Barthélemy et al., 2010). Study 1 was also conducted based on this concept. However, the exact origin of EMG-EMG coherence in the beta and gamma bands remains controversial. For example, impaired perception due to disease or anesthesia has been reported to lead to a decrease in EMG-EMG coherence in the beta band during motor tasks (Fisher et al., 2002; Kilner et al., 2004; Zipser-Mohammadzada et al., 2022). Therefore, because EMG-EMG coherence in the beta band is believed to contain sensory information, the results of the EMG-EMG analysis should be interpreted with enough caution. Furthermore, the definition of the beta and gamma bands has been entrusted to each researcher. For example, one researcher uses the beta band as 15–35 Hz (Jensen et al., 2018) and another as 15–30 Hz (Willerslev-Olsen et al., 2015). Hence, attention should be paid when comparing the findings of different studies.

On the other hand, regarding the muscle synergy analysis used in Study 2, many researchers have used this method to investigate neuromuscular control during human walking. However, there are several methodological concerns. First, because muscle synergies are affected by the number of muscles and type of muscles recorded (Steele et al., 2013), researchers should select muscles in advance, carefully considering the purpose of the study. Second, there are many considerations in the preprocessing of EMG signals for muscle synergy analysis. For example, the structure of the original EMG data set (e.g., EMG data set averaged over several consecutive steps or not averaged over several consecutive steps) would affect the results of muscle synergy analysis (Oliveira et al., 2014).

Furthermore, enough attention should be paid to the choice of low-pass filters to smooth the original EMG signals and the normalization method of the EMG amplitudes (Shuman et al., 2017). Subsequently, researchers should be aware of which matrix factorization algorithm (e.g., NNMF, PCA, independent component analysis, and factor analysis) is used to extract muscle synergies from the processed EMG data set (Ivanenko et al., 2005; Tresch et al., 2006), although NNMF seems to be commonly used in the literature. The way in which the number of muscle synergies is determined in this extraction process is an important issue. Although several criteria have been used to determine the number of muscle synergies in previous studies, VAF >90% has been widely used (Kibushi et al., 2018, 2019; Yokoyama et al., 2019, 2021). Meanwhile, VAF >95% (Hagio et al., 2015) or VAF >75% (Severini et al., 2020) has also been used in several previous studies. As such, detailed methods for muscle synergy analysis have not yet been standardized among researchers. However, despite several methodological differences, the fact that a small number of muscle synergies are extracted from multiple muscle activities during walking suggests that low-dimensional structures that coordinate the activities of multiple muscles during walking reside in the CNS.

4-6. The future direction of split-belt locomotor adaptation study

Although many researchers have been addressed to reveal the neural control underlying the split-belt locomotor adaptation from various perspectives (Morton and Bastian, 2006; Reisman et al., 2007; Choi et al., 2009; Jayaram et al., 2011; Mawase et al., 2017; Sato and Choi, 2019, 2022; Jossinger et al., 2020; Oshima et al., 2021, 2022), changes in brain activity during split-belt locomotor adaptation remain unclear due to methodological difficulties. Considering the importance of supraspinal structures in walking, as reviewed in Chapter 1, studies focusing on brain activity are necessary to

expand our understanding of the neural control of split-belt locomotor adaptation. Recently, electrical activities in the cerebral cortex during steady-state walking have been noninvasively investigated using EEG (Gwin et al., 2011; Bradford et al., 2016; Yokoyama et al., 2020a). Therefore, future studies should incorporate such EEG methods to reveal brain activity during split-belt locomotor adaptation. A challenging study that combines fMRI and an fMRI-compatible treadmill that can mimic the split-belt condition is also needed to investigate the involvement of deep brain activities, such as the basal ganglia, in the split-belt locomotor adaptation (Dalla Volta et al., 2015). As such, combining the split-belt paradigm with neuroimaging techniques advances our understanding of neural control in split-belt locomotor adaptation. Furthermore, if brain electrical activity could be measured using EEG, more detailed neuromuscular control would be revealed during split-belt locomotor adaptation. For example, EEG-EMG coherence (i.e., corticomuscular coherence) is a promising measure (Gwin and Ferris, 2012; Petersen et al., 2012; Yokoyama et al., 2020b).

Meanwhile, neuromodulation has also received considerable interest in the field of motor control research. Although some researchers recently investigated the effect of neuromodulation on the cerebellum and PPC on split-belt locomotor adaptation (Jayaram et al., 2012; Kumari et al., 2020; Young et al., 2020), the effects of neuromodulation in other regions of the CNS (e.g., the motor cortex or spinal cord) have not yet been investigated. Furthermore, in recent years, various neuromodulation techniques, such as transcranial alternating current stimulation (Miyaguchi et al., 2018) and transcutaneous spinal direct current stimulation (Awosika et al., 2019), not only tDCS (Jayaram et al., 2012) have been used to modulate neural activities. Therefore, neuromodulation studies that focus on various regions and incorporate various neuromodulation methods will contribute to a better understanding of the neural control of split-belt locomotor adaptation.

From the above, further studies incorporating various neuroimaging and neuromodulation techniques are necessary to understand what occurs in the CNS during split-belt locomotor adaptation.

4-7. Implications for clinical rehabilitation and sports science

The main measures were EMG-EMG coherence (Study 1) and muscle synergy (Study 2) in this thesis. To date, these measures have been used to compare neuromuscular control during walking between healthy participants and patients with CNS disorders such as SCI (Hansen et al., 2005; Barthélemy et al., 2010; Zipser-Mohammadzada et al., 2022), stroke (Nielsen et al., 2008; Clark et al., 2010; Kitatani et al., 2016), and cerebral palsy (Cappellini et al., 2016; Shuman et al., 2017). EMG-EMG coherence has also been used to investigate changes in neuromuscular control with rehabilitation training in patients with CNS disorders (Norton and Gorassini, 2006; Willerslev-Olsen et al., 2015). Therefore, EMG-EMG coherence and muscle synergy could be promising tools to evaluate the state of the CNS in patients with CNS damage (Hansen et al., 2005; Safavynia et al., 2011). To date, poststroke individuals have been reported to be able to make predictive feedforward adaptation in split-belt locomotor adaptation as healthy participants (Reisman et al., 2007, 2009). However, because the findings were based on kinematics parameters (i.e., apparent movements), whether neuromuscular control during split-belt locomotor adaptation is the same between poststroke patients and healthy participants remains unclear. Investigating EMG-EMG coherence and muscle synergy during split-belt locomotor adaptation in poststroke patients may help clarify the question. Moreover, the split-belt treadmill has been believed to be a therapeutic tool to improve the asymmetric walking patterns observed in poststroke individuals (Helm and Reisman, 2015). In other words, the intervention using the split-belt treadmill can lead to an aftereffect resulting in more symmetrical walking patterns

(Reisman et al., 2007, 2009). However, the effect of the intervention is expected to differ between individuals. Then, EMG-EMG coherence and muscle synergy may be useful to elucidate the causes of the individual differences of the intervention using the split-belt treadmill. Because each study in this thesis was conducted in healthy participants, the present findings will be fundamental knowledge to interpret and discuss the characteristics of neural control during split-belt locomotor adaptation in poststroke patients. Meanwhile, although aging has been reported to influence split-belt locomotor adaptation from a kinematics perspective (Bruijn et al., 2012; Malone and Bastian, 2016; Sato and Choi, 2021), the detailed neural mechanism is not fully revealed. Therefore, if neuromuscular control in locomotor adaptation in older participants would be investigated using EMG-EMG coherence or muscle synergy in the future, the present findings based on healthy young participants might help characterize differences in locomotor adaptability between young and older people.

Although the theme of this thesis was locomotor adaptability, the present findings may also contribute to sports science. One of the main interests in sports science is the difference between a person who can quickly acquire new motor skills and a person who does not. In other words, researchers studying sports science would be interested in the individual difference in motor learning ability. The locomotor adaptation is considered an aspect of motor learning (Reisman et al., 2010). In this thesis, EMG-EMG coherence and muscle synergy were investigated over time in the process in which participants acquire new walking patterns and it is found that those measures change with adaptation. Similarly, if EMG-EMG coherence or muscle synergy were chronologically investigated in the process by which novices acquire new motor skills, individual differences in motor learning ability may be revealed in terms of neuromuscular control. Furthermore, if brain activity during split-belt locomotor adaptation can be clarified in the future, as mentioned above, the findings would also

be fundamental knowledge for exploring individual differences when learning new motor skills.

Finally, future neuromodulation studies based on the findings of this thesis and studies using EEG or fMRI are expected to contribute to both clinical rehabilitation and sports science. Specifically, understanding neuromodulation methods to facilitate split-belt locomotor adaptation could be useful to build rational methods to facilitate the regaining of walking function and the acquisition of new motor skills. From the above, the split-belt locomotor adaptation study may potentially contribute not only to the field of human walking research but also to clinical rehabilitation and sports science.

Chapter 5: Conclusion

This thesis aimed to investigate neuromuscular control during split-belt locomotor adaptation in humans. Based on two separate studies, it is concluded that flexible neuromuscular controls through the corticospinal tract and muscle synergies may underlie the adaptation to the novel walking environment in which walking speeds differ between the right and left sides and the de-adaptation to the normal walking environment. These neuromuscular controls are not mutually exclusive, and both may play an important role in split-belt locomotor adaptation.

The novel findings of this thesis expand our understanding of the neural control that underpins split-belt locomotor adaptation. The present findings may also motivate further studies investigating the neural control of split-belt locomotor adaptation. In the future, the knowledge accumulated in the study of split-belt locomotor adaptation is expected to contribute to walking rehabilitation and sports science.

References

Abd, A. T., Singh, R. E., Iqbal, K., and White, G. (2021). A Perspective on Muscle Synergies and Different Theories Related to Their Adaptation. *Biomech. Model. Mechanobiol.* 1, 253–263.

Armstrong, D. M. (1988). The supraspinal control of mammalian locomotion. *J. Physiol.* 405, 1–37.

Awosika, O. O., Sandrini, M., Volochayev, R., Thompson, R. M., Fishman, N., Wu, T., et al. (2019). Transcutaneous spinal direct current stimulation improves locomotor learning in healthy humans. *Brain Stimul.* 12, 628–634.

Bach, M. M., Daffertshofer, A., and Dominici, N. (2021). Muscle Synergies in Children Walking and Running on a Treadmill. *Front. Hum. Neurosci.* 15, 637157.

Baker, R. (2007). The history of gait analysis before the advent of modern computers. *Gait Posture* 26, 331–342.

Barroso, F. O., Torricelli, D., Moreno, J. C., Taylor, J., Gomez-Soriano, J., Bravo-Esteban, E., et al. (2014). Shared muscle synergies in human walking and cycling. *J. Neurophysiol.* 112, 1984–1998.

Barthélemy, D., Willerslev-Olsen, M., Lundell, H., Conway, B. A., Knudsen, H., Biering-Sørensen, F., et al. (2010). Impaired transmission in the corticospinal tract and gait disability in spinal cord injured persons. *J. Neurophysiol.* 104, 1167–1176.

Bastian, A. J. (2006). Learning to predict the future: the cerebellum adapts feedforward movement control. *Curr. Opin. Neurobiol.* 16, 645–649.

Bernstein (1966). The co-ordination and regulation of movements. *The co-ordination and regulation of movements*. Available at: https://ci.nii.ac.jp/naid/10008376164/.

Bizzi, E., and Cheung, V. C. K. (2013). The neural origin of muscle synergies. *Front. Comput. Neurosci.* 7, 51.

Boccia, G., Zoppirolli, C., Bortolan, L., Schena, F., and Pellegrini, B. (2018). Shared and task-specific muscle synergies of Nordic walking and conventional walking. *Scand. J. Med. Sci. Sports* 28, 905–918.

References

Bohannon, R. W., and Williams Andrews, A. (2011). Normal walking speed: a descriptive meta-analysis. *Physiotherapy* 97, 182–189.

Bradford, J. C., Lukos, J. R., and Ferris, D. P. (2016). Electrocortical activity distinguishes between uphill and level walking in humans. *J. Neurophysiol.* 115, 958–966.

Brown, T. G. (1914). On the nature of the fundamental activity of the nervous centres; together with an analysis of the conditioning of rhythmic activity in progression, and a theory of the evolution of function in the nervous system. *J. Physiol.* 48, 18–46.

Bruijn, S. M., Van Impe, A., Duysens, J., and Swinnen, S. P. (2012). Split-belt walking: adaptation differences between young and older adults. *J. Neurophysiol.* 108, 1149–1157.

Bulea, T. C., Kim, J., Damiano, D. L., Stanley, C. J., and Park, H.-S. (2015). Prefrontal, posterior parietal and sensorimotor network activity underlying speed control during walking. *Front. Hum. Neurosci.* 9, 247.

Calancie, B., Needham-Shropshire, B., Jacobs, P., Willer, K., Zych, G., and Green, B. A. (1994). Involuntary stepping after chronic spinal cord injury. Evidence for a central rhythm generator for locomotion in man. *Brain* 117 (Pt 5), 1143–1159.

Capaday, C. (2002). The special nature of human walking and its neural control. *Trends Neurosci.* 25, 370–376.

Capaday, C., Lavoie, B. A., Barbeau, H., Schneider, C., and Bonnard, M. (1999). Studies on the corticospinal control of human walking. I. Responses to focal transcranial magnetic stimulation of the motor cortex. *J. Neurophysiol.* 81, 129–139.

Capaday, C., and Stein, R. B. (1986). Amplitude modulation of the soleus H-reflex in the human during walking and standing. *J. Neurosci.* 6, 1308–1313.

Capaday, C., and Stein, R. B. (1987). Difference in the amplitude of the human soleus H reflex during walking and running. *J. Physiol.* 392, 513–522.

Cappellini, G., Ivanenko, Y. P., Martino, G., MacLellan, M. J., Sacco, A., Morelli, D., et al. (2016). Immature Spinal Locomotor Output in Children with Cerebral Palsy. *Front. Physiol.* 7, 478.

Cappellini, G., Ivanenko, Y. P., Poppele, R. E., and Lacquaniti, F. (2006). Motor patterns in human

walking and running. *J. Neurophysiol.* 95, 3426–3437.

Carvalho, S., Biro, D., Cunha, E., Hockings, K., McGrew, W. C., Richmond, B. G., et al. (2012). Chimpanzee carrying behaviour and the origins of human bipedality. *Curr. Biol.* 22, R180-1.

Charalambous, C. C., and Hadjipapas, A. (2022). Is there frequency-specificity in the motor control of walking? The putative differential role of alpha and beta oscillations. *Front. Syst. Neurosci.* 16, 123.

Cheung, V. C. K., d'Avella, A., Tresch, M. C., and Bizzi, E. (2005). Central and sensory contributions to the activation and organization of muscle synergies during natural motor behaviors. *J. Neurosci.* 25, 6419–6434.

Cheung, V. C. K., and Seki, K. (2021). Approaches to revealing the neural basis of muscle synergies: a review and a critique. *J. Neurophysiol.* 125, 1580–1597.

Choi, J. T., and Bastian, A. J. (2007). Adaptation reveals independent control networks for human walking. *Nat. Neurosci.* 10, 1055–1062.

Choi, J. T., Bouyer, L. J., and Nielsen, J. B. (2015). Disruption of Locomotor Adaptation with Repetitive Transcranial Magnetic Stimulation Over the Motor Cortex. *Cereb. Cortex* 25, 1981–1986.

Choi, J. T., Vining, E. P. G., Reisman, D. S., and Bastian, A. J. (2009). Walking flexibility after hemispherectomy: split-belt treadmill adaptation and feedback control. *Brain* 132, 722–733.

Christensen, L. O., Petersen, N., Andersen, J. B., Sinkjaer, T., and Nielsen, J. B. (2000). Evidence for transcortical reflex pathways in the lower limb of man. *Prog. Neurobiol.* 62, 251–272.

Chvatal, S. A., and Ting, L. H. (2012). Voluntary and reactive recruitment of locomotor muscle synergies during perturbed walking. *J. Neurosci.* 32, 12237–12250.

Chvatal, S. A., and Ting, L. H. (2013). Common muscle synergies for balance and walking. *Front. Comput. Neurosci.* 7, 48.

Clark, D. J., Ting, L. H., Zajac, F. E., Neptune, R. R., and Kautz, S. A. (2010). Merging of healthy motor modules predicts reduced locomotor performance and muscle coordination complexity post-stroke. *J. Neurophysiol.* 103, 844–857.

References

Conradsson, D., Hinton, D. C., and Paquette, C. (2019). The effects of dual-tasking on temporal gait adaptation and de-adaptation to the split-belt treadmill in older adults. *Exp. Gerontol.* 125, 110655.

Dalla Volta, R., Fasano, F., Cerasa, A., Mangone, G., Quattrone, A., and Buccino, G. (2015). Walking indoors, walking outdoors: an fMRI study. *Front. Psychol.* 6, 1502.

Danna-Dos-Santos, A., Boonstra, T. W., Degani, A. M., Cardoso, V. S., Magalhaes, A. T., Mochizuki, L., et al. (2014). Multi-muscle control during bipedal stance: an EMG–EMG analysis approach. *Exp. Brain Res.* 232, 75–87.

Danner, S. M., Hofstoetter, U. S., Freundl, B., Binder, H., Mayr, W., Rattay, F., et al. (2015). Human spinal locomotor control is based on flexibly organized burst generators. *Brain* 138, 577–588.

De Luca, C. J., and Mambrito, B. (1987). Voluntary control of motor units in human antagonist muscles: coactivation and reciprocal activation. *J. Neurophysiol.* 58, 525–542.

Desrochers, E., Harnie, J., Doelman, A., Hurteau, M.-F., and Frigon, A. (2019). Spinal control of muscle synergies for adult mammalian locomotion. *J. Physiol.* 597, 333–350.

Dietz, V. (2002). Proprioception and locomotor disorders. *Nat. Rev. Neurosci.* 3, 781–790.

Dietz, V., Zijlstra, W., and Duysens, J. (1994). Human neuronal interlimb coordination during split-belt locomotion. *Exp. Brain Res.* 101, 513–520.

Dimitrijevic, M. R., Gerasimenko, Y., and Pinter, M. M. (1998). Evidence for a spinal central pattern generator in humans. *Ann. N. Y. Acad. Sci.* 860, 360–376.

Dominici, N., Ivanenko, Y. P., Cappellini, G., d'Avella, A., Mondì, V., Cicchese, M., et al. (2011). Locomotor primitives in newborn babies and their development. *Science* 334, 997–999.

Drew, T., and Marigold, D. S. (2015). Taking the next step: cortical contributions to the control of locomotion. *Curr. Opin. Neurobiol.* 33, 25–33.

Ebersbach, G., Sojer, M., Valldeoriola, F., Wissel, J., Müller, J., Tolosa, E., et al. (1999). Comparative analysis of gait in Parkinson's disease, cerebellar ataxia and subcortical arteriosclerotic encephalopathy. *Brain* 122 (Pt 7), 1349–1355.

References

Farmer, S. F., Bremner, F. D., Halliday, D. M., Rosenberg, J. R., and Stephens, J. A. (1993). The frequency content of common synaptic inputs to motoneurones studied during voluntary isometric contraction in man. *J. Physiol.* 470, 127–155.

Finley, J. M., Statton, M. A., and Bastian, A. J. (2014). A novel optic flow pattern speeds split-belt locomotor adaptation. *J. Neurophysiol.* 111, 969–976.

Fisher, R. J., Galea, M. P., Brown, P., and Lemon, R. N. (2002). Digital nerve anaesthesia decreases EMG-EMG coherence in a human precision grip task. *Exp. Brain Res.* 145, 207–214.

Frigon, A., Hurteau, M.-F., Thibaudier, Y., Leblond, H., Telonio, A., and D'Angelo, G. (2013). Split-belt walking alters the relationship between locomotor phases and cycle duration across speeds in intact and chronic spinalized adult cats. *J. Neurosci.* 33, 8559–8566.

Fukuyama, H., Ouchi, Y., Matsuzaki, S., Nagahama, Y., Yamauchi, H., Ogawa, M., et al. (1997). Brain functional activity during gait in normal subjects: a SPECT study. *Neurosci. Lett.* 228, 183–186.

Gerasimenko, Y., Gorodnichev, R., Machueva, E., Pivovarova, E., Semyenov, D., Savochin, A., et al. (2010). Novel and direct access to the human locomotor spinal circuitry. *J. Neurosci.* 30, 3700–3708.

Grillner, S. (2011). Neuroscience. Human locomotor circuits conform. *Science* 334, 912–913.

Grillner, S., and El Manira, A. (2020). Current Principles of Motor Control, with Special Reference to Vertebrate Locomotion. *Physiol. Rev.* 100, 271–320.

Gwin, J. T., and Ferris, D. P. (2012). Beta- and gamma-range human lower limb corticomuscular coherence. *Front. Hum. Neurosci.* 6, 258.

Gwin, J. T., Gramann, K., Makeig, S., and Ferris, D. P. (2011). Electrocortical activity is coupled to gait cycle phase during treadmill walking. *Neuroimage* 54, 1289–1296.

Hagio, S., Fukuda, M., and Kouzaki, M. (2015). Identification of muscle synergies associated with gait transition in humans. *Front. Hum. Neurosci.* 9, 48.

Hagio, S., and Kouzaki, M. (2014). The flexible recruitment of muscle synergies depends on the required force-generating capability. *J. Neurophysiol.* 112, 316–327.

References

Halliday, D. M., Conway, B. A., Christensen, L. O. D., Hansen, N. L., Petersen, N. P., and Nielsen, J. B. (2003). Functional coupling of motor units is modulated during walking in human subjects. *J. Neurophysiol.* 89, 960–968.

Halliday, D. M., Rosenberg, J. R., Amjad, A. M., Breeze, P., Conway, B. A., and Farmer, S. F. (1995). A framework for the analysis of mixed time series/point process data—Theory and application to the study of physiological tremor, single motor unit discharges and electromyograms. *Progress in Biophysics and Molecular Biology* 64, 237–278. doi: 10.1016/s0079-6107(96)00009-0.

Hamzey, R. J., Kirk, E. M., and Vasudevan, E. V. L. (2016). Gait speed influences aftereffect size following locomotor adaptation, but only in certain environments. *Exp. Brain Res.* 234, 1479–1490.

Hanakawa, T., Katsumi, Y., Fukuyama, H., Honda, M., Hayashi, T., Kimura, J., et al. (1999). Mechanisms underlying gait disturbance in Parkinson's disease: a single photon emission computed tomography study. *Brain* 122 (Pt 7), 1271–1282.

Hansen, N. L., Conway, B. A., Halliday, D. M., Hansen, S., Pyndt, H. S., Biering-Sørensen, F., et al. (2005). Reduction of common synaptic drive to ankle dorsiflexor motoneurons during walking in patients with spinal cord lesion. *J. Neurophysiol.* 94, 934–942.

Hathout, G. M., and Bhidayasiri, R. (2005). Midbrain ataxia: an introduction to the mesencephalic locomotor region and the pedunculopontine nucleus. *AJR Am. J. Roentgenol.* 184, 953–956.

Hayes, H. B., Chvatal, S. A., French, M. A., Ting, L. H., and Trumbower, R. D. (2014). Neuromuscular constraints on muscle coordination during overground walking in persons with chronic incomplete spinal cord injury. *Clin. Neurophysiol.* 125, 2024‑2035.

Helm, E. E., and Reisman, D. S. (2015). The split-belt walking paradigm: Exploring motor learning and spatiotemporal asymmetry poststroke. *Phys. Med. Rehabil. Clin. N. Am.* 26, 703–713.

Hinton, D. C., Conradsson, D. M., and Paquette, C. (2020). Understanding Human Neural Control of Short-term Gait Adaptation to the Split-belt Treadmill. *Neuroscience* 451, 36–50.

Hoogkamer, W. (2017). Perception of Gait Asymmetry During Split-Belt Walking. *Exerc. Sport Sci. Rev.* 45, 34–40.

References

Iturralde, P. A., and Torres-Oviedo, G. (2019). Corrective Muscle Activity Reveals Subject-Specific Sensorimotor Recalibration. *eNeuro* 6. doi: 10.1523/ENEURO.0358-18.2019.

Ivanenko, Y. P., Cappellini, G., Dominici, N., Poppele, R. E., and Lacquaniti, F. (2005). Coordination of locomotion with voluntary movements in humans. *J. Neurosci.* 25, 7238–7253.

Ivanenko, Y. P., Poppele, R. E., and Lacquaniti, F. (2004). Five basic muscle activation patterns account for muscle activity during human locomotion. *J. Physiol.* 556, 267–282.

Ivanenko, Y. P., Poppele, R. E., and Lacquaniti, F. (2006). Motor control programs and walking. *Neuroscientist* 12, 339–348.

Janshen, L., Santuz, A., Ekizos, A., and Arampatzis, A. (2017). Modular control during incline and level walking in humans. *J. Exp. Biol.* 220, 807–813.

Jayaram, G., Galea, J. M., Bastian, A. J., and Celnik, P. (2011). Human locomotor adaptive learning is proportional to depression of cerebellar excitability. *Cereb. Cortex* 21, 1901–1909.

Jayaram, G., Tang, B., Pallegadda, R., Vasudevan, E. V. L., Celnik, P., and Bastian, A. (2012). Modulating locomotor adaptation with cerebellar stimulation. *J. Neurophysiol.* 107, 2950–2957.

Jensen, P., Frisk, R., Spedden, M. E., Geertsen, S. S., Bouyer, L. J., Halliday, D. M., et al. (2019). Using Corticomuscular and Intermuscular Coherence to Assess Cortical Contribution to Ankle Plantar Flexor Activity During Gait. *J. Mot. Behav.* 51, 668–680.

Jensen, P., Jensen, N. J., Terkildsen, C. U., Choi, J. T., Nielsen, J. B., and Geertsen, S. S. (2018). Increased central common drive to ankle plantar flexor and dorsiflexor muscles during visually guided gait. *Physiol Rep* 6. doi: 10.14814/phy2.13598.

Jossinger, S., Mawase, F., Ben-Shachar, M., and Shmuelof, L. (2020). Locomotor Adaptation Is Associated with Microstructural Properties of the Inferior Cerebellar Peduncle. *Cerebellum* 19, 370–382.

Kamibayashi, K., Nakajima, T., Fujita, M., Takahashi, M., Ogawa, T., Akai, M., et al. (2010). Effect of sensory inputs on the soleus H-reflex amplitude during robotic passive stepping in humans. *Exp. Brain Res.* 202, 385–395.

References

Kamibayashi, K., Nakajima, T., Takahashi, M., Akai, M., and Nakazawa, K. (2009). Facilitation of corticospinal excitability in the tibialis anterior muscle during robot-assisted passive stepping in humans. *Eur. J. Neurosci.* 30, 100–109.

Kenville, R., Maudrich, T., Vidaurre, C., Maudrich, D., Villringer, A., Ragert, P., et al. (2020). Intermuscular coherence between homologous muscles during dynamic and static movement periods of bipedal squatting. *J. Neurophysiol.* 124, 1045–1055.

Kibushi, B., Hagio, S., Moritani, T., and Kouzaki, M. (2018). Speed-Dependent Modulation of Muscle Activity Based on Muscle Synergies during Treadmill Walking. *Front. Hum. Neurosci.* 12, 4.

Kibushi, B., Moritani, T., and Kouzaki, M. (2019). Local dynamic stability in temporal pattern of intersegmental coordination during various stride time and stride length combinations. *Exp. Brain Res.* 237, 257–271.

Kilner, J. M., Fisher, R. J., and Lemon, R. N. (2004). Coupling of oscillatory activity between muscles is strikingly reduced in a deafferented subject compared with normal controls. *J. Neurophysiol.* 92, 790–796.

Kitatani, R., Ohata, K., Aga, Y., Mashima, Y., Hashiguchi, Y., Wakida, M., et al. (2016). Descending neural drives to ankle muscles during gait and their relationships with clinical functions in patients after stroke. *Clin. Neurophysiol.* 127, 1512–1520.

Kumari, N., Taylor, D., Rashid, U., Vandal, A. C., Smith, P. F., and Signal, N. (2020). Cerebellar transcranial direct current stimulation for learning a novel split-belt treadmill task: a randomised controlled trial. *Sci. Rep.* 10, 11853.

Lacquaniti, F., Ivanenko, Y. P., and Zago, M. (2012). Patterned control of human locomotion. *J. Physiol.* 590, 2189–2199.

Latash, M. L. (2007). *Neurophysiological Basis of Movement*. Human Kinetics.

Lee, D. D., and Seung, H. S. (1999). Learning the parts of objects by non-negative matrix factorization. *Nature* 401, 788–791.

Li, S., Francisco, G. E., and Zhou, P. (2018). Post-stroke Hemiplegic Gait: New Perspective and Insights. *Front. Physiol.* 9, 1021.

References

Liu, J., Sheng, Y., and Liu, H. (2019). Corticomuscular Coherence and Its Applications: A Review. *Front. Hum. Neurosci.* 13, 100.

Maclellan, M. J., Ivanenko, Y. P., Massaad, F., Bruijn, S. M., Duysens, J., and Lacquaniti, F. (2014). Muscle activation patterns are bilaterally linked during split-belt treadmill walking in humans. *J. Neurophysiol.* 111, 1541–1552.

Malone, L. A., and Bastian, A. J. (2010). Thinking about walking: effects of conscious correction versus distraction on locomotor adaptation. *J. Neurophysiol.* 103, 1954–1962.

Malone, L. A., and Bastian, A. J. (2016). Age-related forgetting in locomotor adaptation. *Neurobiol. Learn. Mem.* 128, 1–6.

Malone, L. A., Bastian, A. J., and Torres-Oviedo, G. (2012). How does the motor system correct for errors in time and space during locomotor adaptation? *J. Neurophysiol.* 108, 672–683.

Martino, G., Ivanenko, Y. P., d'Avella, A., Serrao, M., Ranavolo, A., Draicchio, F., et al. (2015). Neuromuscular adjustments of gait associated with unstable conditions. *J. Neurophysiol.* 114, 2867–2882.

Martino, G., Ivanenko, Y. P., Serrao, M., Ranavolo, A., d'Avella, A., Draicchio, F., et al. (2014). Locomotor patterns in cerebellar ataxia. *J. Neurophysiol.* 112, 2810–2821.

Masdeu, J. C., Alampur, U., Cavaliere, R., and Tavoulareas, G. (1994). Astasia and gait failure with damage of the pontomesencephalic locomotor region. *Ann. Neurol.* 35, 619–621.

Mawase, F., Bar-Haim, S., and Shmuelof, L. (2017). Formation of Long-Term Locomotor Memories Is Associated with Functional Connectivity Changes in the Cerebellar-Thalamic-Cortical Network. *J. Neurosci.* 37, 349–361.

McCrea, D. A., and Rybak, I. A. (2008). Organization of mammalian locomotor rhythm and pattern generation. *Brain Res. Rev.* 57, 134–146.

Mileti, I., Zampogna, A., Santuz, A., Asci, F., Del Prete, Z., Arampatzis, A., et al. (2020). Muscle Synergies in Parkinson's Disease. *Sensors* 20. doi: 10.3390/s20113209.

Miyaguchi, S., Otsuru, N., Kojima, S., Saito, K., Inukai, Y., Masaki, M., et al. (2018). Transcranial Alternating Current Stimulation With Gamma Oscillations Over the Primary Motor Cortex

and Cerebellar Hemisphere Improved Visuomotor Performance. *Front. Behav. Neurosci.* 12, 132.

Morris, M. E., Iansek, R., Matyas, T. A., and Summers, J. J. (1994). The pathogenesis of gait hypokinesia in Parkinson's disease. *Brain* 117 (Pt 5), 1169–1181.

Morton, S. M., and Bastian, A. J. (2006). Cerebellar contributions to locomotor adaptations during splitbelt treadmill walking. *J. Neurosci.* 26, 9107–9116.

Musselman, K. E., Patrick, S. K., Vasudevan, E. V. L., Bastian, A. J., and Yang, J. F. (2011). Unique characteristics of motor adaptation during walking in young children. *J. Neurophysiol.* 105, 2195–2203.

Nakazawa, K., Kawashima, N., Akai, M., and Yano, H. (2004). On the reflex coactivation of ankle flexor and extensor muscles induced by a sudden drop of support surface during walking in humans. *J. Appl. Physiol.* 96, 604–611.

Nazifi, M. M., Yoon, H. U., Beschorner, K., and Hur, P. (2017). Shared and Task-Specific Muscle Synergies during Normal Walking and Slipping. *Front. Hum. Neurosci.* 11, 40.

Neptune, R. R., Clark, D. J., and Kautz, S. A. (2009). Modular control of human walking: a simulation study. *J. Biomech.* 42, 1282–1287.

Neumann, D. A. (2002). *Kinesiology of the Musculoskeletal System: Foundations for Rehabilitation*. Mosby.

Nielsen, J. B. (2002). M otoneuronal drive during human walking. *Brain Res. Rev.* 40, 192–201.

Nielsen, J. B. (2003). How we walk: central control of muscle activity during human walking. *Neuroscientist* 9, 195–204.

Nielsen, J. B., Brittain, J.-S., Halliday, D. M., Marchand-Pauvert, V., Mazevet, D., and Conway, B. A. (2008). Reduction of common motoneuronal drive on the affected side during walking in hemiplegic stroke patients. *Clin. Neurophysiol.* 119, 2813–2818.

Nitsche, M. A., and Paulus, W. (2000). Excitability changes induced in the human motor cortex by weak transcranial direct current stimulation. *J. Physiol.* 527 Pt 3, 633–639.

References

Norton, J. A., and Gorassini, M. A. (2006). Changes in cortically related intermuscular coherence accompanying improvements in locomotor skills in incomplete spinal cord injury. *J. Neurophysiol.* 95, 2580–2589.

Ogawa, T., Kawashima, N., and Nakazawa, K. (2015). Locomotor adaptation: Significance and underlying neural mechanisms. *The Journal of Physical Fitness and Sports Medicine* 4, 107–110.

Ogawa, T., Kawashima, N., Ogata, T., and Nakazawa, K. (2014). Predictive control of ankle stiffness at heel contact is a key element of locomotor adaptation during split-belt treadmill walking in humans. *J. Neurophysiol.* 111, 722–732.

Oliveira, A. S., Gizzi, L., Farina, D., and Kersting, U. G. (2014). Motor modules of human locomotion: influence of EMG averaging, concatenation, and number of step cycles. *Front. Hum. Neurosci.* 8, 335.

Oliveira, A. S., Gizzi, L., Ketabi, S., Farina, D., and Kersting, U. G. (2016). Modular Control of Treadmill vs Overground Running. *PLoS One* 11, e0153307.

Oshima, A., Nakamura, Y., and Kamibayashi, K. (2022). Modulation of Muscle Synergies in Lower-Limb Muscles Associated With Split-Belt Locomotor Adaptation. *Front. Hum. Neurosci.* 16. doi: 10.3389/fnhum.2022.852530.

Oshima, A., Wakahara, T., Nakamura, Y., Tsujiuchi, N., and Kamibayashi, K. (2021). Time-series changes in intramuscular coherence associated with split-belt treadmill adaptation in humans. *Exp. Brain Res.* 239, 2127–2139.

Petersen, N. T., Butler, J. E., Marchand-Pauvert, V., Fisher, R., Ledebt, A., Pyndt, H. S., et al. (2001). Suppression of EMG activity by transcranial magnetic stimulation in human subjects during walking. *J. Physiol.* 537, 651–656.

Petersen, N. T., Pyndt, H. S., and Nielsen, J. B. (2003). Investigating human motor control by transcranial magnetic stimulation. *Exp. Brain Res.* 152, 1–16.

Petersen, T. H., Willerslev-Olsen, M., Conway, B. A., and Nielsen, J. B. (2012). The motor cortex drives the muscles during walking in human subjects. *J. Physiol.* 590, 2443–2452.

References

Power, H. A., Norton, J. A., Porter, C. L., Doyle, Z., Hui, I., and Chan, K. M. (2006). Transcranial direct current stimulation of the primary motor cortex affects cortical drive to human musculature as assessed by intermuscular coherence. *J. Physiol.* 577, 795–803.

Reisman, D. S., Bastian, A. J., and Morton, S. M. (2010). Neurophysiologic and rehabilitation insights from the split-belt and other locomotor adaptation paradigms. *Phys. Ther.* 90, 187–195.

Reisman, D. S., Block, H. J., and Bastian, A. J. (2005). Interlimb coordination during locomotion: what can be adapted and stored? *J. Neurophysiol.* 94, 2403–2415.

Reisman, D. S., Wityk, R., Silver, K., and Bastian, A. J. (2007). Locomotor adaptation on a split-belt treadmill can improve walking symmetry post-stroke. *Brain* 130, 1861–1872.

Reisman, D. S., Wityk, R., Silver, K., and Bastian, A. J. (2009). Split-belt treadmill adaptation transfers to overground walking in persons poststroke. *Neurorehabil. Neural Repair* 23, 735–744.

Rimini, D., Agostini, V., and Knaflitz, M. (2017). Intra-Subject Consistency during Locomotion: Similarity in Shared and Subject-Specific Muscle Synergies. *Front. Hum. Neurosci.* 11, 586.

Rossignol, S., Dubuc, R., and Gossard, J.-P. (2006). Dynamic sensorimotor interactions in locomotion. *Physiol. Rev.* 86, 89–154.

Safavynia, S. A., Torres-Oviedo, G., and Ting, L. H. (2011). Muscle Synergies: Implications for Clinical Evaluation and Rehabilitation of Movement. *Top. Spinal Cord Inj. Rehabil.* 17, 16–24.

Saito, A., Tomita, A., Ando, R., Watanabe, K., and Akima, H. (2018). Muscle synergies are consistent across level and uphill treadmill running. *Sci. Rep.* 8, 5979.

Santuz, A., Brüll, L., Ekizos, A., Schroll, A., Eckardt, N., Kibele, A., et al. (2020). Neuromotor Dynamics of Human Locomotion in Challenging Settings. *iScience* 23, 100796.

Santuz, A., Ekizos, A., Eckardt, N., Kibele, A., and Arampatzis, A. (2018). Challenging human locomotion: stability and modular organisation in unsteady conditions. *Sci. Rep.* 8, 2740.

Sato, S., and Choi, J. T. (2019). Increased intramuscular coherence is associated with temporal gait symmetry during split-belt locomotor adaptation. *J. Neurophysiol.* 122, 1097–1109.

References

Sato, S., and Choi, J. T. (2021). Neural Control of Human Locomotor Adaptation: Lessons about Changes with Aging. *Neuroscientist*, 10738584211013724.

Sato, S. D., and Choi, J. T. (2022). Corticospinal drive is associated with temporal walking adaptation in both healthy young and older adults. *Front. Aging Neurosci.* 14, 920475.

Savin, D. N., Tseng, S.-C., and Morton, S. M. (2010). Bilateral adaptation during locomotion following a unilaterally applied resistance to swing in nondisabled adults. *J. Neurophysiol.* 104, 3600–3611.

Sawers, A., Allen, J. L., and Ting, L. H. (2015). Long-term training modifies the modular structure and organization of walking balance control. *J. Neurophysiol.* 114, 3359–3373.

Schubert, M., Curt, A., Jensen, L., and Dietz, V. (1997). Corticospinal input in human gait: modulation of magnetically evoked motor responses. *Exp. Brain Res.* 115, 234–246.

Severini, G., Koenig, A., Adans-Dester, C., Cajigas, I., Cheung, V. C. K., and Bonato, P. (2020). Robot-Driven Locomotor Perturbations Reveal Synergy-Mediated, Context-Dependent Feedforward and Feedback Mechanisms of Adaptation. *Sci. Rep.* 10, 5104.

Severini, G., and Zych, M. (2022). Locomotor adaptations: paradigms, principles and perspectives. *Prog. Biomed. Eng.* 4, 042003.

Shik, M. L., Severin, F. V., and Orlovskiĭ, G. N. (1966). [Control of walking and running by means of electric stimulation of the midbrain]. *Biofizika* 11, 659–666.

Shuman, B. R., Schwartz, M. H., and Steele, K. M. (2017). Electromyography Data Processing Impacts Muscle Synergies during Gait for Unimpaired Children and Children with Cerebral Palsy. *Front. Comput. Neurosci.* 11, 50.

Simonsen, E. B. (2014). Contributions to the understanding of gait control. *Dan. Med. J.* 61, B4823.

Singh, R. E., White, G., Delis, I., and Iqbal, K. (2020). Alteration of muscle synergy structure while walking under increased postural constraints. *Cognitive Computation and Systems* 2, 50–56.

Sinkjaer, T., Andersen, J. B., and Larsen, B. (1996). Soleus stretch reflex modulation during gait in humans. *J. Neurophysiol.* 76, 1112–1120.

References

Spedden, M. E., Choi, J. T., Nielsen, J. B., and Geertsen, S. S. (2019). Corticospinal control of normal and visually guided gait in healthy older and younger adults. *Neurobiol. Aging* 78, 29–41.

Statton, M. A., Vazquez, A., Morton, S. M., Vasudevan, E. V. L., and Bastian, A. J. (2018). Making Sense of Cerebellar Contributions to Perceptual and Motor Adaptation. *Cerebellum* 17, 111–121.

Steele, K. M., Tresch, M. C., and Perreault, E. J. (2013). The number and choice of muscles impact the results of muscle synergy analyses. *Front. Comput. Neurosci.* 7, 105.

Takakusaki, K. (2013). Neurophysiology of gait: from the spinal cord to the frontal lobe. *Mov. Disord.* 28, 1483–1491.

Thelen, E., Ulrich, B. D., and Niles, D. (1987). Bilateral coordination in human infants: stepping on a split-belt treadmill. *J. Exp. Psychol. Hum. Percept. Perform.* 13, 405–410.

Thomas, S. L., and Gorassini, M. A. (2005). Increases in corticospinal tract function by treadmill training after incomplete spinal cord injury. *J. Neurophysiol.* 94, 2844–2855.

Ting, L. H., Chiel, H. J., Trumbower, R. D., Allen, J. L., McKay, J. L., Hackney, M. E., et al. (2015). Neuromechanical principles underlying movement modularity and their implications for rehabilitation. *Neuron* 86, 38–54.

Torres-Oviedo, G., Vasudevan, E., Malone, L., and Bastian, A. J. (2011). Locomotor adaptation. *Prog. Brain Res.* 191, 65–74.

Tresch, M. C., Cheung, V. C. K., and d'Avella, A. (2006). Matrix factorization algorithms for the identification of muscle synergies: evaluation on simulated and experimental data sets. *J. Neurophysiol.* 95, 2199–2212.

Tresch, M. C., Saltiel, P., and Bizzi, E. (1999). The construction of movement by the spinal cord. *Nat. Neurosci.* 2, 162–167.

Tyrell, C. M., Helm, E., and Reisman, D. S. (2014). Learning the spatial features of a locomotor task is slowed after stroke. *J. Neurophysiol.* 112, 480–489.

Vasudevan, E. V. L., and Bastian, A. J. (2010). Split-belt treadmill adaptation shows different functional networks for fast and slow human walking. *J. Neurophysiol.* 103, 183–191.

References

Vasudevan, E. V. L., Glass, R. N., and Packel, A. T. (2014). Effects of traumatic brain injury on locomotor adaptation. *J. Neurol. Phys. Ther.* 38, 172–182.

Vasudevan, E. V. L., Hamzey, R. J., and Kirk, E. M. (2017). Using a Split-belt Treadmill to Evaluate Generalization of Human Locomotor Adaptation. *J. Vis. Exp.* doi: 10.3791/55424.

Willerslev-Olsen, M., Petersen, T. H., Farmer, S. F., and Nielsen, J. B. (2015). Gait training facilitates central drive to ankle dorsiflexors in children with cerebral palsy. *Brain* 138, 589–603.

Yang, J. F., and Gorassini, M. (2006). Spinal and brain control of human walking: implications for retraining of walking. *Neuroscientist* 12, 379–389.

Yokoyama, H., Kaneko, N., Masugi, Y., Ogawa, T., Watanabe, K., and Nakazawa, K. (2020a). Gait-phase-dependent and gait-phase-independent cortical activity across multiple regions involved in voluntary gait modifications in humans. *Eur. J. Neurosci.* doi: 10.1111/ejn.14867.

Yokoyama, H., Kaneko, N., Ogawa, T., Kawashima, N., Watanabe, K., and Nakazawa, K. (2019). Cortical Correlates of Locomotor Muscle Synergy Activation in Humans: An Electroencephalographic Decoding Study. *iScience* 15, 623–639.

Yokoyama, H., Kato, T., Kaneko, N., Kobayashi, H., Hoshino, M., Kokubun, T., et al. (2021). Basic locomotor muscle synergies used in land walking are finely tuned during underwater walking. *Sci. Rep.* 11, 18480.

Yokoyama, H., Ogawa, T., Kawashima, N., Shinya, M., and Nakazawa, K. (2016). Distinct sets of locomotor modules control the speed and modes of human locomotion. *Sci. Rep.* 6, 36275.

Yokoyama, H., Sato, K., Ogawa, T., Yamamoto, S.-I., Nakazawa, K., and Kawashima, N. (2018). Characteristics of the gait adaptation process due to split-belt treadmill walking under a wide range of right-left speed ratios in humans. *PLoS One* 13, e0194875.

Yokoyama, H., Yoshida, T., Zabjek, K., Chen, R., and Masani, K. (2020b). Defective corticomuscular connectivity during walking in patients with Parkinson's disease. *J. Neurophysiol.* 124, 1399–1414.

Young, D. R., Parikh, P. J., and Layne, C. S. (2020). The Posterior Parietal Cortex Is Involved in Gait Adaptation: A Bilateral Transcranial Direct Current Stimulation Study. *Front. Hum. Neurosci.*

14, 581026.

Zipser-Mohammadzada, F., Conway, B. A., Halliday, D. M., Zipser, C. M., Easthope, C. A., Curt, A., et al. (2022). Intramuscular coherence during challenging walking in incomplete spinal cord injury: Reduced high-frequency coherence reflects impaired supra-spinal control. *Front. Hum. Neurosci.* 16, 927704.